THE SOURCES AND CYCLES OF IRON AND MANGANESE IN SURFACE WATER SUPPLIES

Zackary William Munger

Dissertation submitted to the faculty of the Virginia Polytechnic Institute and State University in partial fulfillment of the requirements for the degree of

Doctor of Philosophy
In
Geosciences

Madeline E. Schreiber, Chair
Cayelan C. Carey
Adil N. Godrej
J. Donald Rimstidt

June 24, 2016
Blacksburg, VA

Keywords: iron, manganese, water quality, reservoir, oxidation, watershed, oxygenation

The sources and cycles of iron and manganese in surface water supplies

Zackary William Munger

ABSTRACT (ACADEMIC)

Evaluation of the sources and cycles of water quality contaminants in watersheds is critical for effective surface water resource management. In particular, iron (Fe) and manganese (Mn), commonly found in rocks and sediments, have adverse impacts on water quality. However, controlling Fe and Mn in surface water systems is often complex and requires careful consideration of the hydrologic and biogeochemical factors that influence the speciation and mobility of these metals.

This dissertation investigates the sources and cycles of Fe and Mn in surface waters designated for human use. Here, I present the findings from three field- and laboratory-based studies conducted at sites in western Virginia, United States. The first study examines the impacts of reservoir-derived and watershed-derived metals on water quality along the 180 km reach of the Roanoke River downgradient from Leesville Dam. The results from this study showed strong temporal influences on river water quality immediately downgradient of the dam, resulting from seasonal reservoir dynamics. Further downgradient in the Roanoke River, water quality was strongly tied to hydrologic conditions resulting from influences generated in the watershed. The second study investigated the effects of increasing dissolved oxygen (DO) concentrations in the hypolimnion of stratified drinking water reservoir on Fe and Mn oxidation and removal. Results from a whole-ecosystem experiment showed that increasing DO concentrations through hypolimnetic oxygenation was effective for preventing the accumulation of soluble Fe in the water column. Although Mn oxidation increased under well-oxygenated conditions, soluble Mn still accumulated in the hypolimnion. Results from a laboratory

experiment demonstrated that the oxidation of Mn was strongly tied to the activity of Mn oxidizing microbes. The third study examined the relative contribution of external and internal metal loadings to the exchange of metals between sediments and the water column and the source/sink behavior of a seasonally stratified reservoir under varying hydrologic conditions in the inflows and outflows and redox conditions in the reservoir hypolimnion. Results from this study showed that redox conditions strongly influenced the exchange of metals between the sediment and aqueous phase, but had little effect on the source/sink behavior of the reservoir, while external tributary loadings had little effect on internal redox cycles, but was a strong indicator for whether the reservoir behaved as a net metal source or sink. Overall, the findings from these studies exemplify the value of characterizing the hydrologic and biogeochemical drivers of Fe and Mn cycles for managing the water quality effects of these metals in surface water supplies.

ABSTRACT (PUBLIC)

Identifying where drinking water contaminants come from and how they change in river, lake, and reservoir environments is critical for effectively managing surface water resources. In particular, the metals iron (Fe) and manganese (Mn), which are commonly found in rocks and sediments, can pose water quality problems. Controlling Fe and Mn in surface waters requires knowledge of flow conditions and water chemistry, which can both influence how these metals are transported and whether they will reach problematic levels.

This dissertation investigates the sources and chemical cycles of Fe and Mn in surface waters designated for human use. Here, I present the findings from three field- and laboratory-based studies conducted at sites in western Virginia, United States. The first study examines temporal and spatial patterns of Fe and Mn concentrations along the 180 km reach of the Roanoke River downstream from Leesville Dam. The results from this study showed that the chemistry of Leesville Lake, which varies seasonally, is an important influence on the concentration of Fe and Mn in the river just downgradient from the dam. Further downstream in the Roanoke River, metal concentrations in the river were strongly tied to flow conditions in the streams that originate in the watershed and flow into the Roanoke River. The second study investigated the effects of increasing dissolved oxygen (DO) concentrations in a drinking water reservoir on the chemical oxidation and removal of Fe and Mn in the reservoir. Results from a whole-ecosystem experiment showed that increasing DO concentrations in the reservoir using an oxygenation system was effective for preventing the accumulation of dissolved Fe in the water column. Although Mn oxidation increased under when DO concentrations were high, soluble Mn remained problematic in the reservoir. Results from a laboratory

experiment demonstrated that the oxidation of Mn was strongly tied to the activity of Mn oxidizing microbes. The third study examined the effects of DO concentrations in a drinking water reservoir and flow conditions in the major stream flowing into the reservoir on the transfer of Fe and Mn between the reservoir water and sediments. We also examined how stream discharge and DO concentrations in the reservoir influenced the net transfer of metals into or out of the reservoir. Results from this study showed that DO concentrations strongly influenced the transfer of metals between the reservoir water and sediment, but had little effect on the net transfer of metals into or out of the reservoir, while flow conditions in the inflow stream had little effect on metal transfer between the reservoir water and sediments, but was a strong indicator for whether there was a net transfer of metal into or out of the reservoir. Overall, the findings from these studies exemplify the value of characterizing the hydrologic and biogeochemical conditions that effect Fe and Mn for managing water quality in drinking water supplies.

ACKNOWLEDGEMENTS

Thank you Maddy, for always being in my corner through thick and thin. You have helped me become a much better scientist and grow as person. Thank you Cayelan, for supporting my research, giving me an opportunity to contribute to your research group, and helping to me to become a much better writer, collaborator, and scientist. Thank you Adil and Don, for the memorable insight and comments that helped to elevate the engineering and geochemical aspects of my dissertation and for keeping me sharp at our committee meetings.

My PhD research would have been dull and monotonous without Zach Kiracofe's coolness, Alex Gerling's hard-working free spirit, Jon Doubek's organic flow, Kate Hamre's edgy quips and genuine caring, Ryan McClure's seriously intense goofiness, Mary Lofton's great smile and attitude, Charlotte Harrell's interesting stories, and Chris Chen's most excellent nature and likeability.

I would also like to thank Denise Levitan, Katie Krueger, Maddie Ryan, Mariah Haberman, Mariah Redmond, Kevin Bierlein, Quinn Hull, Spencer Klepatzki, Chelsea Delsack, Brady Ziegler, Tiffany VanDerwerker, Amanda VanHaitsma, Bobbie Niederlehner, Athena Tilley, Jeff Parks, Durelle Scott, and John Little for support in the field, lab, office, or conference room.

This work would not have been possible without the support from Dominion Power, American Electric Power, the Virginia Department of Environmental Quality, and the Western Virginia Water Authority. I would also like to thank the Geological Society of America's Student Research Grant, the Institute for Critical Technology and Applied Science at Virginia Tech, Virginia Tech Global Change Center, Fralin Life Sciences

Institute, the Graduate School at Virginia Tech, and the Department of Geosciences for financial support.

I would like to thank my ma and my gma for all the love and support; you gals are one of a kind. Above all else, I would like to thank my gorgeous, loving Shmu; I can't imagine the malnourished wretch I would be without you.

TABLE OF CONTENTS

LIST OF TABLES

LIST OF FIGURES

CHAPTER 1. INTRODUCTION

Globally, surface waters (rivers, swamps, and lakes) comprise ~0.3% of Earth's water (Fetter, 2000), yet it is estimated that surface water sources supply more than 60% of the fresh water withdrawn for human use (Wada et al., 2014). Between 1990-2010, increasing human populations and economic development resulted in a ~1% increase in global surface water withdrawals per year, and combined with the effects of climate change, these drivers are expected to continue to increase demands on surface waters over the foreseeable future (Vörösmarty et al., 2000). Compounding the difficulty of meeting the growing demands placed on surface water resources is the fact that many surface water systems also have water quality that is impaired (i.e., the physical, chemical, or biological composition of the water adversely effects its beneficial use; (Krenkel, 2012). Considering that water quality deterioration can have negative economic impacts or be deleterious to human health (World Health Organization, 2004), effective water quality management is central to the discussion of sustainable surface water use.

In the United States, there are over 100 drinking water standards that are used in regulating water treatment and pollutant discharge practices (United States Environmental Protection Agency, 2016a, 2016b), and similar water quality guidelines exist globally (World Health Organization, 2004). While it is technologically feasible to remove many contaminants during water treatment, a preventive approach is often economically preferable but needs to account for the watershed characteristics (e.g., the geology, hydrology, and anthropogenic activity) that govern the pathway of contaminants towards the water treatment facility (World Health Organization, 2004). Such considerations are essential for characterizing possible contaminant sources, their distribution between solid and aqueous phases, and the reactions that drive their

geochemical cycles in the watershed (Krenkel, 2012). Among the diverse group of water contaminants, iron and manganese are unique in that they are widespread in surface water environments (Hem, 1963; Jones and Bowser, 1978; Smith et al., 2013; Stumm and Lee, 1960), commonly reach problematic levels in surface waters used for drinking water (Kohl and Medlar, 2006; Sommerfeld, 1999), and their geochemical cycles have broad implications for water quality by influencing the availability of phosphorus and trace metals (e.g., arsenic and cadmium; Amirbahman et al., 2003; Appelo and Postma, 2005; Balistrieri et al., 1994; Olivie-Lauquet et al., 2001; Orihel et al., 2015).

Iron (Fe) and manganese (Mn) are redox-sensitive metals that constitute ~5% and ~0.1% of the mass of Earth's crust on average, respectively, as major constituents in Fe- and Mn-minerals and as minor constituents in minerals such as pyroxenes, amphiboles, and olivines (Hem, 1963). Within these minerals, Fe and Mn can exist in both oxidized (Fe^{3+}, Mn^{3+}, and Mn^{4+}) and reduced (Fe^{2+} and Mn^{2+}) forms. The oxidized forms of Fe and Mn have low aqueous solubility and are generally favored in waters with near-neutral pH and dissolved oxygen (DO) concentrations that are in equilibrium with atmospheric oxygen (typical of many streams and shallow lakes; Hem, 1972). However, the reduced forms of Fe and Mn are favored in oxygen-poor or acidic waters, and being water soluble, commonly achieve much higher concentrations than the insoluble, oxidized forms (>0.5 mg/L; Davison, 1993). Not surprisingly, surface waters that develop reducing or acidic conditions either permanently or ephemerally are prone to chronic water quality issues related to Fe and Mn accumulation.

With more than 300 million lakes, ponds, and impoundments globally, these surface water systems represent a major resource for both developed and developing

societies (Downing et al., 2006). In many lakes and reservoirs, the water column develops seasonal density stratification that can lead to anoxia in deeper water strata; when respiration exceeds photosynthesis in isolated water strata, DO will become depleted causing the formation of reducing conditions. Numerous studies have characterized the redox cycles of Fe and Mn in response to internal changes in lakes and reservoirs, where reducing conditions are conducive for the release of metals from the sediments into the water column and oxygenated conditions favor metal oxidation (Aguilar and Nealson, 1998; Beutel et al., 2008; Burdige, 1993; Davison, 1993; Hongve, 1997; Johnson et al., 1995; Lerman et al., 1995; Löfgren and Boström, 1989; Zaw and Chiswell, 1999). However, many difficulties in predicting the cycles of Fe and Mn still persist relating to the complex interactions of abiotic and biotic processes involved in lake and reservoir metal cycles, the relative importance of external watershed and internal metal sources on water quality, and the influence of reservoir dynamics on downstream water quality in dammed river environments.

1. RESEARCH OBJECTIVES

My dissertation investigates the sources and cycles of Fe and Mn in surface water environments used for drinking water supplies. The dissertation is divided into three chapters and focuses on interpreting hydrologic and geochemical data collected in western Virginia, United States in the context of water resource management. The field sites examined in this study are actively used as human water supplies and have historical problems with Fe and/or Mn.

1.1. SOURCES AND FATES OF MANGANESE AND IRON IN A DAMMED RIVER

Chapter 2 examines the sources of Fe and Mn to the Roanoke River in the reach between the Smith Mountain Pumped Storage Project and Kerr Reservoir. This study

uses geochemical and hydrologic data collected in Leesville Lake (which feeds the Roanoke River via Leesville Dam releases), the Roanoke River, and the tributaries to the Roanoke River to assess how the concentrations of Fe and Mn to the Roanoke River change along the watershed in response to varying climatic and hydrologic conditions. A version of this chapter was submitted for publication in Hydrological Processes and is under review.

1.2. THE RESPONSE OF IRON AND MANGANESE CONCENTRATIONS TO HYPOLIMNETIC OXYGENATION IN A SHALLOW RESERVOIR

Chapter 3 investigates the response of Fe and Mn concentrations in a shallow drinking water reservoir to hypolimnetic oxygenation. A hypolimnetic oxygenation system was installed in Falling Creek Reservoir, Virginia, United States to mitigate water quality issues related to hypolimnetic anoxia. Over a two-year period, we manipulated redox conditions in the water column of Falling Creek Reservoir via operation of the hypolimnetic oxygenation system. In this study we used geochemical data collected in the reservoir and laboratory incubation experiments to characterize the effects of DO concentrations and microbial oxidation on Fe and Mn oxidation and removal. A version of this chapter is in review in Water Research.

1.3. INTERNAL AND EXTERNAL CONTROLS ON IRON AND MANGANESE DYNAMICS IN A SHALLOW, EUTROPHIC RESERVOIR

Chapter 4 considers the role of external and internal processes in influencing the exchange of Fe and Mn between reservoir sediments and the water column and how watershed dynamics affect the retention of metals in the reservoir. In this study, we calculate a metals budget in Falling Creek Reservoir to show the relative influence of external and internal loadings to the hypolimnion budget over time, how these loadings are influenced by watershed hydrology and reservoir redox conditions, respectively, and

what conditions are expected to result in metal accumulation in the reservoir. A version of this chapter is in preparation for publication in Applied Geochemistry.

1.4. DISSERTATION SUMMARY AND FUTURE RESEARCH

Chapter 5 synthesizes the findings in Chapters 2-4 and outlines the key areas where additional research is needed to advance the science.

CHAPTER 2. SOURCES AND FATES OF MANGANESE AND IRON IN A DAMMED RIVER

Zackary W. Munger, Madeline E. Schreiber, Thomas D. Shahady
A version of this chapter was submitted for publication in Hydrological Processes and is under review

ABSTRACT

We examined the seasonal variability of manganese (Mn) and iron (Fe) concentrations in a eutrophic, hydropower reservoir and the downgradient river that is fed by water released from the dam over a two-year period. During the stratified period, we observed elevated Mn and Fe concentrations in the reservoir and dam tailrace, which persisted 1-2 months after reservoir turnover. Using discharge and concentration measurements, we calculated a metals mass balance in the 18 km reach downgradient from the dam and found that Mn exhibited a moderate net mass loss (44% of reach inputs) and Fe exhibited minor losses (11% of reach inputs) across this reach during the stratified period. When the reservoir was destratified, Mn concentrations in the dam tailrace were generally lower than when the reservoir was stratified. In contrast, Fe concentrations in the tailrace were elevated during winter and early spring from higher particulate loads entering the reservoir during snowmelt. During the well-mixed period there was no pattern of metal mass loss in the mass balance reach. Further downgradient (>18 km from the dam) we observed increases in Mn and Fe concentrations during all times of the year that were related to suspended particle concentrations that were positively correlated with river discharge. Overall, we found that reservoir stratification was a strong predictor of Mn and Fe concentrations in the dam tailrace but Fe concentrations in the tailrace were also influenced by discharge from the dam. Downgradient of the tailrace, discharge in the river and suspended sediment were the

dominant predictors of both Mn and Fe concentrations. Our model of the temporal and hydrologic drivers of metal concentrations can be applied to other rivers downgradient from seasonally stratified reservoirs.

2. INTRODUCTION

Dams are common and widespread features on the hydrologic landscape, constructed to meet the needs for water supply, electricity demands, flood control and recreation (World Commission on Dams, 2000). Construction of hydropower dams, primarily in developing countries, is expected to increase the world's hydropower electricity capacity by more than 70% over the next 10-20 years (Zarfl et al., 2015). Although dams provide many benefits, they also have environmental consequences to rivers, including disrupting ecological connectivity (Ward and Stanford, 1995), inhibiting sediment transport (Anselmetti et al., 2007; Dai and Liu, 2013) and increasing concentrations of metals such as manganese (Mn) and iron (Fe) downgradient of the dam (Ashby et al., 1999; Dortch and Hamlin-Tillman, 1995; Gordon, 1989; Gordon et al., 1984; Hess et al., 1989).

Elevated concentrations of Mn and Fe cause issues with drinking water discoloration, staining, taste and odor (Sommerfeld, 1999). The World Health Organization (WHO) recommends guidelines for Mn and Fe at 50 μg/L and 300 μg/L, respectively to maintain acceptable water quality (World Health Organization, 2004). Sediments are typically the dominant source of Mn and Fe to most surface waters (Zaw and Chiswell, 1999). At the neutral, oxic conditions typical of most shallow surface waters (Smith et al., 1987), Mn and Fe are present in sediments as insoluble forms, commonly hydroxide and oxide minerals (Gordon et al., 1984). However, reducing conditions commonly develop in thermally stratified reservoirs, which promotes the reductive dissolution of Mn and Fe from the sediments and metal accumulation in the water column (Davison, 1993). In dammed rivers, water released via the dam intake

structures can also be a source of Mn and Fe when the upgradient reservoir is thermally stratified (Ashby et al., 1999).

Reservoir water released from the dam is typically in disequilibrium with respect to temperature (Dripps and Granger, 2013), pH, DO (Ashby et al., 1999) and sediment load (Anselmetti et al., 2007; Dai and Liu, 2013) in river environments, and rapid changes are often observed downgradient from the dam (Baxter, 1977; Kurunc et al., 2006; Wei et al., 2009). For example, decreasing Mn concentrations downgradient from hydropower dams have been attributed to Mn precipitation onto stream sediments (Dortch and Hamlin-Tillman, 1995), sorption (Gordon et al., 1984; Hess et al., 1989) or settling of oxidized particulates (Ashby et al., 1999). Manganese and iron concentrations are also influenced by physical processes, such as changing flow conditions that can dilute metal concentrations via metal-poor inflows or increase metal concentrations via entrainment of watershed sediments (Ashby et al., 1999; Zhang and Huang, 1993).

A major hurdle to evaluating the relative importance of physical and chemical influences on metal concentrations in a dammed river is obtaining data with adequate temporal and spatial resolution. Previous work has largely consisted of monitoring data for limited time range (span of 2-3 months) or reach length (<25 km), making it difficult to interpret the temporal and spatial patterns of Mn and Fe concentrations. Because reservoir stratification is likely an important influence on metal concentrations in dam tailraces, evaluating temporal changes in reservoir metal concentrations, paired with observations in the river, is critical. In this study, we sought to address the temporal and spatial drivers of Mn and Fe concentrations in a dammed river by 1) investigating the influence of seasonal and inter-annual variability in the reservoir on river water quality;

2) conducting a mass balance for Mn and Fe in the 18 km reach downgradient of the dam; and 3) characterizing the changes to water quality that occur across the watershed in response to hydrologic and reservoir conditions. The overarching goal of the study is to link reservoir dynamics to river water quality in dammed river watersheds and interpret the contribution of reservoir-generated and river-generated processes to Mn and Fe cycles.

3. METHODOLOGY

3.1. FIELD SITE

Fieldwork for this study was conducted in the Roanoke River watershed in Virginia, within the southeastern United States (Figure 2.1). The Roanoke River originates in Ordovician age sedimentary rocks of Virginia's Valley and Ridge Province and flows through the Proterozoic rocks of the Blue Ridge Province before entering Smith Mountain Lake, which lies on the western extent of the Piedmont Province. The Piedmont is comprised of Precambrian to Paleozoic igneous and metasedimentary rocks (Espenshade, 1954). The Roanoke River is dammed by the Smith Mountain Project, a pumped-storage hydropower facility comprised of Smith Mountain Dam and Leesville Dam. Leesville Lake is a long, narrow reservoir that is the source of water for the Roanoke River downgradient of the Smith Mountain Project. The maximum depth of Leesville Lake is at an elevation of 166 m above mean sea level (AMSL) and full pond is 187 m AMSL, though water levels in Leesville Lake can fluctuate up to 3 m per day due to pumpback into Smith Mountain Lake (Simmons JR, 1976). Water is withdrawn from two intakes that are 5.8 m in diameter and located at an elevation of 177 m AMSL. Water is released hourly from Leesville Dam into the Roanoke River to meet downgradient flow requirements.

Approximately 15 km downgradient of Leesville Dam, the Roanoke River traverses the southern extent of the James River-Roanoke River Manganese District (JRRRMD). The geology in the JRRRMD is characterized by meta-sedimentary and meta-igneous rocks of late Precambrian to early Paleozoic age. The ores in the JRRRMD are comprised of Mn and Fe-oxides that are reported to be as high as 30% Mn by weight, although a few weight percent is more typical (Espenshade, 1954).

3.2. WATER SAMPLE COLLECTION AND ANALYSIS

We collected data for this study as part of three campaigns: 1) quarterly water sampling at monitoring sites along the Roanoke River and three of its major tributaries between November, 2012 and November, 2014; 2) monthly water sampling in Leesville Lake near Leesville Dam, three sites in the Roanoke River and a major tributary between April-October, 2014 and 3) water sampling and flow monitoring in seven major tributaries in the Roanoke River watershed during a two-day period in July, 2013.

Water samples collected in the river were obtained using a depth-integrating sampler (DH-81) with a 1 L polytetrafluoroethylene bottle (Edwards and Glysson, 1999). At each monitoring site, samples were collected at one location, as close to the thalweg as possible, accessed either by wading or using an inflatable kayak. During sample collection, the depth-integrated sampler was lowered and raised at a steady pace so that 1 L volume was filled by the time the sampler was raised to the water surface (Edwards and Glysson, 1999). Samples were collected along a transect across the width of the river during two sampling events to quantify the variability in Mn and Fe concentrations across the channel. At each sampling site, 2 L of water were collected and divided into two aliquots. A portion of the first 1 L aliquot was partitioned into polyethylene containers for raw sample analyses and the remainder filtered (0.45 μm nylon membrane) in the field

and stored in polyethylene or glass containers for soluble sample analyses. Raw and filtered samples for metals and dissolved organic carbon (DOC) analysis were preserved by lowering the pH to <2 with the addition of nitric and hydrochloric acid, respectively. The other 1 L aliquot was used for the measurement of total suspended sediment (TSS) by filtering water through glass microfiber filters (1.5 μm), drying the filters in an oven (40 degrees C for 48 hours) and measuring the retained mass per volume of water collected.

Raw and filtered samples were analyzed for Mn and Fe using graphite furnace atomic absorption spectrometry (GFAA) or inductively-coupled optical emission spectroscopy (ICP-OES). Filtered samples were also analyzed for sodium (Na), potassium (K), magnesium (Mg) and calcium (Ca) by ICP-OES; chloride (Cl) and sulfate (SO4) using ion chromatography; DOC using a carbon analyzer and alkalinity using titration following the inflection point method (Rounds and Wilde, 2001).

Water samples collected in the water column of Leesville Lake were obtained using a Kemmerer-type sampler (1.2 L polyacrylonitrile; (Lane et al., 2003). Samples were collected from the surface and at three to seven depths from 3 m to the sediment-water interface. These samples were analyzed for Mn, Fe and Ca using ICP-OES for raw and filtered (0.45 μm) aliquots as described above. Temperature, conductivity, pH and DO depth profiles were collected monthly (April-October, 2014) to a depth of 14 m using a Hydrolab Quanta probe.

In July, 2013, samples were collected from seven of the major tributaries to the Roanoke River between Leesville Lake and Kerr Reservoir and at locations in the Roanoke River bracketing the confluence of these tributaries. In addition to water

samples, discharge was measured in six of the tributaries using a Teledyne RDI StreamPro acoustic Doppler current profiler (ADCP). Four velocity profiles were collected at each of the tributary monitoring sites to calculate the mean flow.

For ease of discussion we have divided the study reach into three sections: 1) the 18 km reach between Leesville Dam and Altavista which we will refer to as the mass balance reach (MBR), 2) the 92 km reach between Altavista and Randolph which we refer to as the mid-section reach (MIDR) and 3) the 44 km reach between Randolph and Clarksville which we refer to as the downgradient reach (DGR) (see Figure 2.1).

3.3. MASS BALANCE CALCULATIONS

One of the goals of mass balance was to examine whether Mn and Fe concentration changes in the river can be attributed to mass loss or to dilution from inflows with lower metal concentrations. To do this, we conducted a mass balance for both water and metals in the reach between Leesville Dam and Altavista (MBR) (Figure 2.2). Discharge and water sample measurements in Leesville Dam tailrace (<0.5 km downgradient of Leesville Dam), Goose Creek tributary (5.5 km downgradient from Leesville Dam) and at the Altavista monitoring site (18 km downgradient) were used in the mass balance following the method in (Brown et al., 2007). In addition to these water sources, there are several minor, ungaged surface water inputs to the mass balance reach (see Figure 2.2) that were not sampled in this study. We conducted a water mass balance to quantify the input from these additional surface water inputs (Q_{asw}) to the mass balance reach, which we will refer to as ASW in the text, using Equation 1:

$$Q_{asw} = Q_{downgradient} - Q_{dam} - Q_{tributary} \quad (1)$$

where $Q_{downgradient}$ is discharge measured in the Roanoke River at a USGS gaging station located one km upstream from the Altavista monitoring site, Q_{dam} is the mean hourly

discharge from Leesville Dam, which was provided by the dam operator, and $Q_{tributary}$ is discharge in Goose Creek, measured at a USGS gaging station located 17 km upstream from the Goose Creek monitoring site. We assumed that the additional water inputs to the reach were predominantly surface water based on the presence of ungaged streams entering the reach and groundwater Ca concentrations that were lower than expected for the ASW Ca loads (see Ca mass balance results). In July, 2013 the mean discharge under baseflow conditions was measured at the Goose Creek monitoring site using an ADCP. The results were within 10% of the value reported at the USGS station. We assumed for the other dates that discharge measured at the gaging station was an accurate approximation of flow at the monitoring site. The mean relative uncertainty of discharge measurements at USGS gauging stations is between 2.3 and 5.1% depending on the method employed at the station (Turnipseed and Sauer, 2010). For our data analysis, we used a relative uncertainty of 5.1%.

The metals mass balance was calculated to determine non-conservative changes in mass loading across the mass balance reach (ΔL_{reach}), using Equation 2:

$$\Delta L_{reach} = L_{downgradient} - L_{dam} - L_{tributary} - L_{asw} \quad (2)$$

where the loadings at each boundary were calculated using Equation 3:

$$L_i = C_{metal} \times Q_i \quad (3)$$

where C_{metal} is the Mn or Fe concentration measured at the downgradient, dam, and tributary boundaries. Metal concentrations measured in Leesville Dam tailrace were collected 200 m downgradient from the dam. The metal concentrations in Goose Creek were measured at the monitoring site situated 200 meters upgradient from the confluence

with the Roanoke River. The concentrations of Mn and Fe in Goose Creek were used as a proxy for concentrations in the ASW.

To assess the validity of our mass balance approach, a mass balance was calculated for Ca under the assumption that it behaves conservatively (Teefy, 1996). The uncertainty of the loading calculations was calculated using the standard error propagation formula (Ku, 1966):

$$\frac{\delta L}{L} = \sqrt{\left(\frac{\delta Q}{Q}\right)^2 + \left(\frac{\delta C}{C}\right)^2} \quad (4)$$

where $\delta L/L$ is the relative uncertainty of the calculated load, $\delta Q/Q$ is the uncertainty of the discharge measurements and $\delta C/C$ is the uncertainty of the metal concentration measurements. Water samples were collected along a cross-section transect in Leesville Dam tailrace in July, 2013 and at the Randolph monitoring site in October 2013. The concentration uncertainty used in Equation 4 was determined with the largest standard error calculated from the results of the two transects.

3.4. STATISTICAL ANALYSES

To quantify the relationship between metal concentrations and independent predictors such as total suspended sediment and discharge, multiple regression analyses were performed using standard methods described in (Davis and Sampson, 1986). Where there is correlation between independent predictors, simple linear regressions were used instead of multiple regression.

For comparing Fe to Mn mass ratios between the soil and water compartments we first tested whether the differences in the mass ratios of these compartments were statistically different using the Mann-Whitney test (Davis and Sampson, 1986).

4. RESULTS

4.1. SPATIAL VARIABILITY OF MN AND FE IN THE ROANOKE RIVER AND TRIBUTARIES

4.1.1. MANGANESE

Over the two year monitoring period, total Mn exhibited a range of concentrations in the Roanoke River, with 20% of the 134 total Mn measurements exceeding 50 μg/L (50 μg/L is the WHO guideline for Mn; Figure 2.3). This concentration, which is applied to drinking water sources, is lower than the human health benchmark (0.3 mg/L) and that which is known to cause toxicity to fish, invertebrates and algae (adverse effects occur at soluble Mn concentrations exceeding 1.5 mg/L; (Peters et al., 2011). Since the Roanoke River is a drinking water source near Clarksville, VA, we will refer to the WHO guideline when discussing elevated Mn concentrations in our study site. Total Mn concentrations exceeding 50 μg/L occurred most frequently in Leesville Dam tailrace (38% of our measurements) and at the downgradient extent (DGR) of the study reach (45%). In the mid-section (MIDR) of the study reach, total Mn concentrations rarely exceeded 50 μg/L (11%), including periods when Mn concentrations in Leesville Dam tailrace were greater than 50 μg/L.

With respect to the tributaries to the Roanoke River, total Mn concentrations exceeded 50 μg/L in 38% of our measurements, but also displayed variability between tributaries (Figure 2.3). Samples collected in Cedar Creek, which joins the Pigg River before flowing into Leesville Lake, exceeded 50 μg/L in 50% of our measurements, while total Mn in Goose Creek, which enters the Roanoke River approximately 5 km downgradient of Leesville Dam, never exceeded 50 μg/L. Total Mn concentrations in the Dan River, near the southeastern extent of the watershed, were frequently higher than the other tributaries (89% >50 μg/L). Data from six additional tributaries sampled during our

July, 2013 sampling campaign support a trend of increasing total Mn concentrations southeastward in the watershed, as shown in Figure 2.3.

4.1.2. IRON

Overall, 33% of 124 river measurements for total Fe exceeded 300 μg/L (WHO guideline; Figure 2.3). Total Fe concentrations in Leesville Dam tailrace were consistently lower than downgradient sites in the Roanoke River. Downgradient of Leesville Dam tailrace, total Fe concentrations exhibited an increasing pattern that culminated in the highest total Fe concentrations occurring at the southeastern extent of our study site. Total Fe concentrations in the tributaries were often elevated relative to the Fe concentrations measured in the Roanoke River (73% of the tributary measurements exceeded 300 μg/L).

4.1.3. IRON-TO-MANGANESE MASS RATIOS IN THE ROANOKE RIVER WATERSHED

Using our data, we calculated the mass ratio of total Fe to total Mn in the water compartments of Leesville Lake, Leesville Dam tailrace, the Roanoke River downgradient of Leesville Dam tailrace and the tributaries and compared them to the Fe/Mn mass ratios in watershed soils using data from (Smith et al., 2013); Figure 2.4). Using the Mann-Whitney test we determined that the Fe to Mn ratios in each of the water compartments were significantly different than the soil compartment at 0.05 significance level. The median ratio of Fe to Mn in Leesville Lake was the lowest, and similar to the ratio in Leesville Dam tailrace. The mass ratio increased in the Roanoke River downgradient of the tailrace, likely due to the influence of tributaries, which had the highest ratio among the water compartments. The watershed soils had a mass ratio that was approximately double that of the tributaries.

4.2. TEMPORAL VARIABILITY OF MN AND FE IN LEESVILLE DAM TAILRACE

4.2.1. MANGANESE

Total Mn concentrations measured in Leesville Dam tailrace varied from 5-151 μg/L and exhibited seasonal concentration patterns (Figure 2.5). The highest total Mn concentrations measured in the tailrace occurred in October and November 2012 and between July-November 2014. In 2013, the total Mn concentrations were substantially lower than in 2012 and 2014, never exceeding 50 μg/L.

At Altavista, about 18 km downgradient from Leesville Dam and at the end of the mass balance reach, total Mn exhibited a narrower range of concentrations (5-65 μg/L) and did not exhibit a clear pattern of seasonal variation (Figure 2.5).

4.2.2. IRON

Total Fe concentrations measured in Leesville Dam tailrace varied from 7-400 μg/L, with the highest concentration measured on February 25, 2014 (Figure 2.5). Total Fe concentrations in the tailrace were very similar to the total Mn concentrations measured between May-November in 2014 and higher than total Mn in 2013. However, the elevated total Fe concentrations measured in winter-spring were not also observed in the total Mn data which typically exhibited the lowest concentrations during winter-spring.

At Altavista, total Fe concentrations were also highest during winter-spring and decreased later in the year, exhibiting the lowest concentrations between September-November (Figure 2.5).

4.3. TEMPORAL VARIABILITY OF MN AND FE IN LEESVILLE LAKE

4.3.1. MANGANESE

Total Mn concentrations exhibited seasonal patterns in the water column of Leesville Lake, with low total Mn concentrations (<30 μg/L) throughout the water column during spring and early summer, 2014. As the summer progressed, total Mn concentrations in deeper regions of Leesville Lake increased, reaching a maximum of 406 μg/L (15 m depth) in July (Figure 2.6). Increases in Mn concentrations near the bottom of the reservoir occurred concurrently with the development of hypoxic (DO <2 mg/L) conditions in the benthic region of Leesville Lake, during thermal stratification from late spring-summer (Figure 2.7). After Leesville Lake turned over in September, mixing of metal-rich benthic waters caused total Mn concentrations to increase at shallower depths in the water column. Elevated concentrations were measured throughout the water column in late October, more than a month after turnover.

4.3.2. IRON

Total Fe concentrations in Leesville Lake generally exhibited patterns similar to Mn, with 1) concentrations in the hypolimnion increasing as the stratified period progressed in late summer and 2) mass spreading to shallower depths after turnover. However, in contrast to Mn, the highest total Fe concentrations in Leesville Lake were measured in April 2014 prior to reservoir stratification (Figure 2.6). These high concentrations are concurrent with elevated dam release flows that occurred between February and April, when flow through the reservoir was 2-3 times higher than other times in the remainder of 2014. Total Fe concentrations in Leesville Lake also exhibited patterns similar to Mn, with concentrations in deeper, low DO regions increasing as the stratified period progressed and increases at shallower depths after turnover.

4.4. WATER BALANCE IN THE MASS BALANCE REACH

The results from the water mass balance in the mass balance reach are shown in Figure 2.8. During the two-year period, Leesville Dam releases were the largest water source to the reach (70-94% of the flow leaving the reach); typical discharge from Leesville Dam varied from 14-35 m3/s. However, much higher discharge (>70 m3/s) from the dam was released during periods encompassing two of our sampling events, May 21, 2013 and February 25, 2014, in response to rainfall and snowfall that occurred in the week preceding each event. Discharge entering the reach from the major tributary, Goose Creek, varied from 2-10 m3/s and represented 6-12% of the flow at the downgradient boundary. Peaks in discharge from Goose Creek were also observed during May 21, 2013 and February 25, 2014 monitoring events.

The difference in discharge between the measured inflows from Leesville Dam and Goose Creek and the measured outflow at Altavista was used to quantify the discharge entering the reach from the ungaged tributaries (additional surface water, Q_{asw}) using Equation 1). The magnitude of the Q_{asw} term varied from -0.01 to 17 m^3/s which accounted for up to 22% of the flow at Altavista.

4.5. METALS MASS BALANCE

4.5.1. CALCIUM

The results for the Ca mass balance are shown in Figure 2.8. We used the Ca mass balance to estimate the Ca concentrations in the ungaged tributaries (ASW) by solving Equation 3 for C_{metal}. The L_{asw} term that was used in Equation 3 was obtained by solving Equation 2 for L_{asw}, assuming the change in Ca load in the mass balance reach (ΔL_{reach}) was equal to 0 (treating Ca as conservative). The calculated Ca concentration in the ASW varied from 10-22 mg/L and had a median concentration of 15.7 mg/L, similar to the median Ca concentration in Goose Creek (15.4 mg/L). We also explored the possibility

that the ASW had a groundwater component by examining groundwater Ca data in the Roanoke River watershed from the STORET database (STORET, 2015). The majority of groundwater Ca concentrations in the southeastern portion of the upper Roanoke River watershed (which includes Smith Mountain Lake, Leesville Lake and the mass balance reach) were less than 10 mg/L. However, there was only one groundwater observation within 5 km of the mass balance reach. Based on the low groundwater Ca concentrations and similarity between the estimated Ca for the ASW and Goose Creek, we assumed that the ASW component could be considered a surface water source.

Leesville Dam and Goose Creek contributed 74-97% and 3-12% of the Ca mass, respectively. Similar to the water balance, the largest Ca loads observed in the reach during the study occurred on May 21, 2013 and February 25, 2014. The good agreement between the Ca loads entering and leaving the reach suggests that the mass balance accounts for the major sources of metals to the reach.

4.5.2. MANGANESE

To conduct the Mn mass balance, we first had to calculate the Mn load in the ASW. Because Mn is expected to behave non-conservatively, we could not use the same approach used in estimating Ca concentrations. Our best estimate of a representative Mn concentration in these tributaries was our measurements in Goose Creek, the only sampled tributary in the mass balance reach. Using Goose Creek as a proxy for the ASW, the mean contribution of the ASW component was 8% of the Mn loads input to the mass balance reach. Our results show a net loss of Mn mass in events between July-November (Figure 2.8), which was during the stratified period or after turnover when Mn concentrations in the tailrace were elevated. Elevated loads from Leesville Dam were

also observed in the May 21, 2013 and February 25, 2014 monitoring events due to elevated discharge from the dam, however, no Mn loss was observed on these dates.

4.5.3. IRON

The Fe mass balance was conducted similarly to the Mn balance, using the Fe concentrations in Goose Creek as a proxy for the ungaged tributaries (ASW). Results of the mass balance show that Fe loading in the reach exhibited seasonal variability similar to the Mn mass balance, with net loss of Fe mass loading occurring between August-November (Figure 2.8), although the Fe mass loss (mean change in mass across the reach was -11%) had a much weaker signal of loss than that calculated for Mn (-44%). There were two main differences between the Fe and Mn balances. First, the mean contribution of the ASW component to the Fe loads input to the reach (28%) was much higher than the contribution for Mn (8%). Second, there was a net loss of Fe mass loading in February, 2014, when Fe concentrations in Leesville Dam tailrace were the highest during the year. The Fe loads calculated on February 25, 2014 were by far the highest among all the sampling events due to the elevated discharge from Leesville Dam and Goose Creek and high Fe concentrations in Leesville Lake and tributaries.

4.6. TOTAL SUSPENDED SEDIMENT CONCENTRATIONS IN THE ROANOKE RIVER AND ITS TRIBUTARIES

Total suspended sediment was low in Leesville Dam tailrace in comparison to measurements further downgradient in the Roanoke River and in the tributaries (Figure 2.9). The range of TSS generally increased along the flowpath of the Roanoke River with the highest TSS observed in the downgradient reach. In the tributaries, TSS displayed large variability that was positively correlated with discharge (r-squared=0.54; p-value=0.0005; Goose Creek shown in Figure 2.9). There was no correlation between TSS and discharge in Leesville Dam tailrace, but downgradient of the tailrace, in the Roanoke

River, there was a strong, positive correlation between TSS and discharge (r-squared=0.69; p-value=7×10^{-13}).

4.7. RELATIONSHIP OF MN AND FE WITH DISCHARGE AND TSS

4.7.1. MANGANESE

The relationship of total Mn concentrations in Leesville Dam tailrace, the Roanoke River and Goose Creek with discharge (discharge from Leesville Dam represents the Q in the tailrace, river discharge represents Q elsewhere) and TSS is shown in Figure 2.10. Total Mn concentrations in Leesville Dam tailrace were not correlated with dam discharge or TSS. A multiple regression analysis was conducted to examine the dependence of total Mn on discharge and TSS. Our results indicate that there is a positive relationship between the variance in total Mn, river discharge and TSS (multiple r-squared=0.51; p-value=2×10^{-7}) in the Roanoke River. Because discharge and TSS are strongly collinear in the Roanoke River, we also conducted simple linear regressions between total Mn, discharge and TSS, which suggested that both discharge (r-squared=0.35) and TSS (r-squared=0.51) are statistically significant predictors (p-values $<<0.05$) of total Mn concentrations. Correlation between total Mn, dam discharge and TSS was not observed in Leesville Dam tailrace. In Goose Creek there was a strong positive relationship between total Mn, discharge and TSS (multiple r-squared=0.76; p-value=0.002) and both discharge and TSS were statistically significant predictors (p-values $<<0.05$).

4.7.2. IRON

There was a positive correlation between total Fe concentrations, discharge and TSS (multiple r-squared=0.40; p-value=5×10^{-5}) in the Roanoke River (Figure 2.10). Simple linear regressions indicate that both discharge (r-squared=0.37) and TSS (r-

squared=0.36) were statistically significant (p-values <<0.05). In contrast to Mn, total Fe concentrations in Leesville Dam tailrace were positively correlated with dam discharge and TSS (multiple r-squared=0.69; p-value=0.005), however the influence of dam discharge on total Fe in the tailrace was not statistically significant (p-value=0.13; Figure 2.10). In Goose Creek there was a strong positive relationship between total Fe, discharge and TSS (multiple r-squared=0.69; p-value=0.009) and both discharge and TSS were statistically significant predictors (p-values <<0.05).

5. DISCUSSION

5.1. INFLUENCE OF SEASONAL RESERVOIR CONDITIONS ON DAM TAILRACE AND RIVER MN AND FE CONCENTRATIONS

Total Mn and Fe concentrations in Leesville Dam tailrace were linked to the seasonal stratification of Leesville Lake. During the stratified period between June-September 2014, we observed an increase in total Mn and Fe in the hypolimnion of Leesville Lake that coincided with lower hypolimnetic DO concentrations. As warmer air temperatures prevail in summer, the thermal gradient in the reservoir strengthens and inhibits the transport of DO from the photic zone to deeper, respiration dominated zones where there is net consumption of DO (Horne and Goldman, 1994). Between May-August 2014, Mn and Fe concentrations increased in Leesville Dam tailrace, corresponding with the higher metal concentrations observed in the lake during the stratified period. Patterns of both reservoir stratification and tailrace metal concentrations were different in 2013; milder temperatures and increased dam release flows in spring and early summer 2013 contributed to the weaker stratification and higher DO observed in 2013 compared to 2014. In 2013, DO in Leesville Lake remained above 5 mg/L until August; this higher DO coincided with Mn concentrations in the dam tailrace that did not

exhibit much seasonal variation and were much lower than in 2014. Iron concentrations in the tailrace also did not exhibit any increases during the stratified period in 2013.

After reservoir turnover in September 2014, vertical mixing caused the metal mass to redistribute in the water column, resulting in lower Mn and Fe concentrations in benthic zones and higher concentrations in shallower zones. Elevated total Mn and Fe concentrations were measured throughout the water column in October, indicating that elevated metal concentrations can persist for at least a month after the end of the stratified period, even under oxic (DO >5 mg/L) conditions. As a result, Mn and Fe concentrations in the dam tailrace also remained elevated between September-November 2014. This pattern was also observed for October-November 2012. Not surprisingly, the low Mn concentrations measured during the stratified period in 2013 carried over into the turnover period and for Fe there was little change in concentrations between the stratified and turnover period in 2013.

During winter and spring, after the turnover period and before stratification, the water column was oxic and well-mixed. Under these conditions, Mn and Fe in reservoir sediments are stable as insoluble, oxidized forms (Davison, 1993) resulting in lower concentrations of Mn and Fe in the water column compared to the stratified period. Although reductive dissolution of Mn and Fe can occur in reservoir sediments even when the water column is oxic (Bryant et al., 2011), the presence of oxygen near the sediment-water interface has been shown to suppress the release of soluble Mn and Fe from the sediments into the water column (Bryant et al., 2011; Davison, 1993; Gantzer et al., 2009). As expected, Mn concentrations in Leesville Lake were low during this period. However, the highest total Fe concentrations measured in Leesville Lake occurred during

the well-mixed period in April, 2014. The lack of a concomitant increase in Mn concentrations and decrease in DO suggests that the mechanism driving the spike in total Fe in April is not redox-related. In April 2014, total Fe concentrations in Smith Mountain Dam tailrace were low, suggesting the Fe is entering Leesville Lake from tributaries or watershed runoff. Elevated Fe concentrations have been observed during winter and spring months in other reservoirs as a result of increased precipitation and snowmelt (Hongve, 1997; Zaw and Chiswell, 1999). Increased precipitation and several snowfall events occurred during winter-spring in the Roanoke River watershed and provide a possible explanation for the increases in reservoir Fe concentrations observed during this period. The increase in the Fe to Mn ratio in the reservoir during this period is consistent with suspension of watershed sediments, which have a higher Fe to Mn ratio than the reservoir when redox processes are the dominant source of these metals.

5.2. DRIVERS OF MN AND FE LOSS IN THE MASS BALANCE REACH

5.2.1. MANGANESE

The results from the mass balance show that Mn behaves non-conservatively once released into the river from Leesville Lake. Mass losses across the reach occur during the stratified period and after turnover (July-November). The pattern of Mn loss downgradient of the dam is consistent with the findings from previous studies that examined metal concentrations downgradient of hydropower dams in summer and fall (Ashby et al., 1999; Dortch and Hamlin-Tillman, 1995; Gordon, 1989; Hess et al., 1989). However, only a minor fraction of the Mn measured in Leesville Dam tailrace is in the soluble fraction (median soluble fraction is 19% during the stratified period; see Appendix), indicating that mass loss in the mass balance reach is predominantly of particulate Mn.

A number of factors contribute to the spiraling of particulates containing Mn and Fe, notably the particle size, flow velocity, channel depth and Fe/Mn fingerprint of channel sediments (Whiting et al., 2005), and a comprehensive analysis of the particle transport dynamics is beyond the scope of this study. However, the high-energy flows created by dam releases (Csiki and Rhoads, 2010) and pool-riffle sequences in the mass balance reach provide an environment for entrainment and reworking of the suspended particulates (Sear, 1996; Skalak and Pizzuto, 2010) and a possible explanation for the loss of particulate Mn mass. In Leesville Dam tailrace there is no correlation between total Mn and TSS because the concentration of Mn particulates is driven by reservoir conditions rather than TSS. However, once in the river, the particulates traverse erosional and depositional environments that could lead to deposition of some fraction of the reservoir-derived particulates and entrainment of channel-derived particulate Mn. (Whiting et al., 2005) examined the transport of suspended sediment in an upland river with flow characteristics similar to the Roanoke River and found that the transport distance of suspended particulates could be as short as 3 km due to the presence of quiescent zones (pools) along the flowpath. Our results show that the mass ratio of Fe to Mn in the Leesville Lake and Leesville Dam compartments is lower than the Roanoke River and soils compartments. Without significant changes to TSS concentrations we would expect Mn concentrations to decrease relative to Fe concentrations as dam release water approached equilibrium with those compartments (i.e. the fingerprint of suspended particulates shifts to a higher Fe to Mn mass ratio); these patterns are supported by our data.

During the well-mixed period in Leesville Lake, Mn concentrations in the tailrace are generally low and there is negligible net removal of Mn mass between the dam and Altavista. As long as watershed sediments are being entrained along the flowpath, there will be some baseline Mn concentration that will be supported by the river. When Mn concentrations from Leesville Dam are low and similar in magnitude to the baseline concentration, there will be negligible net mass loss. During higher flow events (such as the May, 2013 event), TSS in Leesville Dam tailrace exhibits little change, likely due to sediment retention by the dam, as has been observed at other dams (Anselmetti et al., 2007). However, between Leesville Dam and Altavista the TSS increased due to the higher energy flow. The increase in suspended sediment resulted in a substantial gain in Mn particulate mass and increase in Mn concentration across the reach.

5.2.2. IRON

Iron also behaved non-conservatively in the mass balance reach with a net loss in Fe mass between August-November and also in February, which are the times when total Fe concentrations in the tailrace are the highest. Interestingly, the Fe concentration between Leesville Dam and Altavista increases for several of these sampling events despite a net mass loss in the reach. This can be accounted for by the higher Fe concentrations in Goose Creek and the ASW. Compared to Mn (8% of inputs), the ASW has a much larger effect on the Fe mass balance (28% of inputs), which increases the uncertainty of the Fe loss calculations. However, Fe load estimates based on ASW Fe concentrations one tenth of the proxy estimate would only cause the February and August 27, 2014 events to shift from losing to gaining and the overall pattern of loss occurring between August-November would remain.

In comparison to Mn, the pattern of Fe loss between August-November is substantially weaker. In the tailrace, the relationship between Fe and TSS and lack thereof between Mn and TSS provides a possible explanation for the different behavior in the mass balance reach. Total Mn concentrations in Leesville Dam tailrace are much higher per unit TSS than the overall trend in the Roanoke River (see Figure 2.10). However, the relationship between total Fe and TSS in the dam tailrace is very similar to that observed in the rest of the Roanoke River, which suggests that particulate Fe concentrations do not need to change significantly to be in equilibrium with TSS-related Fe in Altavista (i.e. total Fe in the tailrace fall on the trendline for Roanoke River data in Figure 2.10). If the TSS remained constant, we would expect Mn mass to decrease and Fe mass to remain steady as the reservoir-derived particles approached equilibrium with channel-derived particles. In reality the TSS concentrations do not remain constant but we generally observe greater loss of Mn within the reach than Fe and when there is an increase in TSS, accompanying increases in Mn (that is partially offset by the equilibration of particles) and Fe.

5.3. INFLUENCE OF HYDROLOGY AND SEDIMENT LOADS ON MN AND FE CONCENTRATIONS IN THE ROANOKE RIVER

River channel discharge and TSS are drivers of total Mn and Fe concentrations in the Roanoke River, which is supported by the positive correlation between total Mn and Fe concentrations, river discharge and TSS downgradient from Leesville Dam tailrace (not including Leesville Dam tailrace measurements). The higher flow velocities that occur when discharge increases lead to larger hydraulic shear stresses that enhance the erosion and transport of sediments (Nearing et al., 1994) which are a source of particulate Mn and Fe to the river. However, the water compartment of the Roanoke River has an Fe

to Mn ratio that is lower than expected if metal particulates were entirely the result of entrainment of watershed soils (in that case the ratios would be approximately equivalent). One possible explanation is that the lower Fe to Mn ratio observed in the Roanoke River is the result of remobilization of reservoir-derived particulates, with lower Fe to Mn mass ratios, that had been previously sequestered in depositional zones of the sediment compartment.

We did not observe a correlation between total Mn, dam discharge and TSS in Leesville Dam tailrace. It is improbable that TSS represents a source of Mn in the Roanoke River but not in the tailrace; it is more likely that the strong influence of reservoir stratification on Mn concentrations is overwhelming the signal from discharge and entrainment of Mn-bearing sediments in the channel. Consistently low TSS concentrations measured in Leesville Dam tailrace, which are characteristic of the sediment retaining capabilities of dams (Anselmetti et al., 2007), also minimizes the channel-derived particulate Mn and Fe. Further downgradient, TSS increases as the sediment load approaches equilibrium with the carrying capacity of the river, which coincides with higher Mn and Fe concentrations.

The concentrations of total Fe in the tributaries were often higher than the Roanoke River even when TSS was not substantially higher, suggesting that the tributaries represent an important source of total Fe to the Roanoke River and that the suspended sediment in the tributaries has a higher concentration of particulate Fe than the Roanoke River.

5.4. TEMPOROSPATIAL MODEL OF MN AND FE CYCLING IN DAMMED RIVER WATERSHEDS

A conceptual model characterizing the temporal and spatial drivers of Mn and Fe concentrations in a dammed river watershed is shown in Figure 2.11 and described with respect to reservoir and flow conditions in the following sections. It is important to note that other watersheds may exhibit differences in the relative concentrations of Mn and Fe as a result of different reservoir conditions and watershed geology.

5.4.1. STRATIFIED RESERVOIR

During the stratified period in Leesville Lake, total Mn and Fe concentrations increase in the benthic region of the reservoir due to diffusive metal flux from anoxic sediments. Some of these metal-rich waters are released from the hypolimnion through dam intakes, resulting in elevated tailrace metal concentrations. Upon entering the tailrace the soluble fraction may be chemically removed via sorption or precipitation onto the channel substrate. However, in the case of the Leesville Dam tailrace, the majority of the metals are present in particulate form. In the mass balance reach, both Mn and Fe both exhibited a pattern of mass loss during the period of reservoir stratification. We are attributing this to mixing of reservoir and tributary-derived particulate Mn and Fe with channel-derived particles that generally had lower concentrations of Mn and Fe per unit mass TSS. Over the mid-section reach, there was little seasonal variability in Mn and Fe concentrations, suggesting that the reservoir influence on metal concentrations is negligible. Increases in Mn and Fe concentrations were measured in the downgradient reach that coincided with higher TSS concentrations, a relationship that is supported by positive correlation between Mn and Fe concentrations and TSS.

5.4.2. RESERVOIR TURNOVER

The conclusion of the stratified period is marked by reservoir turnover, when the surface and benthic layers of the reservoir mix, causing the upward transport of Mn and

Fe contained in deeper zones and downward transport of DO to the sediments. Over time the resupplied DO causes the oxidation of soluble metals to insoluble forms that settle out of the water column. After turnover, we observed the highest Mn concentrations in the tailrace although Fe concentrations were relatively steady during this period. There was a substantial decrease in Mn concentrations that accompanied mass loss and little variation for Fe concentrations with minor mass loss in the mass balance reach. Further downgradient there was negligible influence of seasonal reservoir conditions on metal concentrations; concentrations are instead influenced by the same hydrology and TSS driven patterns as during the stratified period.

5.4.3. WELL-MIXED RESERVOIR

During the well-mixed period the reservoir water column is oxic; Mn and Fe concentrations are generally low due to suppressed internal loading from an oxic sediment-water interface. Metal and TSS concentrations in the dam tailrace are also low, but increase downgradient from entrainment of channel-derived sediment and particulate Mn and Fe. Tributaries in the mass balance reach contribute to increases in metal concentrations observed in the reach. Further downgradient, increases to the metal concentrations are related to flow conditions and TSS in the river.

5.4.4. ELEVATED-RELEASE/FLOW CONDITIONS

Release flows in Leesville Dam (run-of-river) were generally linked to rainfall/snowfall in the watershed and, while these conditions could conceivably occur during any time of the year, during the monitoring period for this study, we observed seasonally high flows during the well-mixed period in winter and spring. Elevated dam releases coincided with the highest Fe concentrations that we measured in Leesville Lake. Combined with lake level fluctuations, the higher flows through the reservoir contributed

to the resuspension of littoral sediments and substantial increases in Fe concentrations. Elevated Fe in the reservoir during elevated flow release events resulted in the highest concentrations measured in the dam tailrace. At the Altavista site we also observed elevated Fe concentrations that exhibited little variation from tailrace concentrations. During these conditions we observed no substantial increase in Mn concentrations in the tailrace, presumably because of the higher concentration of Fe in the littoral sediment source. Downgradient from the mass balance reach we observed Mn, Fe and TSS concentrations that were elevated compared to low-flow conditions.

6. CONCLUSIONS

The results from our two year monitoring study indicate that: 1) seasonal reservoir stratification influences Mn and Fe concentrations in the dam tailrace. Elevated metal concentrations in the dam tailrace persist for 1-2 months after reservoir turnover, when mixing of the reservoir transports metal-rich benthic waters to shallower zones in the water column. Elevated Fe concentrations are also observed in the reservoir and tailrace during higher flow conditions in the well-mixed period due to remobilization of Fe-bearing lake sediments. 2) Total Mn and Fe mass is lost in the mass balance reach during the stratified period and after reservoir turnover. During periods of Mn mass loss we also observe substantial decreases in Mn concentrations. When the reservoir is well-mixed, there is no pattern of mass loss and metal concentrations are generally lower and exhibit little variation in the mass balance reach due to the absence of a redox-driven metal source. 3) Downgradient of the tailrace, there is negligible influence of seasonal reservoir conditions on metal concentrations in the river; metal concentrations in the mid-section reach and downgradient reach are positively correlated with river discharge and TSS where the entrainment of Mn and Fe-bearing sediments are a significant source of metals

to the river. 4) Reservoir conditions are the dominant influence on Mn and Fe concentrations in the dam tailrace, but hydrology and TSS are the dominant drivers further downgradient. The findings from this study show that understanding the temporal and spatial drivers of Mn and Fe concentrations in a dammed river is critical for identifying the sources of metals, how those sources change spatially and when metal concentrations are most likely to be elevated in the river.

ACKNOWLEDGEMENTS

We gratefully acknowledge support from Dominion Power. Support was also provided by the Geological Society of America's Student Research Grant awarded to the first author. This study was made possible using freely available data from the Unites States Geological Survey (http://water. usgs.gov/wateralert/). We appreciate American Electric Power providing access to dam sampling sites and discharge data.

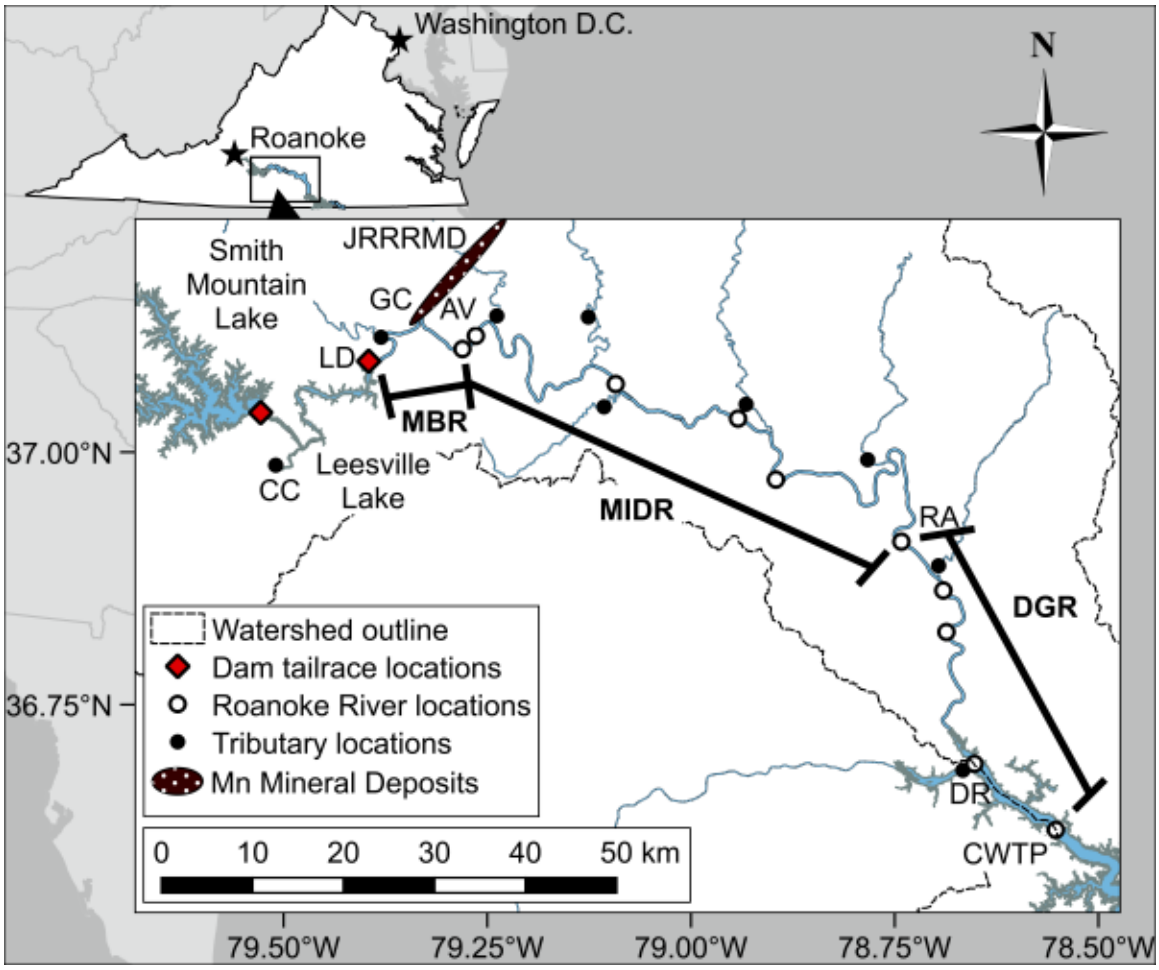

Figure 2.1. Location of the sampling sites along the Roanoke River watershed. Water samples were collected downgradient from Smith Mountain Dam, Leesville Dam, 11 sites in the main channel (labeled sites are Leesville Dam tailrace (LD), Altavista (AV), Randolph (RA) and Clarksville Water Treatment Plant (CWTP)) and 9 tributary sites (labeled sites are Cedar Creek (CC), Goose Creek (GC), and Dan River (DR)). The extent of the mass balance reach (MBR), mid-section reach (MIDR) and downgradient reach (DGR) are shown by black bracket lines. The location of Mn mineral deposits in the James River-Roanoke River Mn District is shown adjacent to the mass balance reach.

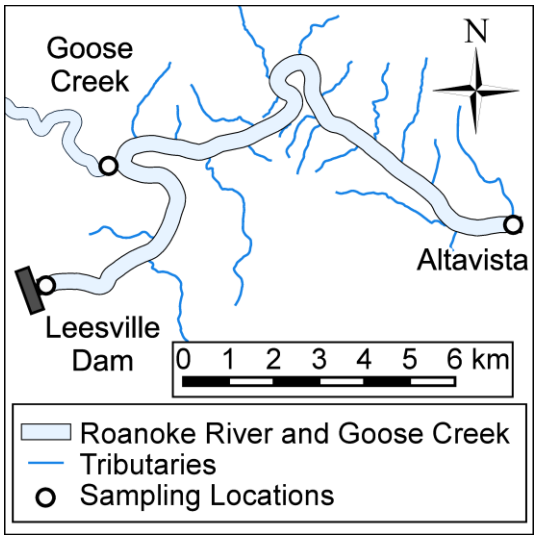

Figure 2.2. Map of the mass balance reach (MBR) and the location of Leesville Dam, Goose Creek and Altavista sampling locations.

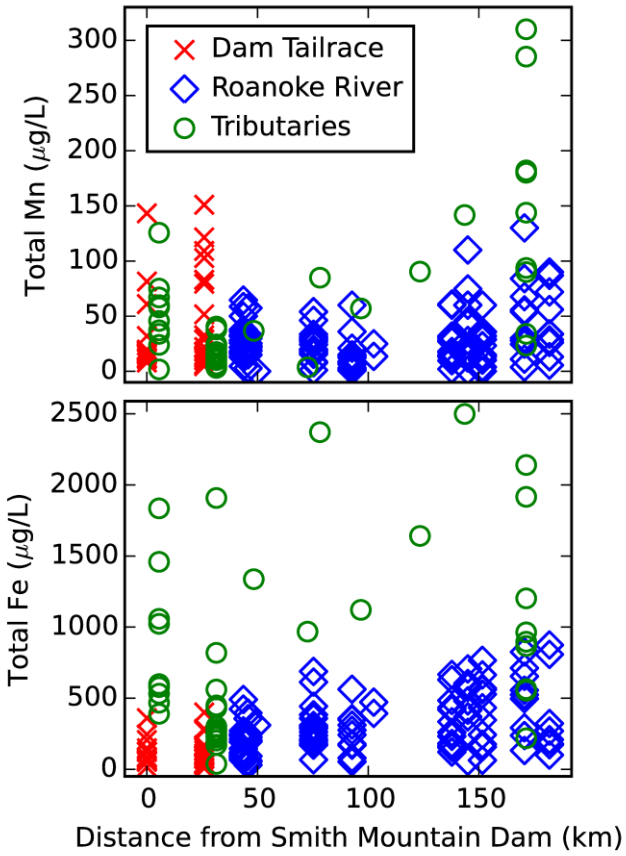

Figure 2.3. Total Mn (top) and Fe (bottom) concentrations in the Roanoke River and tributaries measured between October, 2012 and November, 2014. Tailrace samples include measurements in Smith Mountain Dam (0 km) and Leesville Dam tailraces (26 km). Roanoke River samples were all river measurements collected downgradient from Leesville Dam tailrace.

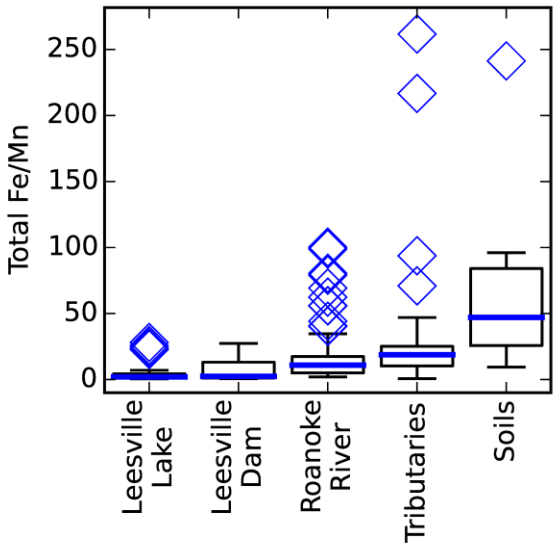

Figure 2.4. Boxplots showing the total Fe to total Mn mass ratio in Leesville Lake (n = 38), Leesville Dam tailrace (n = 32), the Roanoke River downgradient of Leesville Dam tailrace (n = 105), tributaries (n = 40) and soil concentrations (n = 10) in the Roanoke River watershed.

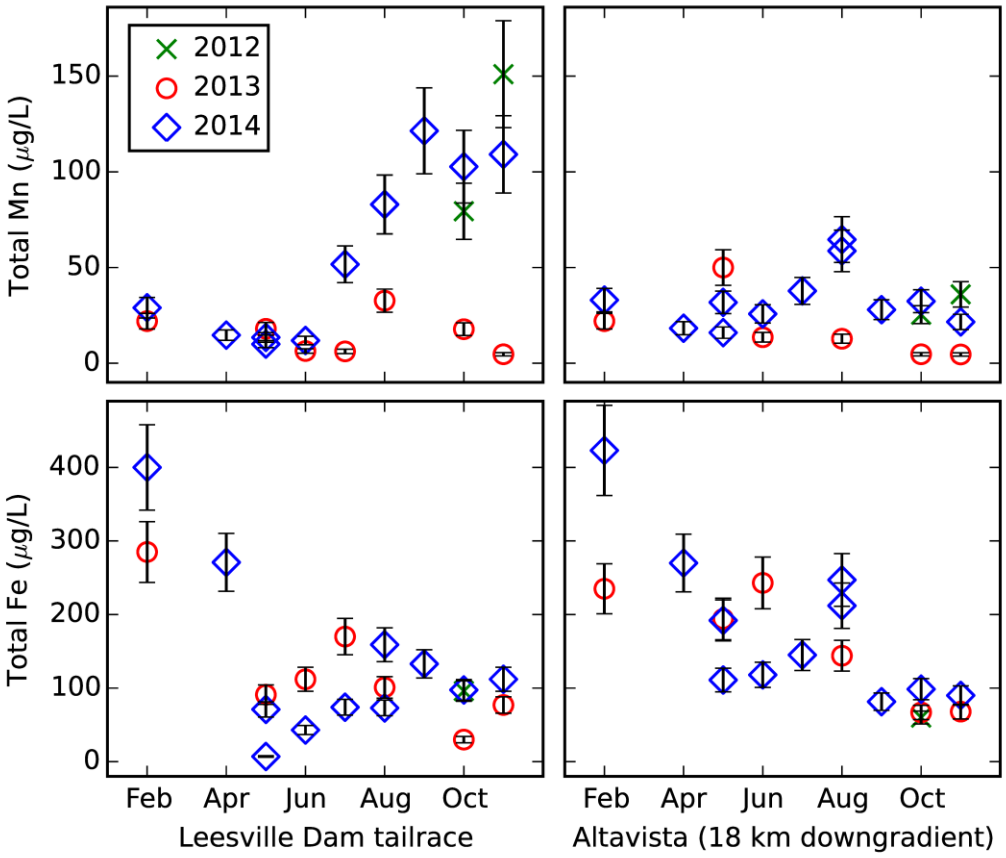

Figure 2.5. Total (top) Mn and Fe (bottom) in Leesville Dam tailrace (left) and Altavista (right) sampling sites. Error bars represent the standard errors of the concentration measurements.

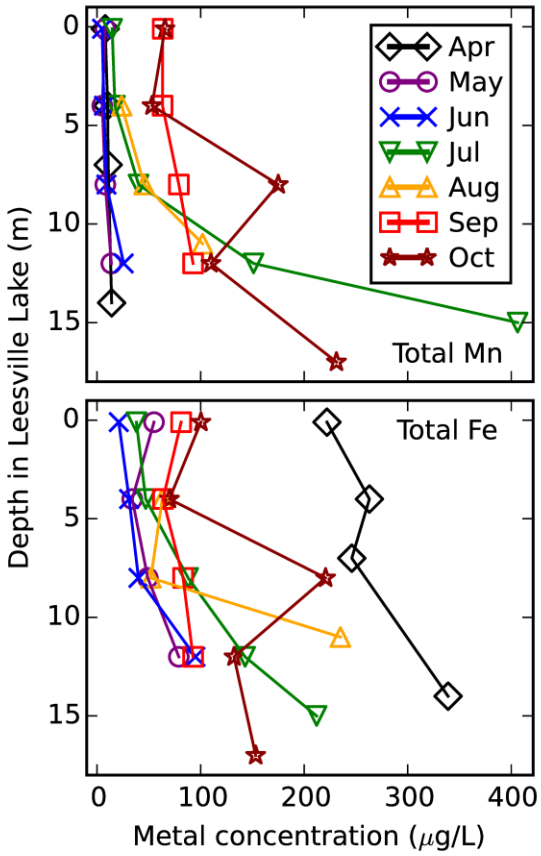

Figure 2.6. Total (top) Mn and Fe (bottom) in Leesville Lake. Profiles represent the water column concentrations in Leesville Lake, 250 meters upstream of Leesville Dam between April-October, 2014.

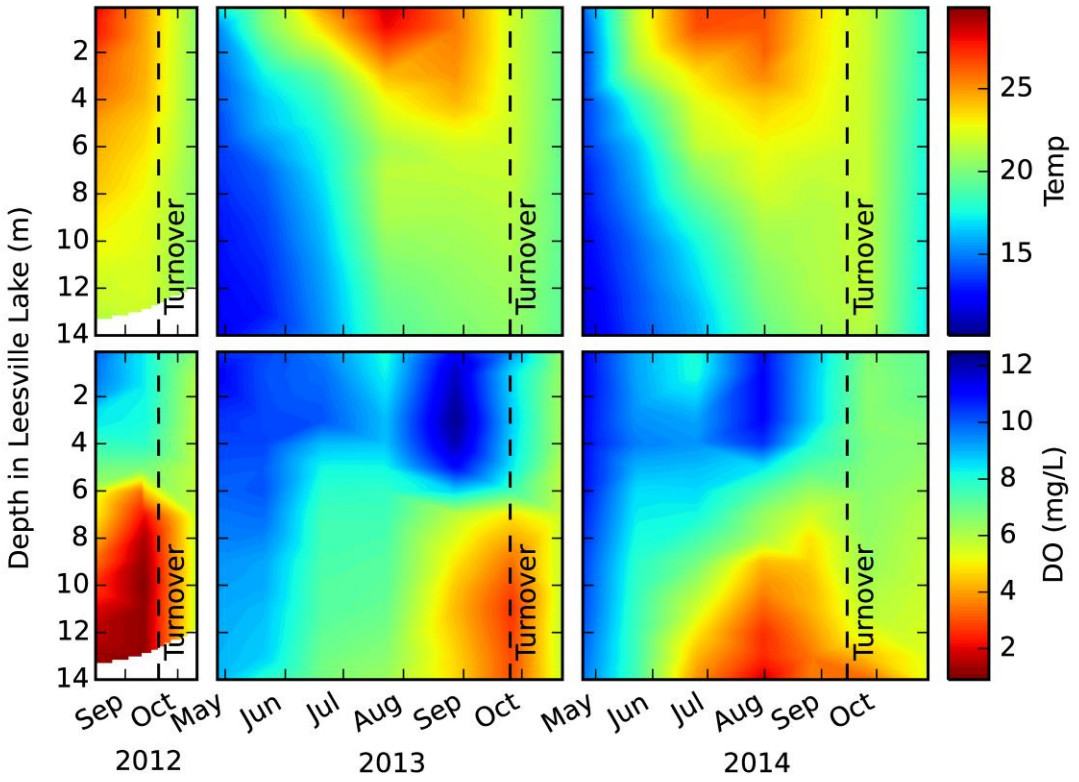

Figure 2.7. Temperature (top) and DO (bottom) in Leesville Lake between October, 2012 and October, 2014. Profiles were collected monthly between April and October. Data for 2012 and 2013 are from Shahady (2013, 2014). Estimates of lake turnover dates are shown as dashed vertical lines.

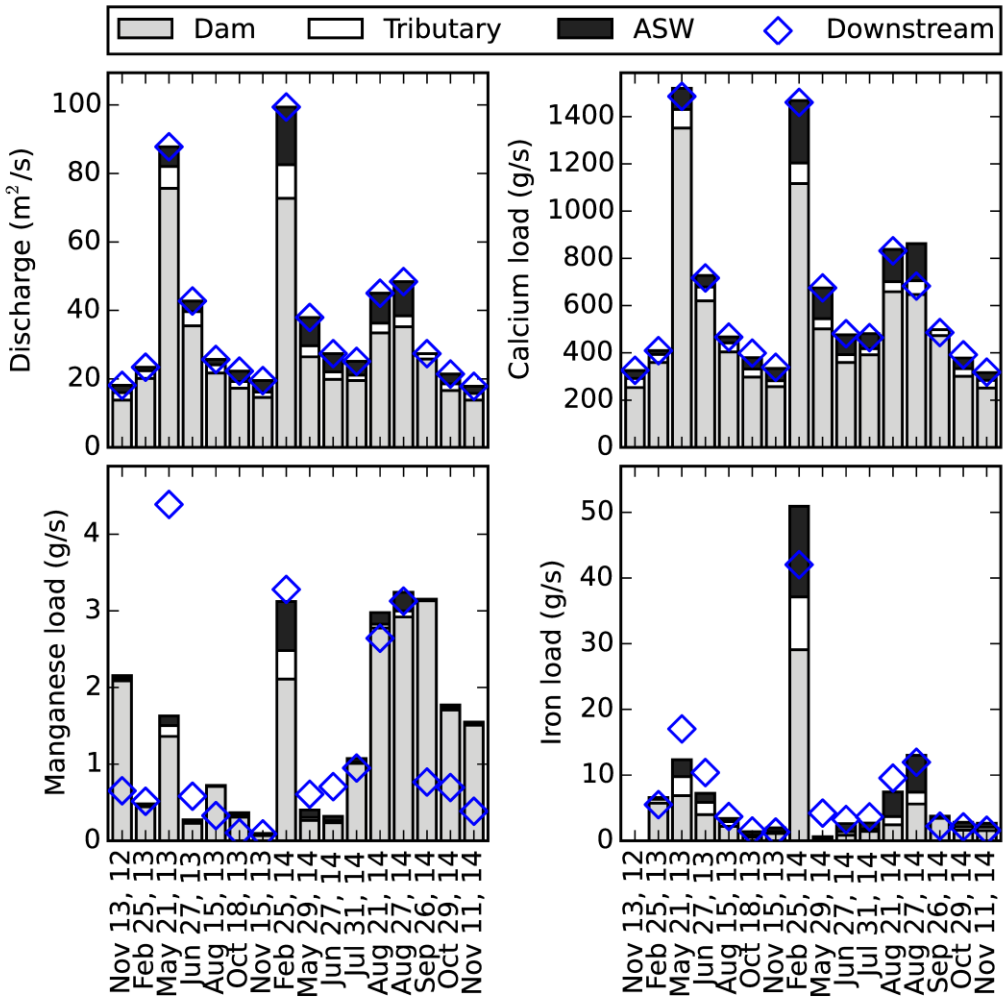

Figure 2.8. Mass balance for discharge (top-left), calcium (top-right), total Mn (bottom-left) and total Fe (bottom-right) in the reach between Leesville Dam and Altavista. The stacked bars represent the load entering the reach from Leesville Dam, Goose Creek tributary and additional surface water sources. The diamonds represent the load exported from the reach at Altavista.

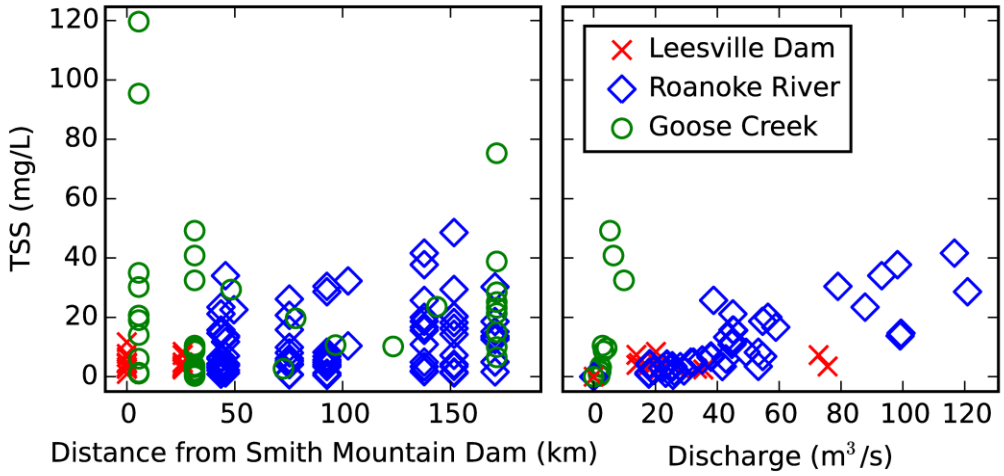

Figure 2.9. Relationship between TSS and distance from Smith Mountain Dam (left) and discharge (right) in the Roanoke River and its tributaries.

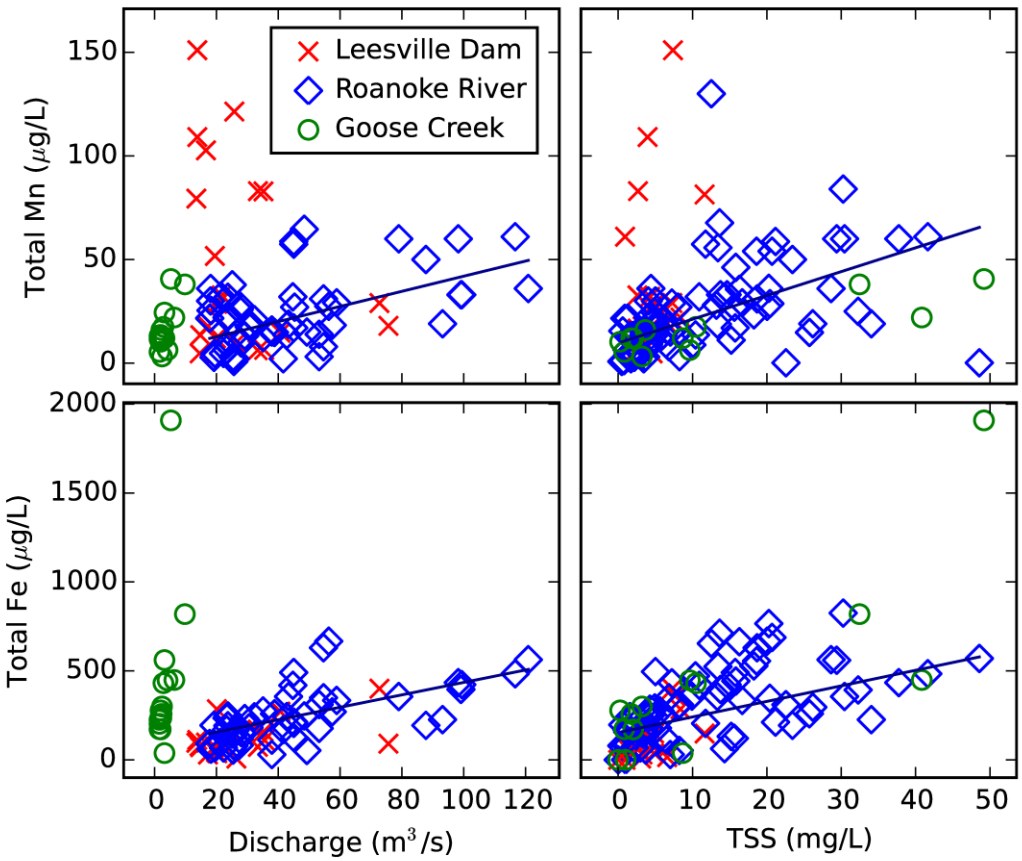

Figure 2.10. The relationship between total Mn (top) and total Fe (bottom) and discharge (left) and TSS (right) in the Roanoke River. Leesville Dam measurements were made in the tailrace downgradient of the dam. Roanoke River measurements were collected downgradient of Leesville Dam tailrace. Dark blue lines show a linear trend line for the Roanoke River data.

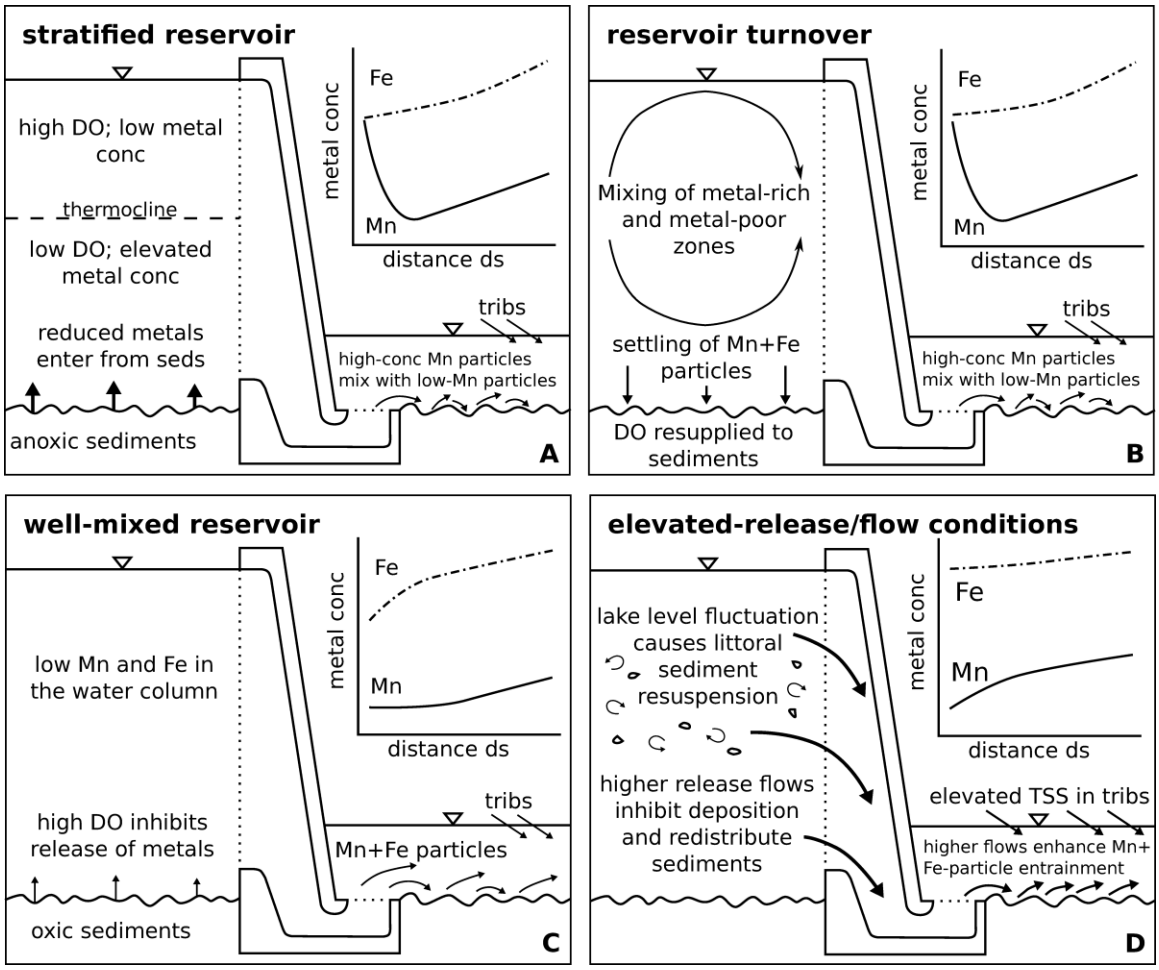

Figure 2.11. Metal cycles in a hydropower dam watershed in response to seasonal reservoir conditions and flow downgradient of the dam.

CHAPTER 3. EFFECTIVENESS OF HYPOLIMNETIC OXYGENATION FOR PREVENTING ACCUMULATION OF FE AND MN IN A DRINKING WATER RESERVOIR

Zackary W. Munger, Alexandra B. Gerling, Cayelan C. Carey, Kathleen D. Hamre, Jonathan P. Doubek, Spencer D. Klepatzki, Ryan P. McClure, Madeline E. Schreiber
A version of this chapter was submitted for publication in Water Research and is under review

ABSTRACT

The accumulation of Fe and Mn in seasonally stratified drinking water reservoirs adversely impacts water quality. To control issues with Fe and Mn at the source, some drinking water utilities have deployed hypolimnetic oxygenation systems to create well-oxygenated conditions in the water column that are favorable for the oxidation, and thus removal, of Fe and Mn. However, in addition to being controlled by dissolved oxygen (DO), Fe and Mn concentrations are also influenced by pH and metal-oxidizing microorganisms. We studied the response of Fe and Mn concentrations to hypolimnetic oxygenation in a shallow drinking water reservoir in Vinton, Virginia, USA by sequentially activating and deactivating an oxygenation system over two summers. We found that maintaining well-oxygenated conditions effectively prevented the accumulation of soluble Fe in the hypolimnion. However, while the rate of Mn oxidation increased under well-oxygenated conditions, soluble Mn still accumulated in the slightly acidic to neutral (pH 5.6 to 7.5) hypolimnion. In parallel, we conducted laboratory incubation experiments, which showed that the presence of Mn-oxidizing microorganisms increased the rate of Mn oxidation in comparison with rates under oxic, abiotic conditions. Combined, our field and laboratory results demonstrate that increasing DO concentrations in the water column is important for stimulating the oxidation of Fe

and Mn, but that the successful management of Mn is also tied to the activity of Mn-oxidizing organisms in the water column and favorable (neutral to alkaline) pH.

1. INTRODUCTION

Controlling iron (Fe) and manganese (Mn) in drinking water is a complex challenge for water utilities because of the adverse effects of these metals on drinking water quality and the difficulties in preventing their accumulation in source reservoirs. Issues with water staining, odor, and taste can be attributed to elevated Fe and Mn concentrations (Sommerfeld, 1999; World Health Organization, 2004), and adverse human health effects have also been associated with chronic exposure from drinking water (Wasserman et al., 2006). In response to the aesthetic water quality effects, the United States Environmental Protection Agency (EPA) has established secondary maximum contaminant limits for Fe and Mn concentrations in drinking water at 0.3 and 0.05 mg/L, respectively (United States Environmental Protection Agency, 2016a), and the World Health Organization (WHO) has recommended similar guidelines (World Health Organization, 2004). Treatment of Fe and Mn is most commonly accomplished by oxidation and filtration techniques (Kohl and Medlar, 2006; Sommerfeld, 1999); however, the accumulation of these metals in raw water increases the cost and difficulty of the water treatment process.

The development of reducing conditions in lake and reservoir sediments during thermal stratification leads to the reductive dissolution of Fe and Mn from the sediments and subsequent diffusion of these metals into the water column (Davison, 1993; Hem, 1972). Under oxidizing conditions (dissolved oxygen (DO) concentrations >2 mg/L), Fe and Mn occur naturally as oxidized, insoluble forms (Fe^{3+}, Mn^{3+}, and Mn^{4+}) in watershed sediments (Jones and Bowser, 1978). However, anoxic conditions (DO concentrations <0.5 mg/L) commonly develop within the sediments of lakes and reservoirs during thermal stratification that are favorable for the reduction of Fe and Mn to soluble forms

(Fe^{2+} and Mn^{2+}; Davison, 1993; Lerman et al., 1995). The reduction of Fe and Mn is known to occur abiotically via redox reactions with sulfides, organic acids, and Fe^{2+} (Mn reduction only); however, microbial activity also plays an important role in metal reduction through the production of sulfide, organic acids, and anaerobic respiration, which couples the mineralization of organic carbon to Fe and Mn reduction (Burdige, 1993; Lovley, 1987; Nealson and Saffarini, 1994). Reductive dissolution of Fe and Mn causes accumulation of soluble Fe and Mn in anoxic sediment pore waters, where concentration gradients drive their diffusion into the overlying water column (Davison, 1993; Hongve, 1997; Zaw and Chiswell, 1999). Transport of reduced Fe and Mn back into oxidizing zones in the sediments or water column can lead to these metals becoming oxidized, often precipitating as insoluble Fe- and Mn-oxyhydroxides that are subject to sedimentation out of the water column (Hem, 1972).

Hypolimnetic oxygenation is increasingly used as the first stage in treating Fe and Mn *in situ* by maintaining well-oxygenated conditions in the hypolimnion of seasonally stratified lakes and reservoirs (Beutel and Horne, 1999; Bryant et al., 2011; Burns, 1998; Debroux et al., 2012; Dent et al., 2014; Gantzer et al., 2009; Gerling et al., 2014). Hypolimnetic oxygenation (HOx) systems increase DO concentrations by injecting air, pure oxygen, or oxygenated water into the hypolimnion (Beutel and Horne, 1999; Gerling et al., 2014; Singleton and Little, 2006). Physical mixing induced by the HOx system operation often accompanies the injection of oxygen, aiding in distributing DO throughout hypolimnion (Figure 3.1; Beutel and Horne, 1999; Gantzer et al., 2009; Gerling et al., 2014). Successful management Fe and Mn using hypolimnetic oxygenation depends on maintaining a sufficiently oxidizing environment to quickly precipitate

oxidized metals in the water column, where they will settle back to the bottom sediments, or ideally, to cause metals to precipitate prior to being released from the sediment pore waters into the hypolimnion water column.

The rate of metal oxidation in the water column is primarily influenced by DO concentrations, pH, and microbial activity (Diem and Stumm, 1984; Hem, 1981, 1972). The abiotic oxidation of Fe is faster than Mn under similar DO and pH conditions. For example, in air-saturated water with pH >6, abiotic Fe oxidation is rapid, with soluble Fe having a half-time, defined as the time required for half of the initial mass of soluble Fe to become oxidized, of <24 hrs (Davison, 1993). However, under similar conditions the half-time for soluble Mn can be >1 year (Morgan, 1967). Soluble Mn oxidation occurs much faster in oxic lake water than observed under abiotic conditions, with several studies observing soluble Mn oxidation half-times between 1-30 days at pH between 6.5-8.4 (Chapnick et al., 1982; Diem and Stumm, 1984; Kawashima et al., 1988; Tipping et al., 1984). Chapnick et al. (1982) and Diem and Stumm (1984) identified Mn-oxidizing organisms in the reservoir water and showed that when these organisms were removed by filtration, Mn oxidation was negligible within the duration of their incubation experiments (10-30 days). The mechanisms of biotic Mn oxidation are not fully understood, but there is evidence that strains of actinobacteria, cyanobacteria, firmicutes, proteobacteria, and fungi have some ability to cause Mn oxidation and are ubiquitous in aquatic environments (Aguilar and Nealson, 1998; Richardson et al., 1988; Tebo et al., 2005), suggesting that the rates of Mn oxidation in lakes and reservoirs are strongly influenced by the activity of Mn-oxidizing organisms.

Although decreased concentrations of Fe and Mn have been observed in oxygenated reservoirs, sediments can continue to release metals, even in oxic hypolimnia (Aguilar and Nealson, 1998; Bryant et al., 2011; Gantzer et al., 2009). For example, Gantzer et al. (2009) reported a 97% decrease in Mn concentrations in the hypolimnion of Carvins Cove, Virginia, USA following the installation and continuous operation of a HOx diffuser system. However, elevated Mn concentrations were still observed in the sediment pore waters while the overlying hypolimnion was well-oxygenated, indicating that upward diffusion of Mn mass continued during HOx operation (Bryant et al., 2011; Gantzer et al., 2009). Similarly, Dent et al. (2014) reported decreases of the mean hypolimnetic Fe and Mn concentrations in North Twin Lake, Washington, USA, by 71% and 73%, respectively, within 8 hrs of activating the oxygenation system; however, the mean concentrations reported in that study did not account for volume difference along the profile, which makes it difficult to determine whether the decrease in hypolimnetic metal concentrations can be attributed to rapidly enhanced oxidation or whether redistribution of mass in response to HOx-induced physical mixing also influenced concentrations along the depth profile.

Managing Fe and Mn treatment in drinking water systems is challenging and expensive. Thus, accurately characterizing the processes controlling metal removal in drinking water reservoirs at the whole-ecosystem scale is needed to optimize management strategies. As discussed above, metal concentrations are affected by a host of biogeochemical and physical processes in waterbodies (Aguilar and Nealson, 1998; Bryant et al., 2011; Diem and Stumm, 1984; Gantzer et al., 2009). While previous studies have examined the impacts of specific processes of metal concentrations in laboratory

incubations or examined larger scale patterns at the lake or reservoir scale (Beutel et al., 2008; Diem and Stumm, 1984; Gantzer et al., 2009; Gerling et al., 2014), it remains unknown how redox and pH-dependent processes in the water column and sediments, physical mixing across concentration gradients, and the activity of metal-oxidizing bacteria together affect metal concentrations at the reservoir scale.

The goal of this study was to investigate the effects of hypolimnetic oxygenation on Fe and Mn oxidation at the whole-ecosystem scale in a drinking water reservoir. We manipulated the HOx system to experimentally create intermittent periods of hypolimnetic anoxia and well-oxygenated conditions over two years. Throughout the two-year experiment, we measured the effects of HOx system activation on soluble and total Fe and Mn accumulation in the hypolimnion and the rate of particulate metal sedimentation. In parallel, we conducted laboratory incubation experiments to evaluate the influence of microbial activity on Mn oxidation in the reservoir. We used the field and laboratory data to evaluate the importance of biogeochemical processes in Fe and Mn oxidation in oxygenated reservoirs.

2. METHODS

2.1. STUDY SITE

Falling Creek Reservoir (FCR) is a shallow (maximum depth=9.3 m), eutrophic drinking water reservoir located in a forested watershed in southwestern Virginia, USA, as shown in Figure 3.2. The primary source of water to the reservoir is a surface water stream that enters along the northeastern shoreline (Gerling et al., 2016). FCR typically experiences thermal stratification between April and October, during which time the hypolimnion develops anoxic conditions (Gerling et al., 2016, 2014).

2.2. HYPOLIMNETIC OXYGENATION SYSTEM DESCRIPTION

In autumn 2012, a side-stream supersaturation hypolimnetic oxygenation system was deployed in FCR (see Gerling et al., 2014, for a full system description). The HOx system at FCR consists of a submersible pump (positioned at 8.5 m depth), inlet piping, an oxygen source, an oxygen contact chamber, outlet piping, and distribution headers (positioned at 8.5 m depth). Water is withdrawn from the reservoir via the submersible pump and transferred to the oxygen contact chamber, where it is supersaturated with oxygen supplied by the oxygen source. The water is then transported to the distribution headers via the outlet piping, where it is injected back into the hypolimnion. A schematic showing the side-stream supersaturation HOx system in FCR is depicted in Figure 3.1.

The distribution header used 15 evenly-spaced eductor nozzles to promote rapid dilution of the oxygenated water and physical mixing throughout the hypolimnion. For every 1 L of oxygenated water injected through the nozzle, 4 L of hypolimnion water was suctioned through the nozzle. For example, at a flow rate of 10 L/min at the submersible pump, 40 L/min of hypolimnetic water was also being suctioned through the nozzle, giving a total flow through the nozzle of 50 L/min. The distribution header was 76.2 m long, designed to cover the length of the deepest region of the reservoir. The nozzles were angled upwards by 10° from horizontal to minimize sediment disturbance. Additional details about the HOx system in FCR are described in Gerling et al. (2014).

2.3. OXYGENATION SYSTEM OPERATION

To examine the effects of hypolimnetic oxygenation on Fe and Mn concentrations in FCR, we created alternating periods of well-oxygenated and hypoxic (DO <2 mg/L) conditions in the hypolimnion during the summer stratified period (see Table 3.1). In both 2014 and 2015, we began operation of the HOx system in early May; the initial period of HOx system activation lasted ~4 weeks. In 2014, the HOx system was

deactivated for two extended intervals, following the initial activation period, to allow anoxic conditions to develop at the bottom sediments. After anoxic conditions were established, the HOx system was reactivated to restore oxic conditions in the bottom of the hypolimnion. In 2015, the HOx system was deactivated for one week beginning June 1 and for 1.5 hr on July 28; however, the HOx system was continuously operated over the majority of the stratified period to maintain well-oxygenated conditions at the bottom sediments. The oxygen addition rates over both years varied between 12.5-25 kg/d (Table 3.1). The pump flow rate for all oxygenation periods was set at 227 L/min, with a total flow through the eductor nozzles of 1135 L/min. At this flow rate, the hypolimnion volume was circulated through the eductor nozzles every 20-30 days.

2.4. SAMPLE COLLECTION AND ANALYSES

2.4.1. METAL CONCENTRATIONS, TEMPERATURE, DISSOLVED OXYGEN, AND PH IN RESERVOIR WATER

We collected water samples to measure total and soluble Fe and Mn along a depth profile at the deepest site in FCR in 2014 and 2015 (see Sampling Location in Figure 3.2). Water samples were collected at nine depths in 2014 (0.1, 0.8, 1.6, 2.8, 3.8, 5.0, 6.2, 8.0 and 9.0 m) and seven depths in 2015 (0.1, 1.6, 3.8, 5.0, 6.2, 8.0 and 9.0 m) using a 4 L Van Dorn sampler (Wildlife Supply Company). These sampling depths correspond to the depths where water can be withdrawn from the reservoir for water treatment. Reservoir water samples were collected from the deepest site of the reservoir, adjacent to the dam, shown in Figure 3.2. Samples were collected weekly between April and October, and monthly through November in both years. After collection, we poured raw water samples directly into HDPE bottles for total metal analyses and syringe-filtered water using 0.45 μm nylon filters into HDPE bottles for soluble metal analyses. The samples were acidified with trace metal grade nitric acid to pH <2 to preserve them until

analysis. After collection, the samples were analyzed for Fe and Mn using an ICP-MS (Thermo Electron X-Series) following APHA Standard Method 3125-B (American Public Health Association et al., 1998).

We measured temperature and DO concentrations along a depth profile in the water column of FCR in both years at the same site where we collected water samples. Temperature and DO were measured using a Seabird Electronics SBE 19plus high-resolution profiler (CTD), which allowed us to collect data at about 0.1 m vertical increments. Gerling et al. (2014) collected CTD profiles at six additional sites on a transect between the reservoir's inflow and dam in FCR, which showed that DO concentrations measured at the sampling site used in this study were a good representation of conditions throughout the reservoir. To examine how DO concentrations change vertically within the water column as a result of HOx system-induced mixing, we collected a DO profile immediately before activation in June 2014, and seven additional DO profiles at 1, 2, 3, 5, 24, 48, and 72 hours after HOx system activation. Measurements of pH were collected weekly during the summer stratified period in 2014 at 0.1, 1.6, 3.8, and 6.2 m depths and at all seven of the sampling depths in 2015 using a YSI multiparameter meter.

The volume-weighted hypolimnetic (VWH) DO and metal concentrations were calculated using bathymetry data from Gerling et al. (2014) and profiles collected in FCR. We first determined the hypolimnetic masses of DO, Fe and Mn by linearly interpolating the measured concentrations in the hypolimnion at the depths in the bathymetry data (~0.3 m intervals) and multiplying the interpolated concentration data by the volume of water in each layer corresponding to those depths. The total hypolimnion

mass was the sum of the masses in each layer below the thermocline. The thermocline depth was determined from the CTD temperature profiles collected on each sampling date and analyzed using Lake Analyzer, a Matlab program (Mathworks; Read et al., 2011), and the hypolimnion volume was calculated as the cumulative volume from the sediments to the mean thermocline depth for each year, following Gerling et al. (2014). We calculated the VWH concentrations by dividing the hypolimnion mass by the total volume in the hypolimnion. The mean thermocline depths were 4.1±0.8 m (1 standard deviation) and 4.6±0.9 m in 2014 and 2015, respectively.

2.4.2. SEDIMENTATION TRAPS AT 4 M AND 8 M DEPTH IN THE RESERVOIR

We deployed sedimentation traps (KC Denmark A/S) at 4 m and 8 m depth near the dam in FCR to capture particulate metal sedimentation. Each trap contained two tubes with openings of 7.2 cm in diameter. The sedimentation traps were deployed between May-December in 2014 and April-November in 2015, and particulate samples were retrieved every 14 days during summer and every 28 days in autumn. During sampling, the traps were brought to the surface and the mixture of water and particulates was poured into 1 L bottles. The samples in these bottles were vacuum-filtered through pre-weighed glass microfiber filters (1.5 μm; Whatman 934-AH). The filters containing particulates were dried at 45°C in a drying oven and the retained mass was calculated by difference from the final and starting mass of the filter.

We determined the particulate metal flux by digesting the raw particulate matter retained on the filters and analyzing the digestion solution for Fe and Mn concentrations. The raw particulates were microwave-digested with trace metal grade nitric acid following EPA Method 3051A (United States Environmental Protection Agency, 1995). We analyzed the resulting digestion solution for Fe and Mn using ICP-MS, as described

above. The mass of particulate metal was calculated by multiplying the metal concentration by the known volume of acid added to each sample. We calculated the particulate metal sedimentation flux by dividing the trapped metal mass by the trap opening area and duration of trap deployment. Measurement uncertainty was calculated using the standard deviation between the replicate flux measurements at each depth.

We estimated zero-order Fe and Mn oxidation rates in the hypolimnion of FCR using the sediment trap data. To do this, we assumed that the metal sedimentation rate represented the rate of particulate metal production in the water column (via oxidation). To calculate the hypolimnion oxidation rate, we first subtracted the flux calculated at 4 m (allochthonous particulates) from the 8 m flux. The hypolimnion flux ($M/L^2/T$) was divided by the water column thickness between traps (4 m) to calculate an average zero-order oxidation rate (K; $M/L^3/T$) in the hypolimnion. We used the volume-weighted hypolimnion soluble metal concentration at the beginning of the trap deployment interval as the initial concentration (C_0).

Using the zero-order oxidation rate, we then calculated an oxidation "half-time" for each rate, a characteristic time that reflects how long soluble Fe and Mn persist in the hypolimnion of FCR prior to being oxidized and removed via particulate settling. We calculated the oxidation half-time, $t_{i,0.5}$, for both Fe and Mn with the equation (Rimstidt, 2013):

$$t_{0.5} = \frac{0.5C_0}{K} \quad (1)$$

2.5. MANGANESE OXIDATION INCUBATIONS

We designed a laboratory incubation experiment to evaluate the relative influence of biotic and abiotic processes on Mn oxidation in the reservoir. Our experiment had five

treatments with four replicates each: 1) a slurry of reservoir particulates spiked with Mn (PMn), 2) reservoir water spiked with Mn (WMn), 3) a slurry of particulates without the Mn spike (P), 4) a slurry of sterilized particulates spiked with Mn (SPMn), and 5) sterilized reservoir water spiked with Mn (SWMn).

We conducted the incubation experiments in 250 mL sterilized Erlenmeyer flasks. Each flask received 100 mL of live or sterilized reservoir water according to its treatment. The particulates and reservoir water used in the experiments were collected in September 2015 from a sedimentation trap deployed at 4 m depth in the same manner as described in Section 2.4.2. The reservoir water (19°C at collection) was siphoned from the 1 L bottle and 1 mL of the resulting slurry was transferred to the experiment flasks assigned to the particulate treatments. We sterilized the flasks and sample material by autoclaving them at 121°C for 45 minutes; the sterilized particulates also received 1 g sodium azide to kill all microorganisms. We spiked the samples with Mn^{2+} using 1 mL aliquot of 250 mg/L $MnCl_2$ aqueous solution. All flasks were covered in aluminum foil and placed on a shaker table in the dark at room temperature (21°C).

The experiment was sampled at regular intervals to quantify the rate of soluble Mn (Mn^{2+}) loss for 18 days. Three of the flask replicates were sampled for soluble Mn and the fourth replicate was used to measure temperature, pH, and DO concentrations. During sampling, a 1 mL aliquot was collected from each of the three sample replicate flasks at 0.5 hr, 3 hr, 6 hr, 12 hr, 1 d, 2 d, and every 3 d between 3-18 d using a sterile syringe. Temperature, pH, and DO concentrations were measured in the fourth replicate flasks simultaneous with the water sample collection. After collection, samples were filtered (0.2 μm nylon filter), diluted to 10 mL with deionized water, and preserved with

trace metal grade nitric acid. The samples were analyzed for soluble Mn using ICP-AES following EPA Method 200.7 (Creed et al., 1994). Measurement uncertainty was determined using the standard deviation of the triplicate measurement results. We calculated zero-order Mn oxidation rates (K; $M/L^3/T$) by fitting a linear model to the Mn data as described in Rimstidt (2013), assuming that any decrease in soluble Mn concentration was the result of oxidation. The half-time of soluble Mn in the incubations was calculated using the zero-order oxidation rates with Equation 2.

3. RESULTS

3.1. TEMPERATURE, DISSOLVED OXYGEN, AND PH IN THE RESERVOIR

Activation and deactivation of the HOx system successfully established intermittent periods of oxic and anoxic hypolimnetic conditions in 2014 (Figure 3.3). In early April 2014, DO concentrations and temperature were relatively uniform throughout the water column. By mid-April, thermal stratification had intensified, causing the volume-weighted hypolimnetic (VWH) DO concentration to decrease at a rate of 0.14 mg/L/d between April and early May. The HOx system was activated in early May 2014 (see Table 3.1 for HOx system activation dates), which caused the VWH DO concentration to increase at a rate of 0.04 mg/L/d. Over the summer stratified period when the HOx system was deactivated, the VWH DO concentration decreased at a mean rate of 0.16±0.02 mg/L/d (1 SD), which resulted in anoxic conditions (DO <0.5 mg/L) in the bottom layer of the hypolimnion in June and August. When the system was activated in June/July and August/September, the VWH DO concentration increased at a mean rate of 0.04±0.03 mg/L/d.

Along the depth profile, DO concentrations changed most rapidly in the bottom layer of the hypolimnion in response to HOx system activation (Figure 3.3). During the

three-day periods after the HOx system was activated in May, June, and August 2014, DO concentrations at 9 m depth increased by a mean rate of 0.67±0.12 mg/L/d, ~30 times faster than the bulk hypolimnion. CTD profiles showed that DO concentrations quickly increased below ~7 m depth and decreased slightly at shallower depths in the hypolimnion after the HOx system was activated (Figure 3.4). Within 24 hrs after HOx system activation, DO concentrations throughout the hypolimnion were uniform due to the system's mixing of anoxic bottom layers with oxic water from shallower depths in the hypolimnion.

Continuous operation of the HOx system maintained oxic conditions for most of the summer stratified period in 2015 (Figure 3.3). Similar to 2014, the VWH DO concentration decreased at a rate of 0.13 mg/L/d prior to HOx system activation. After the HOx system was activated in early May, the VWH DO concentration increased at a rate of 0.07 mg/L/d. In 2015, we only observed anoxia in the bottom of the hypolimnion after a one-week period when the HOx system was deactivated in early June. After the HOx system was reactivated in June, the VWH DO concentration remained >4 mg/L for the rest of the summer stratified period, including a brief, 1.5 hr interval when the HOx system was deactivated in July 2015. Despite DO concentrations >8 mg/L throughout most of the hypolimnion during the summer in 2015, the VWH DO concentration never exceeded ~7 mg/L due to the persistence of anoxia just below the thermocline. In both 2014 and 2015, anoxia developed in the metalimnion and persisted until the water column destratified in autumn, suggesting that physical mixing across the thermocline did not increase substantially when the HOx system was activated.

During the summer stratified period in 2014 and 2015, we measured a mean pH of 6.8±0.4 (6.2 m depth only in 2014) and 6.2±0.3, respectively, in the hypolimnion. Between April and May in 2014, the pH was ~0.5 units higher than that measured between June and September. Similarly, in 2015 the pH was ~0.2 units higher between April and May compared to pH measured between June and September.

3.2. IRON CONCENTRATIONS IN THE RESERVOIR WATER COLUMN AND SEDIMENTATION TRAPS

Total Fe concentrations increased in the hypolimnion during the summer stratified period, even when the HOx system was activated (Figure 3.5). During the early stratified period (between April and May) in both 2014 and 2015, total Fe concentrations in the hypolimnion remained ~0.5 mg/L. However, later in the stratified period, between June and September, total Fe concentrations increased throughout the hypolimnion. The average rates at which total Fe concentrations increased between June and September in 2014 (0.016 mg/L/d) and 2015 (0.015 mg/L/d) were similar, despite the higher DO concentrations that were measured during these months on average in 2015 compared to 2014 (Figure 3.6). Although the rates of total Fe accumulation in the hypolimnion were similar during intervals of anoxia and well-oxygenated conditions, we measured the highest total Fe concentrations near the bottom of the reservoir (33 mg/L at 9 m depth in August 2014) when the hypolimnion was anoxic in response to HOx system deactivation (Figure 3.6). When the HOx system was activated, total Fe concentrations near the bottom of the reservoir were much lower than observed during anoxic intervals; however, the VWH total Fe concentrations reached similar levels regardless of HOx system operation (Figure 3.6).

Soluble Fe concentrations were generally low (<1 mg/L) throughout the hypolimnion when the HOx system was activated, even between June and September when we observed total Fe accumulating in the hypolimnion (Figure 3.5). Soluble Fe constituted a relatively minor fraction (<50%) of the total Fe concentrations throughout the hypolimnion when the HOx system was activated; however, when anoxic conditions developed in response to HOx system deactivation in August 2014, soluble Fe increased to >90% of the total Fe concentrations measured in the bottom of the reservoir (9 m depth; Figure 3.6). Soluble Fe did not accumulate in the hypolimnion when the HOx system was activated; however, during the periods of HOx system deactivation in June and July-August 2014, the VWH soluble Fe concentrations increased by a mean rate of 0.007±0.001 mg/L/d (Figure 3.6), which was substantially lower than the accumulation rate measured for total Fe.

We observed increases in total and soluble Fe concentrations concurrent with the development of anoxia in the metalimnion in 2015 (Figure 3.5). In July 2015, total Fe concentrations reached >4 mg/L at 5 m depth (Figure 3.6). By the end of August 2015, soluble Fe concentrations at 5 m decreased to ~1 mg/L and remained at or below this level until destratification, despite the persistence of anoxia in the metalimnion. However, total Fe remained elevated at 5 m between July-September (Figure 3.6).

The rate of particulate Fe sedimentation increased as the VWH total Fe concentration increased over the summer stratified period in both 2014 and 2015 (Figure 3.7). There was negligible change in particulate Fe sedimentation at 4 m during the summer stratified period, which averaged 0.16±0.06 $g/m^2/d$ during both years. The most significant changes in particulate sedimentation occurred in the 8 m trap. During the

onset of thermal stratification, particulate Fe sedimentation at 8 m was <0.2 g/m^2/d, but the flux reached >2 g/m^2/d by August in both 2014 and 2015, despite differences in HOx system operation.

3.3. MANGANESE CONCENTRATIONS IN THE RESERVOIR WATER COLUMN AND SEDIMENTATION TRAPS

Similar to the Fe results, total Mn accumulated in the hypolimnion over the summer stratified period, regardless of HOx system operation (Figure 3.8). During the early stratified period, between April and May, total Mn concentrations were <0.3 mg/L throughout the hypolimnion and did not substantially increase during these months in either year (Figure 3.9). However, between June and September, the VWH total Mn concentration increased at rates of 0.009 mg/L/d and 0.010 mg/L/d in 2014 and 2015, respectively. Although total Mn accumulation in the hypolimnion occurred at similar rates in both years, we observed total Mn concentrations up to 4.1 mg/L during anoxia at 9 m depth in August 2014 (following a period of HOx system deactivation), which was much higher than total Mn concentrations measured anywhere in the hypolimnion during HOx system activation (Figure 3.9).

In contrast to the Fe data, soluble Mn accumulated in the hypolimnion between June and September regardless of DO concentrations (Figure 3.8). During these months in both years, the VWH soluble Mn constituted 89±10% of the VWH total Mn concentration measurements on average (Figure 3.9). When the HOx system was deactivated soluble Mn concentrations were much higher in the bottom of the reservoir (8 m and 9 m depths) than at shallower depths in the hypolimnion (Figure 3.9). Immediately after HOx system reactivation the soluble Mn concentrations decreased rapidly at 8 m and 9 m. For example, reactivating the HOx system in both June and August 2014 caused

the soluble Mn concentrations at 9 m depth to decrease by 47% and 39% within one week, respectively (Figure 3.9). However, there was not a consistent pattern of decreasing soluble Mn concentrations throughout the hypolimnion; the VWH soluble Mn concentration decreased by 2% and increased by 53% one week after HOx system reactivation in June and August 2014, respectively. Furthermore, soluble Mn concentrations at 8 m and 9 m depths generally continued to increase in the weeks following HOx system activation, indicating that, similar to Fe, Mn also continued to be released from the sediments when the HOx system was activated (Figure 3.9).

Particulate Mn sedimentation was higher in response to extended periods of HOx system activation in October 2014 and between July and September 2015 (Figure 3.7). Mn sedimentation at 4 m exhibited a minor decrease between 2014 and 2015 (the mean sedimentation rates in 2014 and 2015 were 0.036±0.014 $g/m^2/d$ and 0.028±0.014 $g/m^2/d$, respectively; Figure 3.7). In 2014, Mn sedimentation at 8 m did not increase until late September, with the highest rate occurring after destratification. In 2015, particulate Mn sedimentation increased earlier, in July, and remained elevated until reservoir destratification in October. Examination of the DO data revealed that the highest rates of particulate Mn sedimentation in the hypolimnion (8 m trap) occurred when DO concentrations were generally >8 mg/L (Figure 3.3).

3.4. MANGANESE INCUBATION EXPERIMENTS

We observed soluble Mn oxidation only in the biologically active incubation experiments containing particulates and/or water from FCR (Figure 3.10). The treatment containing live reservoir particulates (PMn) exhibited the greatest rate of soluble Mn removal at 0.042 mg/L/d, and the treatment containing live reservoir water (WMn) exhibited a lower removal rate of 0.0017 mg/L/d (Table 3.3). The sterilized treatments,

consisting of particulates (SPMn) and reservoir water (SWMn), exhibited negligible change in soluble Mn concentration during the experiment. DO and pH conditions in the experiments (Table 3.2) were consistently maintained to reflect reservoir conditions. The mean DO concentration in the treatments was 8.3±0.7 mg/L, similar to DO concentrations in well-oxygenated conditions of the hypolimnion in FCR; the mean pH in the flasks was 7.0±0.7; within the pH range observed in the FCR water column (mean 6.6±0.6).

3.5. OXIDATION RATES AND HALF-TIMES FOR SOLUBLE FE AND MN IN THE HYPOLIMNION

The half-time of soluble Fe in the water column of FCR was much shorter (~2 d) compared to soluble Mn (~15-33 d) in both years (Table 3.3 and Figure 3.11). Our results showed that the mean half-time of soluble Fe in the hypolimnion of FCR was 1.6±1.7 d over the summer stratified period in both 2014 and 2015, with negligible difference between years (Figure 3.11). However, the half-time for soluble Mn was ~50% shorter over the summer stratified period in 2015 (15±13 d), when the HOx system was continuously operated, compared to the same period in 2014 (33±21 d), when the hypolimnion exhibited intermittent anoxia.

4. DISCUSSION

4.1. EFFECTS OF HOX SYSTEM ACTIVATION ON FE AND MN ACCUMULATION IN THE HYPOLIMNION

Operation of the HOx system successfully prevented the accumulation of soluble Fe in the hypolimnion of FCR, but had little effect on soluble Mn accumulation. When the HOx system was activated, DO concentrations increased and became uniform throughout the hypolimnetic water column. Our results show that maintaining well-oxygenated conditions increased Fe oxidation, resulting in the formation of Fe-

oxyhydroxides, to prevent significant soluble Fe accumulation in the water column (Figure 3.5). However, under these same conditions, soluble Mn concentrations increased throughout the hypolimnion and persisted even in well-oxygenated zones (Figure 3.8). Although the oxidation rate of soluble Mn increased when the HOx system was continuously activated in 2015 (Table 3.3), maintaining well-oxygenated conditions did not increase the rate of Mn oxidation enough to prevent soluble Mn accumulation in the hypolimnion.

The HOx system did not inhibit the accumulation of total Fe or Mn, which includes both the soluble and particulate fractions, during the summer stratified period in either year. The rate at which the VWH total Fe concentration increased over the summer stratified period exhibited little change when the HOx system was activated, suggesting that oxic conditions increased the rate of soluble Fe oxidation (conversion from soluble to particulate Fe), but did not suppress the release of Fe from the sediments and its accumulation in the overlying water column. Total Mn concentrations also increased over the summer stratified period reflecting the accumulation of soluble Mn, which constituted the majority of the total Mn concentrations (Figure 3.8).

Our Mn results deviate from the findings of several other studies which support the effectiveness of hypolimnetic oxygenation for controlling Mn concentrations in source reservoirs (e.g., Bryant et al., 2011; Dent et al., 2014; Gantzer et al., 2009). We believe these contrasting results are due to the application of different methods for characterizing the effects of HOx system operation on metal concentrations and differences in reservoir biogeochemistry that influence metal oxidation. For example, Dent et al. (2014) observed a 73% decrease in total Mn concentrations along a depth

profile collected in North Twin Lake, 8 hrs after activating a bubble-plume HOx system; however, these measurements were not weighted by volume and, after one week, 94% of the Mn remained in soluble form, suggesting that mixing and dilution induced by the HOx system may have influenced their observed Mn concentrations. Gantzer et al. (2009) reported a 97% decrease in the volume-weighted total Mn concentration in the bulk hypolimnion of Carvins Cove Reservoir after a year of continuous HOx system operation; however, the pH in Carvins Cove Reservoir is typically between 8-9 (Bryant et al., 2011), which is much more favorable for rapid Mn oxidation compared to the pH <7 observed in FCR (Diem and Stumm, 1984; Hem, 1981; Morgan, 1967). The following discussion examines the role of DO, pH, and microorganisms in mediating the effects of HOx system operation on Fe and Mn concentrations.

4.1.1. EFFECTS OF DO, PH, AND MICROORGANISMS ON METAL OXIDATION

The combined results of water column metal concentrations and sedimentation rates suggest that Fe oxidation was enhanced sufficiently during HOx system activation to prevent the accumulation of soluble Fe in the hypolimnion (Figure 3.6), but that soluble Mn oxidation occurred more slowly, which allowed soluble Mn to accumulate in the hypolimnion even under well-oxygenated conditions (Figure 3.9). Previous studies have demonstrated that oxidation of Fe and Mn is influenced by both DO concentration and pH; however, the oxidation rate of Fe is much faster than Mn at similar DO concentration and pH (Appelo and Postma, 2005; Millero et al., 1987; Morgan, 1967). For example, using the rate equation in Appelo and Postma (2005), the abiotic oxidation of soluble Fe at a DO concentration of 8.5 mg/L and pH 6.6, conditions observed in the hypolimnion of FCR, gives a half-time for soluble Fe of ~1.5 hr. In contrast, using the rate equation for Mn in Morgan (1967) with the same pH and DO conditions, gives a

half-time for soluble Mn of 10^5 days (approximately 275 years). The predicted half-time for soluble Fe under abiotic conditions is within the range of oxidation half-times calculated for Fe in the water column of FCR (half-time between 5 hr and 7 d); however, the predicted half-time for soluble Mn under the same conditions was much longer than what we calculated in FCR (half-time <60 d; Figure 3.11; Table 3.3), indicating factors other than DO concentration and pH have a greater effect on Mn oxidation compared to Fe oxidation.

The concentration of hydrogen ions (pH) exerts a substantial effect on metal oxidation rates, but pH in the hypolimnion of FCR did not substantially change during the summer stratified period. For example, doubling DO concentration would cause the abiotic oxidation rate of Mn to double using the rate equation in Appelo and Postma (2005); however, doubling the hydrogen ion concentration would cause the abiotic oxidation rate to increase by a factor of four. Despite the comparatively larger effect of pH on abiotic metal oxidation, pH in the hypolimnion generally varied by less than 0.3 units and were slightly lower later in the summer stratified period, suggesting that the changes in metal oxidation rates calculated between the anoxic and well-oxygenated intervals between June and September were not substantially influenced by pH.

Our incubation experiment results show negligible abiotic Mn oxidation occurring at a DO concentration of ~8.5 mg/L and pH 6.6 within 18 d (Figure 3.10). These results agreed with oxidation rates calculated using the rate equation in Morgan (1967); even at the highest DO concentration observed in FCR during the summer stratified period (10.5 mg/L), the predicted half-time for soluble Mn was $>10^4$ d under abiotic conditions. At higher pH, between 8-9, the predicted half-time for soluble Mn would be between 1-100

d, suggesting that abiotic Mn oxidation may have been much faster if the pH in FCR were more alkaline, similar to the reservoirs studied in Bryant et al. (2011); Dent et al. (2014; and Gantzer et al. (2009).

Manganese oxidation occurred most rapidly in the biotic incubation treatments (Figure 3.10). The oxidation half-time of soluble Mn in water collected from FCR (WMn treatment) was ~32 days, which is similar to results observed in previous studies conducted on oxic lake water samples (Table 3.3; Chapnick et al., 1982; Diem and Stumm, 1984; Kawashima et al., 1988; Tipping et al., 1984), and much shorter than the 10^5 days predicted from the abiotic oxidation rate equation. The half-time for soluble Mn measured in the particulates treatment was 50 times shorter than the reservoir water alone, suggesting that Mn-oxidizing organisms are concentrated in suspended particulates and that greater abundances can dramatically increase oxidation rates.

Higher DO concentrations in the hypolimnion in 2015 (Figure 3.3) caused Mn oxidation to occur more quickly compared to 2014 (Table 3.3 and Figure 3.11). Although maintaining well oxygenated conditions would not substantially increase the abiotic rate of Mn oxidation, the faster oxidation rates observed in the hypolimnion suggest that higher DO concentrations may promote the oxidizing activity of Mn-oxidizing organisms (Figure 3.11). It has been previously shown that DO is consumed proportionally to the production of oxidized Mn by *Leptothrix* bacteria (Boogerd and De Vrind, 1987); however, we do not know of any published literature that has demonstrated the effects of DO concentration on biotic Mn oxidation rates. Such a rate equation would be invaluable for optimizing future HOx system operation.

4.1.2. IMPLICATIONS FOR CONTROLLING FE AND MN WITH HYPOLIMNETIC OXYGENATION

Our results show that continuous operation of the HOx system during the summer stratified period is essential to optimizing its effectiveness for controlling soluble metals. Continual operation of the HOx system prevented the development of anoxic zones where we observed the highest concentrations of soluble Fe in 2014 (Figure 3.6); when the HOx system was continuously operated, soluble Fe did not accumulate near the benthic sediments where we had previously measured soluble Fe concentrations >30 mg/L. Although soluble Mn still accumulated under well-oxygenated conditions, the concentrations near the benthic sediments were twice as high when anoxia was allowed to develop (Figure 3.9). Hypolimnetic oxygenation effectively prevented soluble Fe accumulation, even under slightly acidic conditions, because of the fast oxidation kinetics of Fe. The oxidation of Mn is generally slower and is sensitive to pH and microbial activity, but the shorter oxidation half-times calculated for soluble Mn during continual operation of the HOx system demonstrates that maintaining high DO concentrations (>8 mg/L) is also useful for stimulating the oxidation and removal of soluble Mn. Accumulation of soluble Mn in the water column in FCR in both 2014 and 2015 reflects the relatively slow oxidation kinetics that are inherent to Mn.

Results of the incubation experiment support previous work showing that biotic activity, likely resulting from the presence of Mn-oxidizing microorganisms, is a key part of the Mn redox cycle in natural systems and thus are critical elements of engineered systems to treat Mn *in situ*. Additional work is needed to identify the community of metal-oxidizing organisms, their distribution in the water column, and the optimal DO concentration and pH needed to maximize their oxidizing behavior in FCR.

5. CONCLUSIONS

The goal of this study was to investigate the effects of hypolimnetic oxygenation on Fe and Mn dynamics at the reservoir scale in a drinking water reservoir. Overall, our results showed that hypolimnetic oxygenation was effective for controlling soluble Fe in a shallow, dimictic drinking water reservoir. However, although continuous operation of the HOx system increased the rate of Mn oxidation, soluble Mn ultimately accumulated in the water column. Several other patterns emerged from our results in FCR that are important for water quality management: 1) Increasing DO concentrations to >8 mg/L is essential for maximizing the rate of soluble Mn oxidation. 2) The rate of Mn oxidation in the water column is influenced by the presence of Mn-oxidizing organisms that are associated with water column particulates. 3) Although the HOx system maintained oxidizing conditions in the hypolimnion, it did not prevent the continued release of Fe and Mn from the sediments, thus limiting its effectiveness to the rate at which metals may oxidize in the water column. In summary, hypolimnetic oxygenation may be a favorable management strategy for controlling soluble Fe, but future work is needed to optimize it effectiveness in promoting soluble Mn oxidation.

ACKNOWLEDGEMENTS

We thank the staff at the Western Virginia Water Authority for their long-term support and funding. In particular, we would like to thank Cheryl Brewer, Jamie Morris, Jeff Booth, Bob Benninger, and Gary Robertson. Jeffrey Parks, Mariah Redmond, Mariah Haberman, Madeline Ryan, Charlotte Harrell, Athena Tilley, and Bobbie Niederlehner provided critical help in the field and laboratory. We also thank Don Rimstidt for help in modeling metal oxidation rates. This work was supported by the Institute for Critical Technology and Applied Science at Virginia Tech, Virginia Tech Global Change Center, and Fralin Life Sciences Institute.

Table 3.1. Dates of activation and oxygen addition rates for the HOx system.

Year	Dates of activation	Oxygen addition rate (kg/d)
2014	May 5–Jun 3	20
2014	Jun 29–Jul 22	20
2014	Aug 18–Nov 10	25
2015	May 5–Jun 1	15
2015	Jun 8–Jun 23	12.5
2015	Jun 23–Jul 27	20
2015	Jul 28–Aug 8	15
2015	Aug 8–Nov 20	20

Table 3.2. Experimental conditions and calculated Mn oxidation half-times (t0.5) from the laboratory incubations. The treatments included a slurry of reservoir particulates spiked with Mn (PMn), reservoir water spiked with Mn (WMn), a slurry of particulates without the Mn spike (P), a slurry of sterilized particulates spiked with Mn (SPMn), and sterilized reservoir water spiked with Mn (SWMn). Half-times were not calculated for the P, SPMn, or SWMn treatments because there was a negligible decrease in the initial soluble Mn concentration. Values in parentheses are the standard deviation of the measurements over the 18 day-long experiment. Incubation flasks were kept at 22°C.

Experiment	Mean DO (mg/L)	Mean pH	$t_{0.5}$ (days)
PMn	8.6(1.07)	6.7(0.35)	0.98
WMn	8.3(0.55)	6.6(0.32)	30
P	8.3(0.61)	6.8(0.22)	
SPMn	8.3(0.64)	8.2(0.22)	
SWMn	8.2(0.62)	6.9(0.40)	

Table 3.3. Summary of zero-order Mn oxidation rates in this study and collected from the published literature. All experiments were conducted under air-saturated conditions at room temperature. The initial Mn concentration, rate, and half-time values for the intermittent anoxia and well-oxygenated treatments are an average over the summer stratified period.

Reservoir	Mean pH	Initial Mn concentration (mg/L)	Mn oxidation rate (mg/L/d)	Half-time (d)	Experiment type	Sample treatment
FCR (this study)	6.7	1.69	0.86	0.98	Laboratory	Slurry of reservoir particulates
FCR (this study)	6.6	2.36	0.039	30	Laboratory	Reservoir water
FCR (this study)	6.8[4]	0.94	0.014	33	Field (reservoir-scale)	Intervals of HOx system deactivation in FCR (2014)
FCR (this study)	6.6	0.84	0.028	15	Field (reservoir-scale)	Continuous HOx system activation in FCR (2015)
Lake Zurich[1]	7.5	0.385	0.0058-0.084	2.3-33	Laboratory	Reservoir water spiked with "Mn-bacteria"
Lake Biwa[2]	7	0.100-0.750	0.0008-0.0021	1-3	Laboratory	Anoxic hypolimnetic waters aerated in the lab
Lake Oneida[3]	8-8.4	0.066	0.016	2.1	Laboratory	Hypolimnetic water

[1]Diem and Stumm (1984)
[2]Kawashima et al. (1988)
[3]Chapnick et al. (1982)
[4]pH measured at 6.2 m depth only

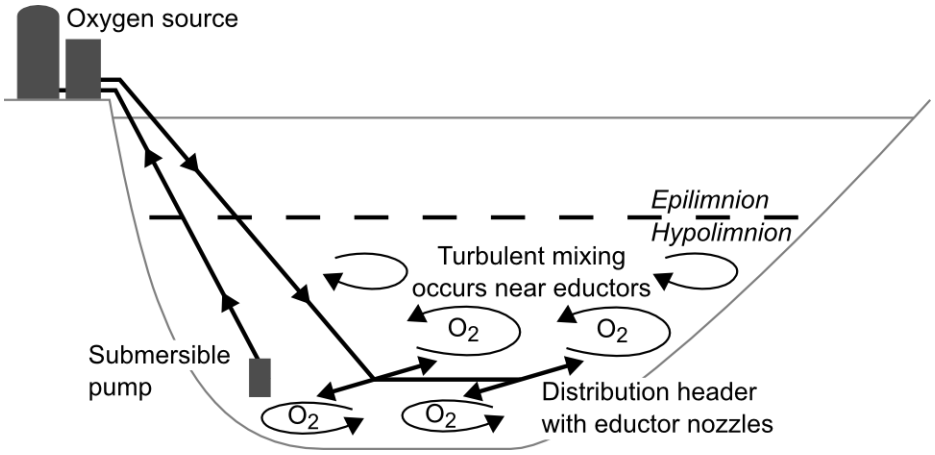

Figure 3.1. Hypolimnetic oxygenation systems cause turbulence in the water column that may lead to physical mixing of the hypolimnion. This figure depicts the mixing induced by the side-stream supersaturation system installed in FCR. This figure is adapted from (Gerling et al., 2014).

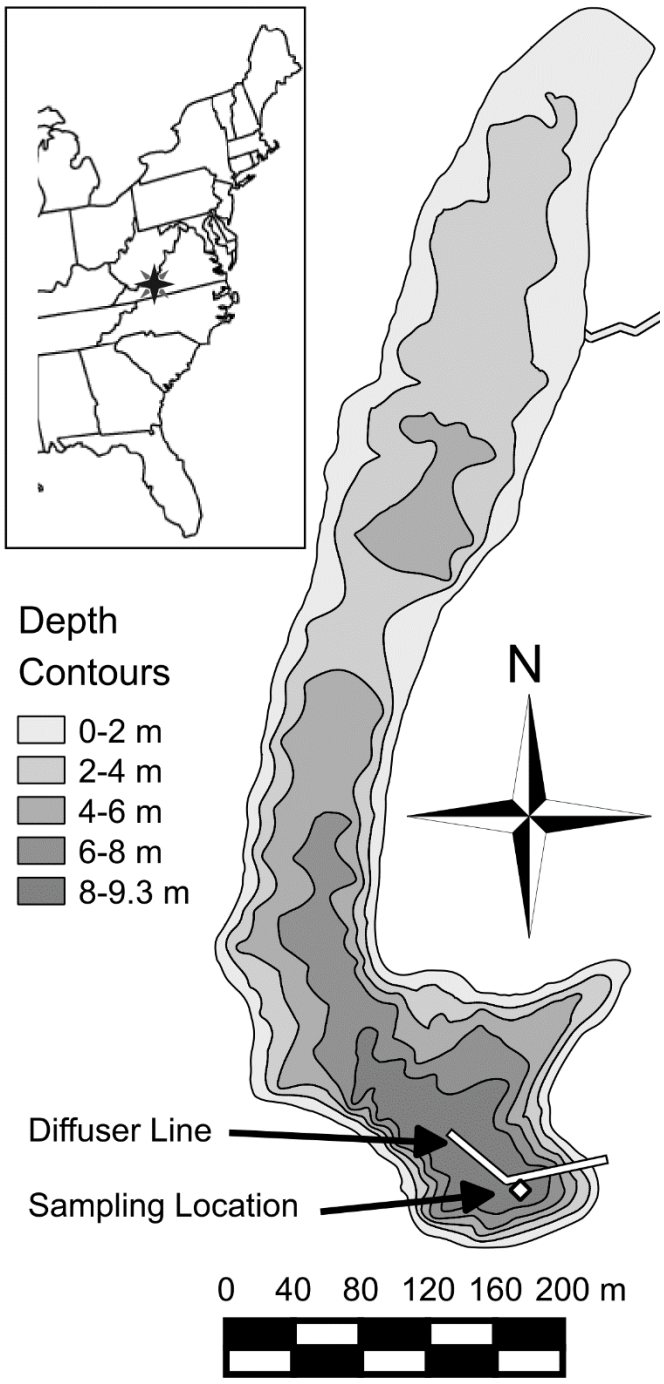

Figure 3.2. Falling Creek Reservoir bathymetry, location of oxygenation system diffuser lines, and water sample collection site.

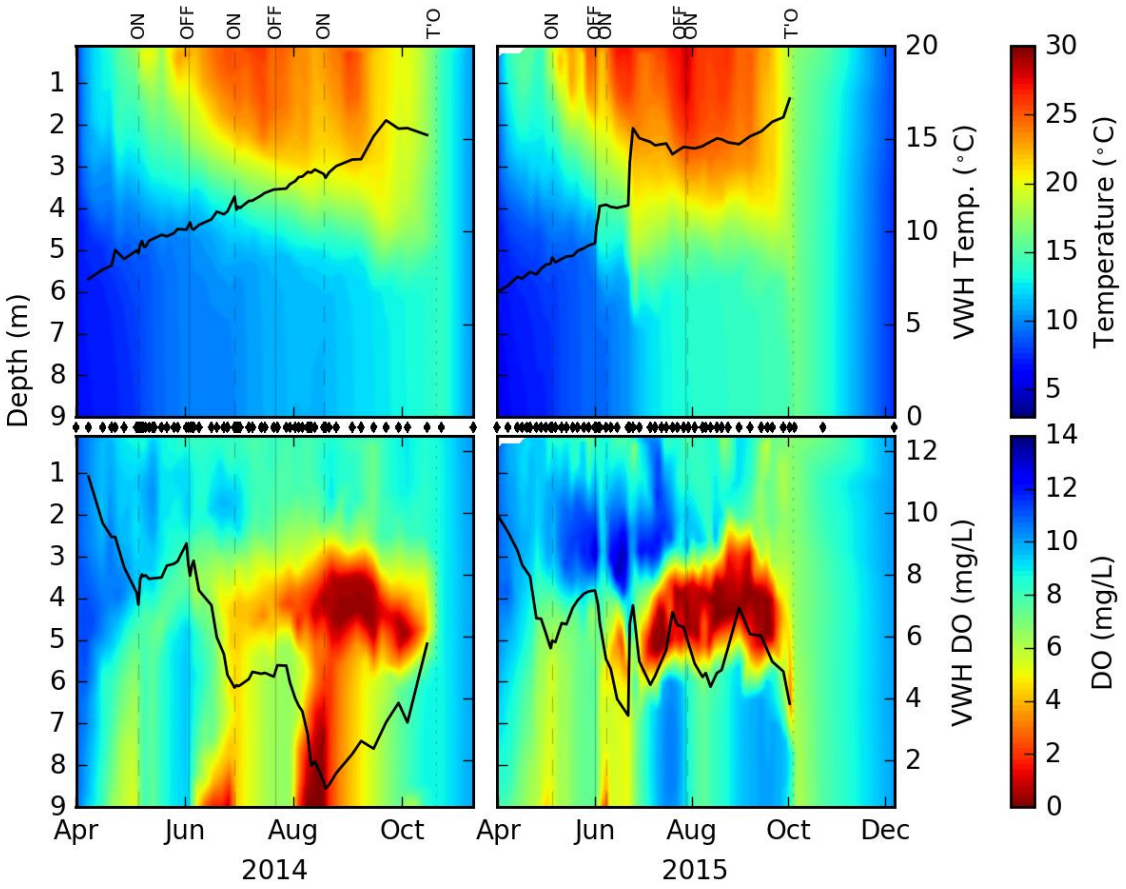

Figure 3.3. Temperature (top) and DO concentrations (bottom) at the deepest location in FCR during 2014 (left) and 2015 (right). The volume-weighted hypolimnion temperature and volume-weighted hypolimnetic DO concentrations are shown as the solid line in the top and bottom panels, respectively. Sampling dates are shown as the black diamonds between panels, with linear interpolation between them. Vertical dashed lines indicate when the HOx was activated ('ON'), vertical solid lines indicate when the HOx system was deactivated ('OFF'), and the vertical dotted lines indicate the approximate date of reservoir destratification ('T/O').

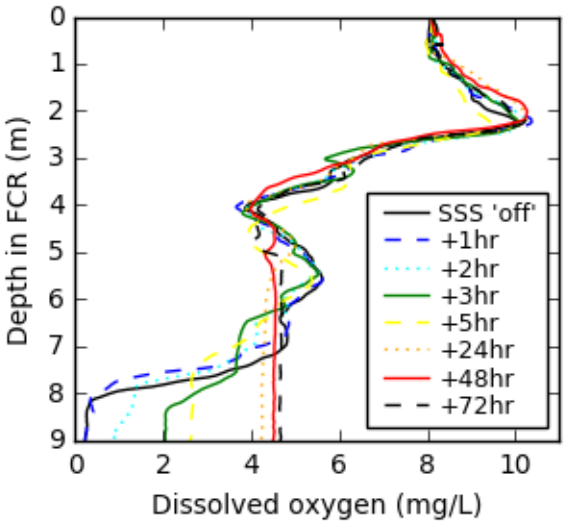

Figure 3.4. Dissolved oxygen profiles at the deepest location in FCR immediately prior to activating the HOx on 29 June, 2014 and at specified intervals afterwards: e.g., +1 hr indicates the profile was collected one hour after the HOx was activated.

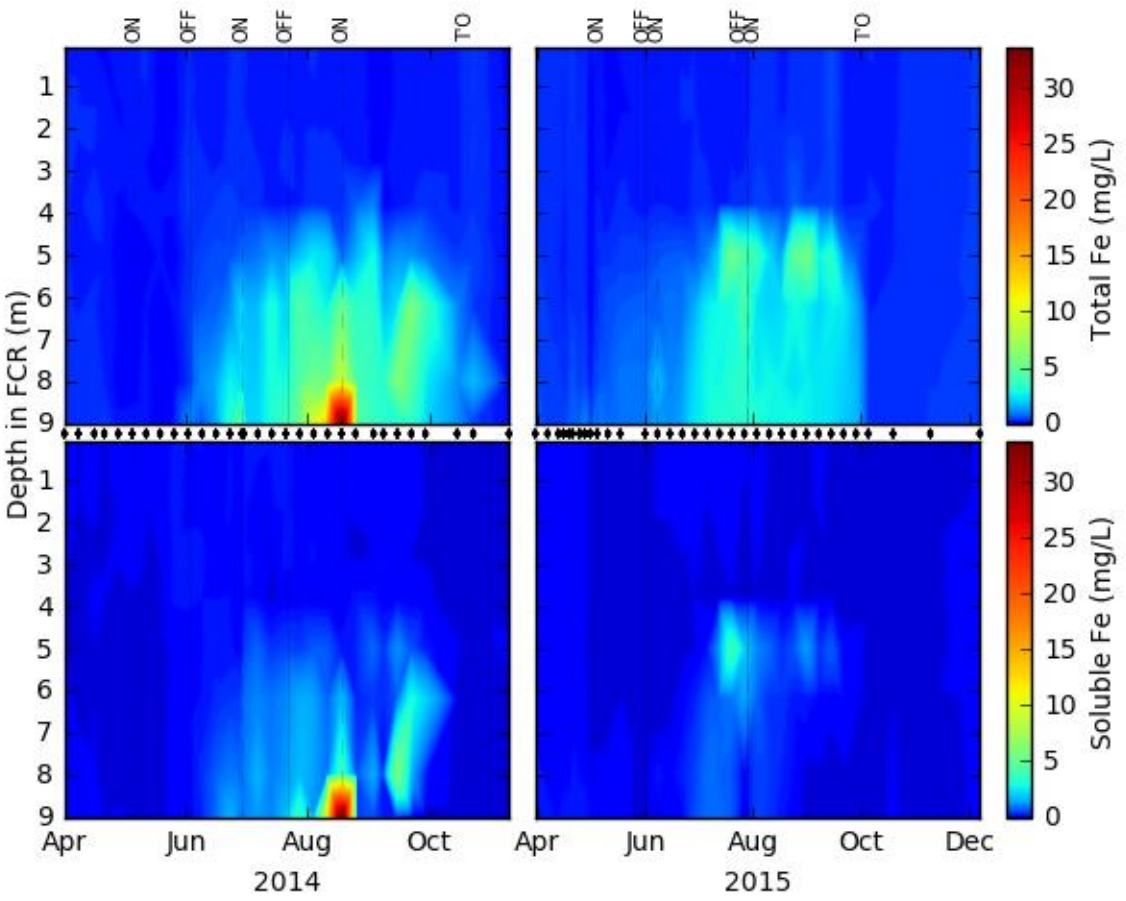

Figure 3.5. Total (top) and soluble (bottom) Fe concentrations in FCR during 2014 (left) and 2015 (right). Samples were collected from nine depths in 2014 and seven depths in 2015; sampling dates are shown as the black diamonds between panels. The color map has been skewed to better illustrate patterns at concentrations <10 mg/L. Vertical dashed lines indicate when the HOx was activated (’ON’), vertical solid lines indicate when the HOx system was deactivated (’OFF’) and the vertical dotted lines indicate the approximate date of reservoir destratification (’T/O’).

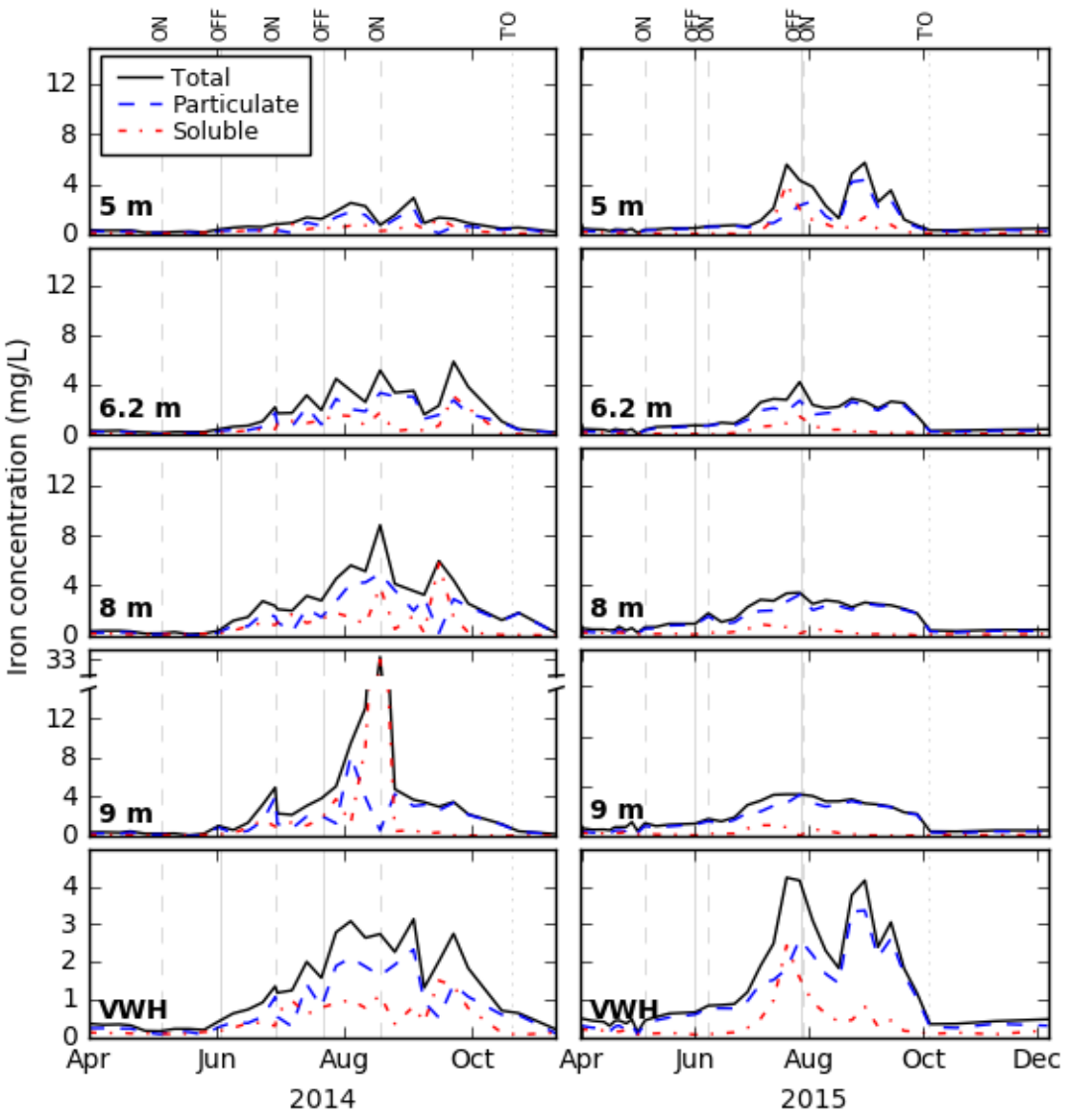

Figure 3.6. Total (black solid line), particulate (blue dashed line) and soluble Fe (red dotted line) concentrations in the four hypolimnetic sample depths and the volume-weighted hypolimnetic Fe concentrations ('VWH') during 2014 (left) and 2015 (right). Vertical dashed lines indicate when the HOx was activated ('ON'), vertical solid lines indicate when the HOx system was deactivated ('OFF') and the vertical dotted lines indicate the approximate date of reservoir destratification ('T/O').

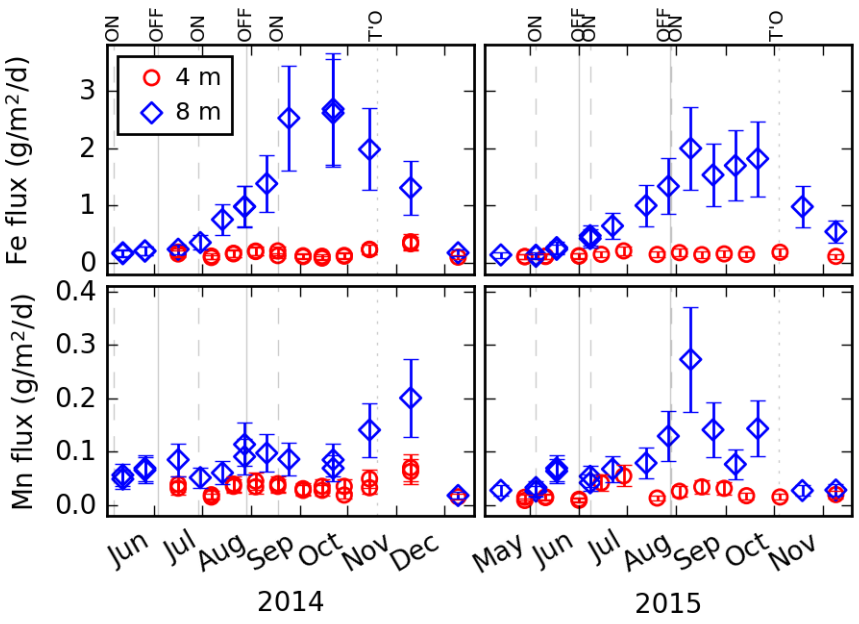

Figure 3.7. Particulate Fe (top) and particulate Mn (bottom) flux at 4 m (red circles) and 8 m depth (blue diamonds) in FCR during 2014 (left) and 2015 (right). Samples were collected every 14-28 days and each data point represents the average daily flux over the preceding interval. Vertical dashed lines indicate when the HOx was activated ('ON'), vertical solid lines indicate when the HOx system was deactivated ('OFF'), and the vertical dotted lines indicate the approximate date of reservoir destratification ('T/O'). The error bars represent the standard deviation of replicate measurements.

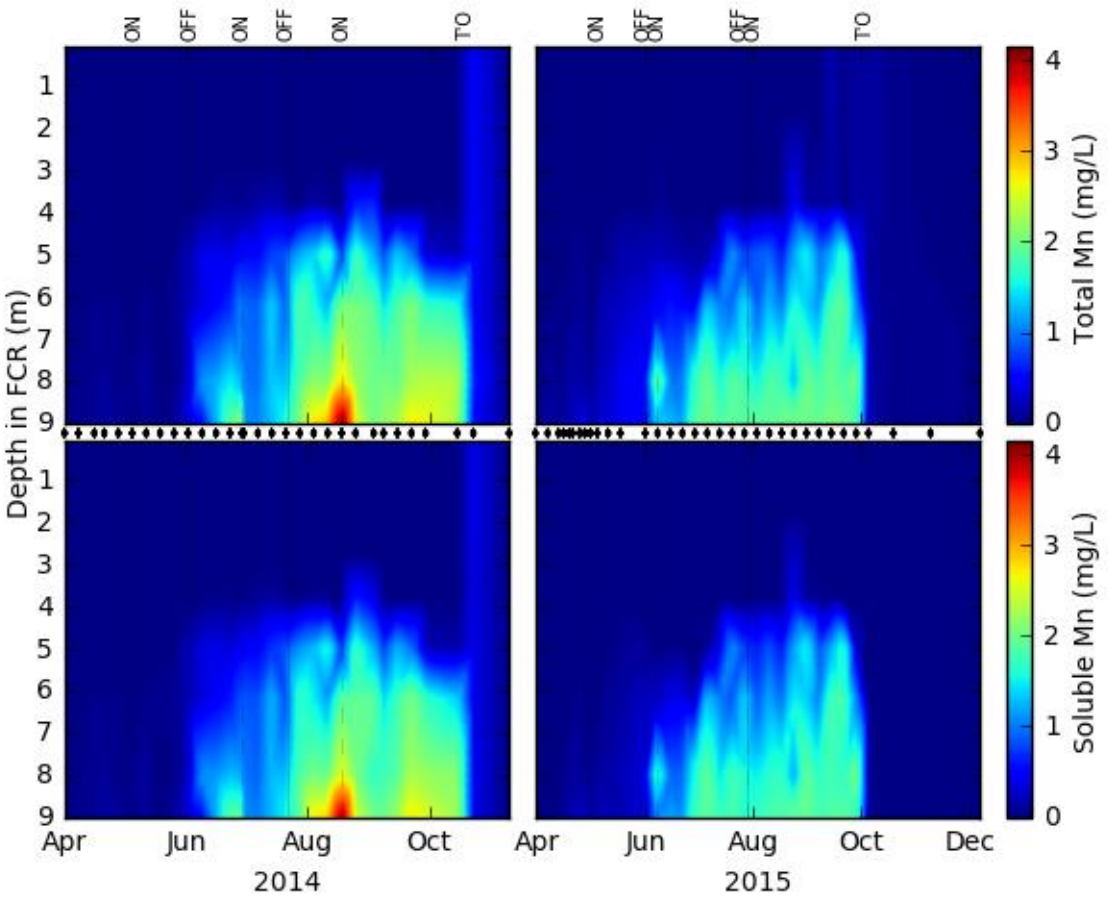

Figure 3.8. Total (top) and soluble (bottom) Mn concentrations in FCR during 2014 (left) and 2015 (right). Samples were collected from nine depths in 2014 and seven depths in 2015; sampling dates are shown as the black diamonds between panels. Vertical dashed lines indicate when the HOx was activated (’ON’), vertical solid lines indicate when the HOx system was deactivated (’OFF’) and the vertical dotted lines indicate the approximate date of reservoir destratification (’T/O’).

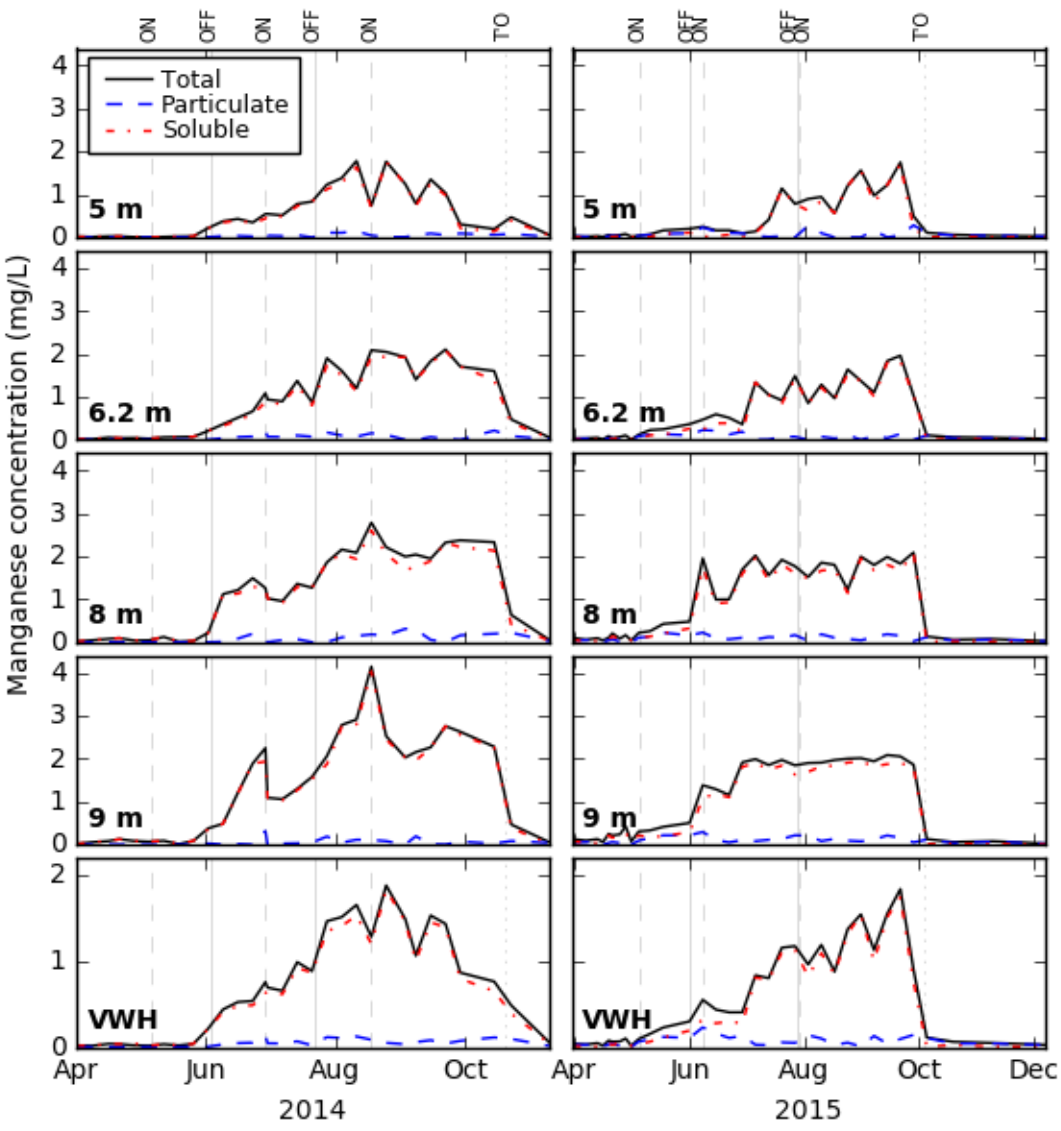

Figure 3.9. Total (black solid line), particulate (blue dashed line) and soluble Mn (red dotted line) concentrations in the four hypolimnetic sample depths and the volume-weighted hypolimnetic Mn concentrations ('VWH') during 2014 (left) and 2015 (right). Vertical dashed lines indicate when the HOx was activated ('ON'), vertical solid lines indicate when the HOx system was deactivated ('OFF') and the vertical dotted lines indicate the approximate date of reservoir destratification ('T/O').

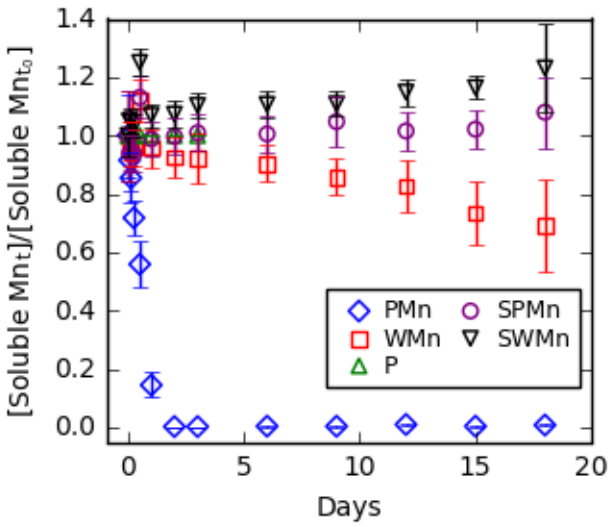

Figure 3.10. Change in Mn concentration over time in incubation flasks containing reservoir particulates and water collected from the 4 m sedimentation traps deployed in FCR. The treatments included a slurry of reservoir particulates spiked with Mn (PMn), reservoir water spiked with Mn (WMn), a slurry of particulates without the Mn spike (P), a slurry of sterilized particulates spiked with Mn (SPMn), and sterilized reservoir water spiked with Mn (SWMn). Error bars represent the standard deviation of three replicate measurements. Experimental conditions are shown in Table 3.2.

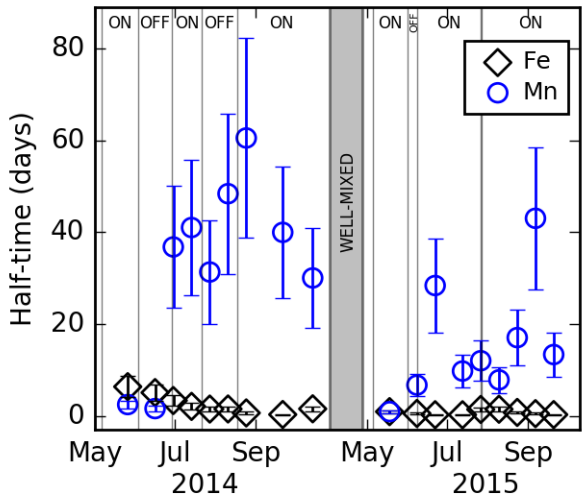

Figure 3.11. Half-time of soluble Fe (black diamonds) and Mn (blue circles) in the hypolimnion of FCR during 2014 and 2015. The shaded area represents the well-mixed period between years. Vertical dashed lines indicate the transition between HOx system activation ('ON') and deactivation ('OFF').

CHAPTER 4. HYDROLOGIC AND GEOCHEMICAL CONTROLS ON FE AND MN MASS BUDGETS IN A DRINKING WATER RESERVOIR

Zackary W. Munger, Alexandra B. Gerling, Cayelan C. Carey, Kathleen D. Hamre, Jonathan P. Doubek, Ryan P. McClure, Madeline E. Schreiber
A version of this chapter is in preparation for publication in Applied Geochemistry

ABSTRACT

In seasonally stratified lakes and reservoirs, shifting redox conditions in the hypolimnion and hydrologic conditions in the watershed can influence the retention of metals and their exchange between the sediments and water column. We calculated a mass budget for iron (Fe) and manganese (Mn) in a shallow drinking water reservoir over a two-year period in which we manipulated the discharge in the tributary inflow (external loads) and dissolved oxygen (DO) concentrations (internal loads) in the hypolimnion at the whole-ecosystem scale. We found that the rate of release of Fe and Mn from the sediments into the water column was influenced by water column DO concentrations, with greater release occurring during longer periods of anoxia; however, both metals were released from the sediments, even during well-oxygenated conditions. Surprisingly, the redox conditions in the hypolimnion had no effect on the net retention of metals in the reservoir. Instead, the net retention of Fe and Mn was generally higher (i.e., the reservoir behaved as a metal sink) when the external metal loads were elevated during periods of increased inflow discharge. In summary, we found that manipulating hypolimnion DO concentrations had a large effect on the internal redox cycles of Fe and Mn, but that the source/sink behavior of the reservoir in the watershed was driven primarily by external loads.

1. INTRODUCTION

The biogeochemical cycles of iron (Fe) and manganese (Mn) can have substantial effects on water quality in freshwater lakes and reservoirs. For example, the accumulation of Fe and Mn in the water column causes issues with staining, odor, and taste that require treatment for potable use (Fe and Mn concentrations are regulated in drinking water at 0.3 mg/L and 0.05 mg/L, respectively; United States Environmental Protection Agency, 2016; World Health Organization, 2004). Furthermore, the reductive dissolution of oxidized, insoluble Fe- and Mn-oxyhydroxides can cause adsorbed trace metals, some of which are toxic at low concentrations (e.g., arsenic and cadmium), to enter the water column (Appelo and Postma, 2005; Balistrieri et al., 1994; Olivie-Lauquet et al., 2001). Similarly, phosphorus adsorbed onto Fe-oxyhydroxides can also be released during Fe reduction (Amirbahman et al., 2003; Rozan et al., 2002), which can stimulate cyanobacterial bloom formation (Orihel et al., 2015). Although laboratory- and field-based studies have characterized some of the drivers of Fe and Mn cycles in lakes and reservoirs (e.g., Aguilar and Nealson, 1998; Beutel et al., 2008; Davison, 1993; Davison and Woof, 1984; Hongve, 1997; Johnson et al., 1995; Shaked et al., 2004; Stauffer, 1986), examining the response of these cycles to systematic changes in both internal redox-sensitive loads, which are largely controlled by climatic conditions and net heterotrophy, and external metal loads, which are derived from watershed sediments, is challenging in most systems because these forcings are not easily manipulated at the whole-ecosystem scale.

Redox conditions drive the internal cycling of Fe and Mn between insoluble, oxidized and soluble, reduced forms in lakes and reservoirs. In natural environments, Fe and Mn occur in both reduced (Fe^{2+} and Mn^{2+}) and oxidized (Fe^{3+}, Mn^{3+}, and Mn^{4+})

forms (Appelo and Postma, 2005). In the presence of oxygen, the oxidized forms of Fe and Mn are stable in most surface water environments (Hem, 1972). However, the development of anoxia (DO concentration <0.5 mg/L) in thermally stratified lakes and reservoirs can shift the redox potential to favoring the reduced metal forms (Hem, 1972; Lerman et al., 1995). Reducing conditions in the sediments can cause the reductive dissolution of oxidized Fe and Mn, where the soluble forms can accumulate in the sediment pore waters and diffuse into the overlying water column (Davison, 1993).

The depletion of DO has been well-recognized as a factor in the accumulation of Fe and Mn, and as a result, whole-lake manipulation of water column DO concentrations is increasingly used to manage Fe and Mn in drinking water systems (Beutel and Horne, 1999; Bryant et al., 2011; Gantzer et al., 2009; Gerling et al., 2014; Zaw and Chiswell, 1999). To effectively manage these manipulations and understand potential cascading effects on ecosystem function, it is critical to characterize the influence of hypolimnetic DO on exchange of metals between sediments and the water column.

In addition to the effects of DO on internal metal loadings, external metal loadings also have large effects on water column concentrations and the stock of Fe and Mn available for sediment exchange. For example, Davison (1993) found that ~10% of the soluble Fe released from the sediments into the water column of a meromictic lake was lost via surface water outflows, while the remaining 90% was eventually oxidized and returned to the sediments to complete a redox cycle. Without an external supply, the inventory of Fe available to participate in internal cycles would become smaller each year due to export via the outflows. The magnitude of external Fe and Mn loads to lakes and reservoirs has been quantified in several studies, which have reported loadings that were

between 10-50% of the water column metal mass annually (Davison, 1981; Graham et al., 2002; Hongve, 1997).

There is inherent variability in the metal loading from external sources across the broad spectrum of lake and reservoir systems. For example, Hongve (1997) reported external loading of Fe and Mn into a reservoir that varied by more than a factor of ten during the year in response to changing streamflow conditions. However, previous studies, have not investigated the influence of long-term (months to years) changes in stream discharge on lake or reservoir metal cycles or the net retention of metals in these systems. Understanding the effects of changing external loads within a lake or reservoir is needed for predicting how changes in watershed hydrology (e.g., resulting from climate change, channelization, or flow-regulation) can alter Fe and Mn cycles.

While many studies have examined the effects of manipulating internal and/or external loadings on nutrient (e.g., N and P) dynamics in lakes and reservoirs (e.g., Gerling et al., 2016; Köhler et al., 2005; Marsden, 1989; Van der Molen and Boers, 1994), the response of whole-ecosystem Fe and Mn budgets to similar manipulations remains unknown. Examining these effects on the exchange of metal between the sediments and water column is particularly important for understanding the relative importance of internal and external loadings on lake and reservoir water quality and how the recycling of metals may influence the release of adsorbed phosphorus and trace metals. Furthermore, quantifying the retention of Fe and Mn mass under different external streamflow and internal redox conditions is critical for understanding when the waterbody behaves as a source or sink for Fe and Mn in the watershed.

We conducted whole-ecosystem manipulations of a shallow, drinking water reservoir in a temperate, forested watershed to examine the relative importance of changing inflow discharge (external loads) and internal redox conditions (internal loads) on reservoir Fe and Mn budgets. By manipulating a hypolimnetic oxygenation system in the reservoir, we established both anoxic and well-oxygenated conditions during the summer stratified period. By manipulating the inflow water entering the reservoir, we also created intermittent periods of elevated and lower flow. We calculated the rate of Fe and Mn exchange between the reservoir water column and sediments as well as the net retention of these metals in the reservoir under elevated discharge, intermittent anoxia, and well-oxygenated scenarios. Our overarching goal of the experimental manipulations was to evaluate how changing external and internal loads altered the ability of the reservoir to serve as a sink or source of Fe and Mn to downstream environments.

2. METHODS

2.1. STUDY SITE

Falling Creek Reservoir (FCR) is a shallow (maximum depth=9.3 m), dimictic drinking water reservoir located in a forested watershed in southwestern Virginia (Figure 4.1). The reservoir is primarily fed by a surface water tributary that receives water from upgradient Beaverdam Reservoir (BVR; Figure 4.1). Both FCR and BVR become thermally stratified each year between April and October, which leads to the development of hypolimnetic anoxia. During the summer stratified period in previous years, FCR has exhibited summer cyanobacterial blooms and elevated concentrations of Fe, Mn, and P associated with hypolimnetic anoxia (Gerling et al., 2016, 2014). We monitored the Fe and Mn budgets in FCR during whole-ecosystem manipulations that we conducted in 2014 and 2015.

2.2. HYPOLIMNETIC OXYGENATION

A side stream supersaturation oxygenation system was deployed at FCR in 2012 to manage DO concentrations in the hypolimnion (Gerling et al., 2014). The hypolimnetic oxygenation (HOx) system is comprised of a submersible pump, inlet piping, an oxygen contact chamber, an oxygen source, outlet piping, and a distribution header. The submersible pump positioned at 8.5 m depth withdraws water from the hypolimnion and transfers it through inlet piping to the onshore oxygen contact chamber. Oxygen gas is injected into the water in the contact chamber, resulting in DO concentrations that are supersaturated with respect to hypolimnion conditions. The oxygenated water is transferred through outlet piping to a distribution header positioned at 8.5 m depth, where it is injected back into the hypolimnion. Evenly spaced eductor nozzles on the distribution header were angled upwards to promote mixing of oxygenated water throughout the hypolimnion without disturbing the bottom sediments (see Gerling et al., 2014, for a more detailed description of the oxygenation system in FCR). Gerling et al. (2014) showed that operation of the HOx system in FCR successfully increased hypolimnetic DO concentrations by up to ~1 mg/L/week without disrupting thermal stratification.

2.3. EXTERNAL FLOW CONDITIONS

The stream flow rate in the tributary inflow that enters FCR from BVR can be manipulated via an intake valve in the epilimnion of BVR. Flow from BVR is channeled through an underground pipe for ~750 m before discharging into the tributary (Figure 4.1). After entering the tributary, the water flows an additional ~950 m through riffle-pool sequences in a shallow, meandering channel (<1 m depth) before entering FCR.

Discharge in the tributary inflow is measured with a contracted rectangular weir located ~300 m upgradient from FCR (see Gerling et al., 2014).

We manipulated flow conditions in the tributary inflow by opening the intake valve within BVR. On 28 April 2014, we opened the intake valve to recreate the high flow conditions observed after very heavy precipitation events in the watershed (Gerling et al., 2016). The intake remained continuously open after 28 April, 2014. However, during the four months after we opened the intake valve, the water level in BVR decreased; by late September the water level was below the intake opening and discharge in the tributary inflow returned to normal levels.

2.4. INTERNAL REDOX CONDITIONS

We created alternating intervals of anoxic and well-oxygenated conditions in the hypolimnion of FCR by manipulating HOx system operation (see Table 4.1 for the dates of HOx system activation). Prior to the onset of thermal stratification each year, the HOx system was not operational. During the summer stratified period in both 2014 and 2015, we activated the HOx system after DO concentrations near the bottom sediments reached approximately 50% of oxygen saturation levels. In 2014, we deactivated the HOx system during two intervals each lasting ~4 weeks; during each period of deactivation, the bottom waters became anoxic (DO concentration <0.5 mg/L). In 2015, we continuously operated the HOx system throughout the summer stratified period, except for a one-week interval after 1 June, and a several hour period on 27 July for HOx system maintenance.

2.5. DATA COLLECTION

We monitored temperature, DO, and water quality parameters at least weekly in FCR and the tributary inflow between April and October in 2014 and 2015. Depth profiles of temperature and DO were collected at the deepest site in FCR (Sampling

Location, Figure 4.1) 1-3 times per week using a Seabird Electronics SBE 19plus high-resolution profiler (CTD) as described in (Gerling et al., 2014). Temperature and water level in the tributary inflow were measured every 15 minutes at the weir (Figure 4.1) using an INW Aquistar PT2X pressure sensor. We also measured the water level in the reservoir each day using a staff gage. The flow velocity over the spillway was measured using a current meter and the discharge was calculated using the velocity-area method (Fetter, 2000). Measurements of flow velocity over the spillway were collected at three different stages to construct a rating curve. Daily measurements of precipitation were collected using a rain gauge at the water sample collection site.

We measured Fe and Mn concentrations weekly in FCR and its tributary inflow between April and October in 2014 and 2015. We collected water samples from nine depths in the water column of FCR in 2014 (0.1, 0.8, 1.6, 2.8, 3.8, 5.0, 6.2, 8.0 and 9.0 m) and seven depths in 2015 (0.1, 1.6, 3.8, 5.0, 6.2, 8.0 and 9.0 m) using a 4 L Van Dorn sampler (Wildlife Supply Company). We also collected water samples in the inflow stream at the weir (~150 m upgradient from FCR). We collected both raw and filtered water samples, which were analyzed for total and soluble metal fractions, respectively. Filtered samples were filtered (0.45 μm pore size) immediately after collection. Raw and filtered water samples were preserved by lowering the pH to <2 with trace metal grade nitric acid prior to analysis. We analyzed the samples for Fe and Mn using an ICP-MS (Thermo Electron X-Series) following APHA Standard Method 3125-B (American Public Health Association et al., 1998).

2.6. DATA ANALYSIS

We calculated a water budget to quantify the inflows and outflows to FCR. Using those data, we calculated a metals (Fe and Mn) budget in FCR (refer to Figure 4.2 for the

inflows and outflows) to quantify the net rates at which metals were released from the sediments into the water column in FCR under different tributary inflow discharge and hypolimnion redox scenarios. We examined the net release of Fe and Mn from the sediments into the hypolimnion because the HOx system only influences hypolimnion DO concentrations (Gerling et al., 2014). We also calculated the net retention of Fe and Mn in the reservoir to quantify the influence of inflow and redox conditions on the net retention of Fe and Mn in the reservoir.

2.6.1. WATER BUDGET

The water budget was calculated using:

$$\frac{dV}{dt} = Q_{tri} + PA - Q_{spw} - Q_{wtp} - EA \pm Q_{gw} \quad (1)$$

where dV/dt (m^3/d) is the daily change in reservoir volume, Q_{tri} (m^3/d) is the daily tributary inflow discharge, P (m/d) is the daily precipitation, A (m^2) is the reservoir surface area at full pond (119900 m^2), Q_{spw} (m^3/d) is the daily spillway discharge, Q_{wtp} (m^3/d) is the daily water treatment withdrawal rate, E (m/d) is the daily direct evaporation rate, and Q_{gw} (m^3/d) is the flow rate contributed by groundwater and runoff. We measured all inflows and outflows with exception of Q_{gw}, which we solved for using Equation 1.

We calculated the daily change in reservoir volume using the water level measurements in FCR from:

$$V = 51.88z^4 - 1662.83z^3 + 21341.78z^2 - 131246.01z + 324105.13 \quad (2)$$

where z (m) is the depth of the water level in FCR below full pond (508 m above mean sea level). The coefficients in Equation 2 were determined from a polynomial regression of the cumulative reservoir volume as a function of depth. We calculated the mean daily

discharge in the tributary inflow using the water level measurements at the weir as described by (Gerling et al., 2014). We calculated the discharge over the spillway using:

$$Q_{spw} = 3.583z_s^2 + 0.122z_s \quad (3)$$

where z_s (m) is the water level above the spillway crest. Direct evaporation from the reservoir was calculated using the Priestley-Taylor method modified from (Rosenberry et al., 2007):

$$E = \alpha \frac{m_{vap}}{m_{vap} + \gamma} \times \frac{R_{net}}{l_{vap}\rho} \quad (4)$$

where α (1.26) is the Priestley-Taylor constant, m_{vap} (kPa/°C) is the slope of the saturated vapor pressure-temperature curve at the mean daily temperature, γ (kPa/°C) is the psychometric constant, R_{net} (MJ/m^{2}d) is the net radiation, l_{vap} (2.26 MJ/kg) is the latent heat of vaporization, and ρ (998 kg/m^3) is the density of water. Daily air temperature data were obtained for Roanoke-Blacksburg Regional Airport from NOAA's National Climatic Data Center (Menne et al., 2016). Radiation fluxes were obtained from NASA's CERES SYN1deg-Day Ed3A dataset (Wielicki et al., 1996).

The tributary inflow water was consistently colder than the water at the surface of FCR, thus we assumed that the tributary water was entrained in the hypolimnion upon entering FCR, following Gerling et al. (2016). To balance the addition of the tributary inflow into the constant hypolimnion volume, we assumed that water was being entrained from the hypolimnion across the thermocline at a rate equivalent to the tributary inflow discharge into the hypolimnion. We determined the thermocline depth for each CTD temperature profile by analyzing those data with Lake Analyzer, a Matlab program (Mathworks; Read et al., 2011).

2.6.2. METALS BUDGET

We calculated the metals budget in the hypolimnion at weekly intervals using:

$$\frac{dM_{hyp}}{dt} = L_{inf} - L_{th} \pm L_{exch} \quad (5)$$

where dM_{hyp}/dt (kg/d) is the rate of change in metal (Fe or Mn) mass in the hypolimnion water column between weekly measurements, L_{inf} (kg/d) is the metal loading in the tributary, L_{th} (kg/d) is the metal loading across the thermocline, and L_{exch} (kg/d) is the net internal metal loading from the sediments into the hypolimnion water column. We used metal concentrations measured at 5 m depth, which was always just below the thermocline in both years, in calculating the metal loading across the thermocline. The vertical transfer of water across the thermocline was the only outflow from the hypolimnion; the spillway and intakes for the water treatment plant were situated in the epilimnion. The net internal loading, L_{exch}, represents the balance between the rate of metal release from the sediments into the water column and the return of metals from the water column back to the sediments, where positive L_{exch} values indicate that the rate of metal release from the sediments into the water column was greater than the rate at which metals returned to the sediments.

The metal mass in the hypolimnion was calculated for each sampling date using:

$$M_{hyp} = \sum C_z V_z \quad (6)$$

where M_{hyp} (kg) is the metal (Fe or Mn) mass in the hypolimnion, C_z (kg/m^3) is the metal concentration at depth z in the hypolimnion and V_z (m^3) is the volume of the water at depth z in the hypolimnion. The volume at each depth z was determined from the reservoir bathymetry in Gerling et al. (2014). We linearly interpolated the metal concentrations at the depths of the bathymetry data (~0.3 m intervals); we only

interpolated metal concentrations measured below the thermocline. We calculated dM_{hyp}/dt as the difference between M_{hyp} over the preceding week divided by 7 days.

We calculated weekly inflow and outflow metal loadings as the sum of the daily loads divided by 7 days. To calculate daily loadings, we first linearly interpolated the metal concentrations in the tributary, spillway, and water treatment at each day. We calculated the loadings using the daily flow measurements with:

$$L_j = C_j \times Q_j \tag{7}$$

where L_j (kg/d) is the metal (Fe or Mn) loading at location j (e.g., tributary inflow, spillway outflow, water treatment intakes), C_j (kg/m^3) is the metal concentration at j, and Q_j (m^3/d) is the flow rate at j.

Finally, we calculated the net export loading of Fe and Mn in the reservoir following the approach used in Cook et al. (2010):

$$L_{net} = L_{spw} + L_{wtp} - L_{inf} \tag{9}$$

where L_{net} is the net export metal (Fe or Mn) loading in the reservoir, L_{inf} (kg/d) is the metal loading in the tributary, L_{spw} (kg/d) is the metal loading in the spillway, and L_{wtp} (kg/d) is the metal loading in the water treatment intakes. The net retention rate, L_{net}, represents the balance between metal export and import in the reservoir, where positive L_{net} indicates that more metal is being exported from the reservoir via the spillway and water treatment intakes than is being imported via the tributary inflow. Over time, consistently negative L_{net} indicates that metal mass is accumulating in the reservoir and its sediments, which can be subsequently released into the water column.

3. RESULTS

3.1. WATER BALANCE AND TRIBUTARY FLOW

We successfully manipulated both inflow discharge and hypolimnetic oxygen conditions during the two-year whole-ecosystem experiment. During the four-month period after opening the intake in BVR in April 2014, the mean discharge in the tributary over this period (8.1±0.3 ML/d; 1 SD) was ~144% higher than the mean discharge observed during the rest of the study (3.3±1.8 ML/d; Figure 4.3). The groundwater/runoff term, which was determined from Equation 1, was also a substantial water source to FCR, comprising 42±21% and 29±30% of the total water input on average in 2014 and 2015, respectively. Direct inputs from precipitation were generally a minor component of the total input, comprising 3±7% and 5±13% of the input on average in 2014 and 2015, respectively. The outflows were dominated by the spillway at the surface of the reservoir, which contributed 56±27% of the total outflow on average in both years. The water treatment intakes removed ~3.3 ML/d when the treatment plant was operational; however, no water was removed from FCR via the water treatment intakes after 19 September 2014 or after 9 July 2015 throughout autumn in both years. Direct evaporation from the surface of FCR contributed 13±18% of the total outflow on average across both years.

3.2. DISSOLVED OXYGEN CONDITIONS IN FCR

By manipulating the HOx system, we were able to create alternating periods of anoxia and well-oxygenated conditions in the hypolimnion of FCR during the summer stratified periods in 2014 and 2015 (Figure 4.4). The onset of thermal stratification in FCR began in April and stratified conditions were maintained until October in both years. When the HOx system was deactivated, the volume-weighted mean hypolimnion (VWH) DO concentration decreased at a mean rate of 0.16±0.04 mg/L/d (1 SD; Figure 4.4). After the HOx system was activated, the VWH DO concentration increased at a mean rate of

0.04±0.03 mg/L/d, and DO concentrations rapidly homogenized throughout the hypolimnion due to mixing induced by the HOx system (Figure 4.4).

Operation of the HOx system controlled the development of anoxic or well-oxygenated conditions throughout both years (Figure 4.4). In early April 2014, we measured DO concentrations >10 mg/L throughout the hypolimnion; however, DO concentrations decreased throughout the hypolimnion as thermal stratification intensified, reaching ~5 mg/L near the bottom sediments in late April prior to HOx system activation. After the HOx system was activated, DO concentrations throughout the hypolimnion increased, including the water adjacent to the bottom sediments. After deactivating the HOx system, DO concentrations decreased throughout the hypolimnion, with the most rapid decreases along the depth profile occurring near the bottom sediments. During the two deactivation periods in summer 2014, the benthic layer became anoxic within a week after deactivation.

We continuously operated the HOx system for the majority of the summer stratified period in 2015, resulting in well-oxygenated conditions (Figure 4.4). Similar to 2014, we observed decreasing DO concentrations throughout the hypolimnion. When the HOx system was activated, DO concentrations in the bottom of the hypolimnion (~9.3 m depth) remained consistently >5 mg/L until anoxia developed during the one-week period of HOx system deactivation in early June 2015. In late July, the HOx system was deactivated for a several hours, during which time we observed a decrease in hypolimnion DO concentrations, but DO concentrations never decreased below 6 mg/L in the bottom of the hypolimnion.

3.3. HYPOLIMNETIC FE AND MN MASS

Total Fe and Mn mass increased in the hypolimnion during the summer stratified period regardless of HOx system operation, but the mass of soluble Fe and Mn in the hypolimnion was lower during well-oxygenated conditions in 2015 (Figure 4.5). During the early stratified period (between April and May), total Fe and Mn mass in the hypolimnion was low, but later in the summer stratified period (between June and September) of both 2014 and 2015, the total Fe mass in the hypolimnion increased by a factor of 8 or more and total Mn mass increased by a factor of 60 or more (Figure 4.5). When the hypolimnion was well-oxygenated between June and September in 2015, the mean soluble Fe and Mn mass in the hypolimnion was 43% and 39% lower, respectively, compared to the same period in 2014 when the hypolimnion was intermittently anoxic (Figure 4.5).

3.4. INTERNAL LOADING OF FE AND MN IN THE HYPOLIMNION OF FCR

We observed net release (positive L_{int}) of total and soluble Fe and Mn from the sediments into the hypolimnion during the majority of the summer stratified period in 2014 and 2015 (Figure 4.6). Early in the summer stratified period (between April and May), the internal loading of total and soluble Fe and Mn was generally near 0; however, between May and June 2014 when the tributary inflow discharge was elevated, we calculated negative L_{int} values for total Fe and, to a lesser degree, soluble Fe and total Mn, indicating that these metal fractions were accumulating in the reservoir sediments faster than they were being released into the water column (Figure 4.6). Between June and September in both years, the net internal loading of total and soluble Fe and Mn shifted towards consistently positive values, including when the hypolimnion was well-oxygenated in 2015 (Figure 4.6), indicating increased release of metals from the sediments into the water column. The positive internal loading between June and

September also corresponded to periods when the mass of total Fe and Mn in the hypolimnion water column was elevated (Figure 4.5).

The internal loading of both total and soluble metals was higher during intermittent anoxia in 2014 compared to the well-oxygenated conditions of 2015 (Figure 4.6). During the intermittent anoxic period in 2014, the mean internal loading of total Fe and Mn was 38% and 340% higher, respectively, than the mean internal loading of total Fe and Mn during the well-oxygenated period in 2015 (Figure 4.6). We observed the largest positive L_{net} values for both fractions of Fe and Mn in July and August in both years, indicating that the largest net release of metal mass from the sediments into the water column occurred during these two months of the summer stratified period.

3.5. IMPORT AND EXPORT OF FE AND MN IN FCR

After opening the inflow intake in BVR in late April 2014, the loading of total and soluble Fe and Mn into the reservoir from the tributary inflow (L_{inf}) increased and remained elevated until September 2014 (Figure 4.7). Between late April and late August 2014, the loading of total Fe and Mn in the tributary inflow was more than twice as high as the metal loadings measured during the rest of the study on average. Although the loading of soluble Fe and Mn in the tributary inflow was generally low in comparison to total fractions, during the period of elevated tributary flow (between late April and late August 2014) the loading of soluble Fe and Mn was higher by a factor of 5 or more on average compared to soluble metal loading observed during periods in the study (Figure 4.7).

Total and soluble Fe and Mn loading in the reservoir outflows was elevated between April and May in both years and throughout the period of elevated tributary inflow discharge (Figure 4.7). The metal loading in the spillway outflow constituted more

than 70% of the total and soluble metal loadings in the outflow (sum of spillway and water treatment intake outflows). Increased loadings of total and soluble Fe and Mn in the outflow between April and May in both years corresponded to higher discharge measurements in the spillway; discharge in the water treatment intakes did not vary during the year except for periods when the intakes were closed, which caused the metal loadings in the water treatment intakes to exhibit much less variation than observed in the spillway.

When the outflow metal loadings were elevated relative to the tributary inflow loadings early in the summer stratified period in both years, we observed net export of total and soluble Fe and Mn mass from FCR (positive L_{net}), but later in the summer stratified period the outflow loadings became small relative to the inflow loadings and we observed net import of these metals into the reservoir (negative L_{net}; Figure 4.7). Although the loading of Fe and Mn in the outflow generally was not higher between April and May 2014 compared to later in the stratified period in 2014, the inflow loadings were relatively low between April and May in comparison to the outflow loadings, which caused the net export of both fractions of Fe and Mn (Figure 4.7). After the intake valve in BVR was opened in late April, there was a shift towards negative L_{net} values, indicating that the import of total and soluble Fe and Mn mass exceeded its export. Between April and May 2015, we observed much higher loadings of total Fe and Mn and soluble Fe in the outflow, resulting in large calculated net export of these metals during this period (Figure 4.7). Later in the summer stratified period (between June and September) in 2015, the loading of both total and soluble Fe and Mn in the inflow and

outflow was lower compared to 2014, and as a result the L_{net} values were negative or close to 0 during this period (Figure 4.7).

Examining the combination of internal redox and external hydrologic conditions on the net export of metals from FCR, we observe that the reservoir behaves predominantly as a sink for metals in the watershed (Figure 4.8). The only condition under which the reservoir behaves as a source of metals is during high outflow, which reflects periods when additional sources of water, including runoff and groundwater inputs, are elevated. Comparing the high inflow-oxic and high inflow-anoxic conditions shows that the net export of both total Fe and Mn exhibited negligible difference under these different redox conditions in the hypolimnion (Figure 4.8).

4. DISCUSSION

The biogeochemical cycles of Fe and Mn in FCR were affected by the redox environments created in the hypolimnion and the manipulation of flow conditions in the tributary inflow. Below, we discuss the effects of the reservoir treatments on the exchange of Fe and Mn between the sediments and water column, the retention of metals in the reservoir, and the implications of manipulating reservoir conditions for water quality management.

4.1. INFLUENCE OF EXTERNAL AND INTERNAL SOURCES ON HYPOLIMNION METAL MASS

Our results show that the release of metals from the sediments had a substantial effect on the accumulation of Fe and Mn mass in the hypolimnion. Later in the summer stratified period of both years (between June and October), when the net internal loading (L_{int}) of metals between the hypolimnion sediments and water column was positive (Figure 4.6), we observed large increases in the masses of both total and soluble Fe and Mn in the hypolimnion (Figure 4.5). Predictably, the hypolimnion total and soluble Fe

and Mn masses reached their highest levels between July and August in both years (Figure 4.5), when anoxic conditions in the sediments are typically well-established in seasonally stratified lakes and reservoirs (Davison, 1993). Although we did not observe anoxic conditions near the sediments after June 8 in 2015 due to activation of the HOx system, we still observed the highest hypolimnetic total and soluble Fe and Mn masses in late summer (Figure 4.5).

The internal loading (L_{int}) of total and soluble Fe and Mn from the sediments into the water column was sensitive to DO concentrations in the hypolimnion. The net release of Fe and Mn from the sediments to the water column was higher (positive L_{int}) for most of the summer stratified period when the HOx system was intermittently deactivated in 2014 in comparison to extended periods of well-oxygenated conditions in 2015 (Figure 4.6). When the HOx system was deactivated for two four week-long intervals in 2014, the mean net release of Fe and Mn into the hypolimnion was 1.4 and 4.5 times higher than during continuous HOx system operation in 2015, respectively, suggesting that allowing anoxic conditions to develop near the bottom sediments greatly increased the release of metals into the water column, even after well-oxygenated conditions were reestablished in the water column. Furthermore, the continued release of Fe and Mn after oxygenated conditions were reestablished in 2014 suggests that conditions in the sediments, where the reduced Fe and Mn originates, are decoupled from the well-oxygenated conditions in the water column. In a nearby oxygenated reservoir, Bryant et al. (2011) found that although Mn concentrations in the water column decreased by up to 97% under well-oxygenated conditions, Mn concentrations in the sediment pore water continued to increase during HOx operation. Our results from 2015 also corroborate the continued

release from the sediments under a continuously oxygenated water column, although the release rates were lower in comparison to intermittent anoxia in 2014.

The tributary loading of Fe and Mn into FCR had a negligible immediate effect on metal mass in the water column. Early in the summer stratified period in both years (between April and May), we observed relatively minor changes to the masses of Fe and Mn in the hypolimnion (Figure 4.5). Between April and May in 2014, the loading of total Fe and Mn in the tributary inflow increased by a factor of six or more, up to 4.4 kg/d and 0.32 kg/d, respectively (Figure 4.7); however, the metal masses in the hypolimnion did not substantially increase until early June (Figure 4.5). The lack of increase in hypolimnion metal masses in response to increasing tributary inflow loading suggests that, while the tributary inflow was importing a large amount of metal mass daily compared to the total amount in the hypolimnion (mean hypolimnion masses of total Fe and Mn prior to June 2014 were 11.2 kg and 1.2 kg, respectively), the metals entering the reservoir from the tributary did not remain in the water column long enough to cause those metals to accumulate. In the early summer stratified period in 2015, we observed ~50% decrease in the loading of total Fe and Mn in the tributary inflow between mid-April and early June, yet the hypolimnion metal mass exhibited a slight increase during the same period, likely the result of increased release from the sediments, represented by L_{int}.

4.2. NET METAL IMPORT AND EXPORT IN FCR

We observed a shift from net export of total Fe and Mn early in the summer stratified period in both years to net import of these metals later in the summer stratified period in response to changing flow conditions (Figure 4.7). In general, we observed negligible changes in total Fe and Mn concentrations in the tributary inflow or outflows

during thermal stratification in FCR, suggesting that internal redox conditions had little effect on the amount of total Fe and Mn mass being retained in the reservoir. However, we generally observed net export of Fe and Mn from the reservoir when the tributary inflow discharge was low relative to the outflow discharge. Prior to opening the intake valve in BVR in early 2014, flow in the tributary inflow was relatively low (~2 ML/d) compared to the outflows (~10 ML/d), and although Fe and Mn concentrations in the tributary inflow were always higher than metal concentrations in the outflows, the higher outflow discharge caused the net export of total Fe and Mn. Similarly, in early 2015, the outflow discharge greatly exceeded the tributary inflow discharge and the result was a large net export of Fe and Mn from the reservoir (positive L_{net}). After the intake valve in BVR was opened in April 2014, we observed a shift from net metal export to net metal import as the metal loading into FCR exceeded the outflow loading (Figure 4.7). We also observed an increase in Fe and Mn concentrations with discharge in the tributary inflow, likely caused by greater entrainment of metal-bearing watershed sediments under high energy conditions, which resulted in the large net import of both total Fe and Mn. Later in the summer stratified period 2015, the tributary inflow discharge rarely exceeded 4 ML/d and the reservoir was generally net neutral in terms of net metal import and export. However, we did calculate a positive net import of both total Fe and Mn in July, when both the discharge in the spillway and water treatment intakes became 0.

Extended periods of elevated discharge in the tributary inflow or outflows dramatically changed the net metal import or export in FCR (Figure 4.7). In both monitoring years we observed periods of net export (positive L_{net}) early in the summer stratified period and net import (negative L_{net}) later in the summer stratified period.

However, the elevated tributary inflow discharge in 2014 caused the consistent net import of total Fe and Mn in 2014 and the elevated outflow discharge between April and May in both years caused the consistent net export of total Fe and Mn during these two months in both years. Although the tributary inflow discharge in 2014 was 45% higher on average compared to 2015, similar long term changes in annual streamflow are not uncommon (Fu et al., 2007), which could have long term implications for the accumulation of metals in many lakes and reservoirs.

Overall, FCR behaves as a sink for Fe and Mn in the watershed under most conditions (Figure 4.8). Redox conditions in the hypolimnion have limited influence on the net export (compare high inflow-oxic to high inflow-anoxic in Figure 4.8). Higher inflow conditions result in increasing the retention of metals in FCR (compare high inflow-oxic to low inflow-oxic). However, under high outflow conditions, which reflect elevated runoff and groundwater inputs, FCR behaves as a source of Fe and Mn to the watershed (high outflow-oxic condition in Figure 4.8). Further work is needed to quantify these other hydrologic influences, which can contribute both flow and metals to the reservoir.

5. CONCLUSIONS

The goal of this study was to examine the sensitivity of internal metal cycles and the net import/export behavior of a seasonally stratified reservoir in response to changing internal biogeochemical and external hydrologic conditions. Overall, our results showed that prior to onset of thermal stratification, there was a net transfer of Fe and Mn mass from the water column to the sediments supplied by allochthonous inputs. However, after the onset of thermal stratification, the internal exchange shifted to net release of Fe and Mn from the sediments into the water column, under both well-oxygenated and

intermittently anoxic conditions. The net release of both Fe and Mn from the sediments into the water column was greater when the water column was intermittently anoxic compared to continuous oxygenation.

We observed that the reservoir behaved as a source (net export downstream) for metals during the spring when outflow discharge was typically elevated compared to inflow discharge, reflecting additional sources of water to the reservoir, including runoff and groundwater inputs. Later in the stratified period, the reservoir shifted to a metal sink (net import to the reservoir), which began prior to the increase in internal metal release from the sediments.

In summary, the cycling of Fe and Mn within FCR was strongly influenced by internal redox conditions, but that cycling had little effect on the net import or export of metals from the reservoir. Conversely, hydrologic conditions in the inflows and outflows had little effect on the release of metals from the sediments into the water column, but had a large impact on the accumulation (net import) of metals in the reservoir.

ACKNOWLEDGMENTS

We thank the staff at the Western Virginia Water Authority for their long-term support and funding. In particular, we would like to thank Cheryl Brewer, Jamie Morris, Jeff Booth, Bob Benninger, and Gary Robertson. Jeffrey Parks, Mariah Redmond, Mariah Haberman, Madeline Ryan, Charlotte Harrell, Athena Tilley, and Bobbie Niederlehner provided critical help in the field and laboratory. This work was supported by the Institute for Critical Technology and Applied Science at Virginia Tech, Virginia Tech Global Change Center, and Fralin Life Sciences Institute.

Table 4.1. Dates of HOx system activation.

Year	Dates of activation
2014	May 5–Jun 3
2014	Jun 29–Jul 22
2014	Aug 18–Nov 15
2015	May 5–Jun 1
2015	Jun 8–Jun 23
2015	Jun 23–Jul 27
2015	Jul 28–Aug 8
2015	Aug 8–Nov 20

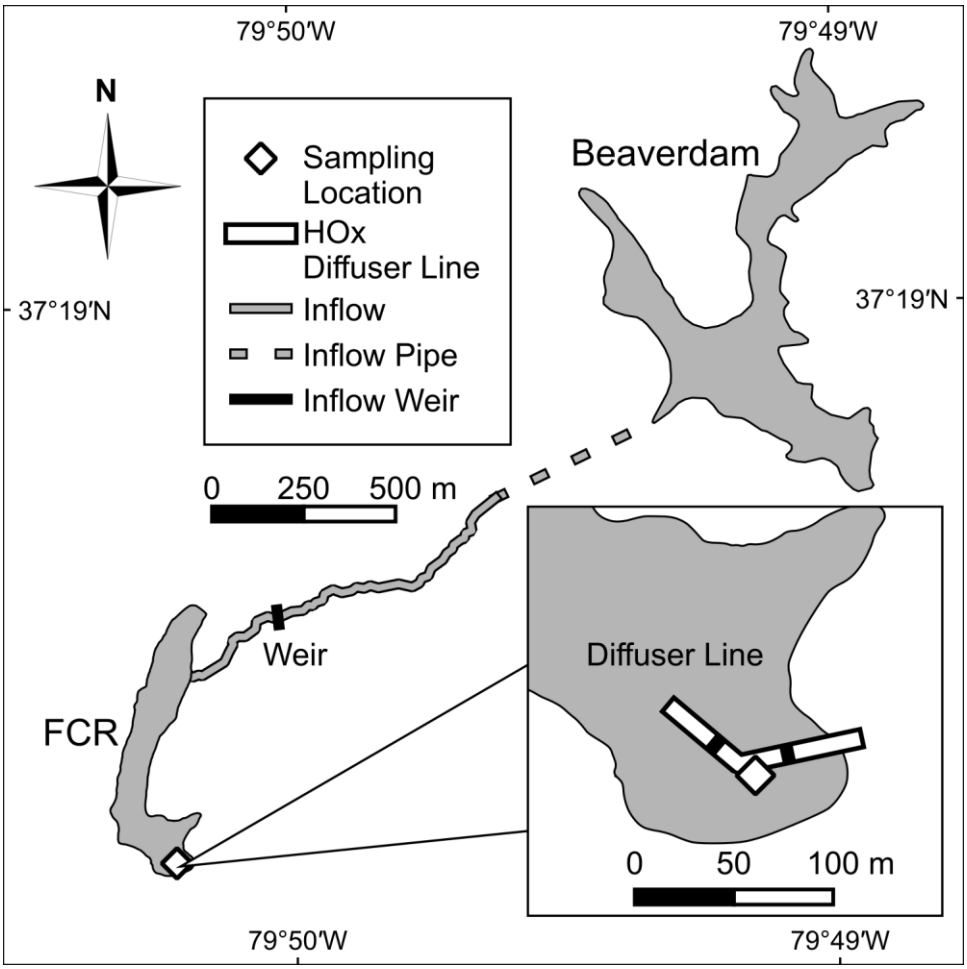

Figure 4.1. Falling Creek Reservoir (FCR) and Beaverdam Reservoir, located near Vinton, Virginia, USA. Reservoir water samples were collected from the sampling location (diamond) and inflow samples were collected from the weir. The inset shows the approximate orientation of the hypolimnetic oxygenation diffuser line.

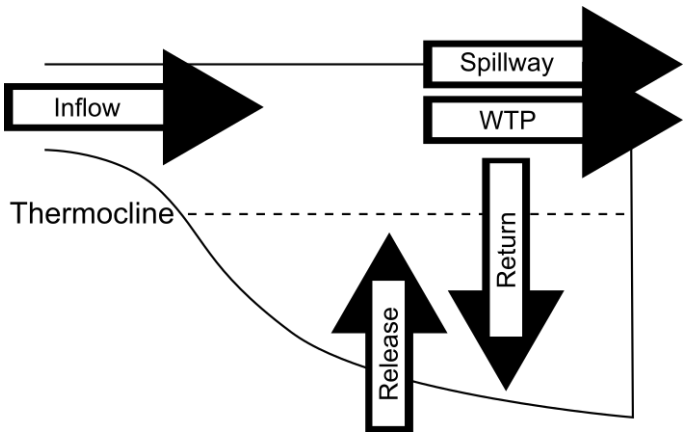

Figure 4.2. Depiction of the metal inputs and outputs to the water column in FCR.

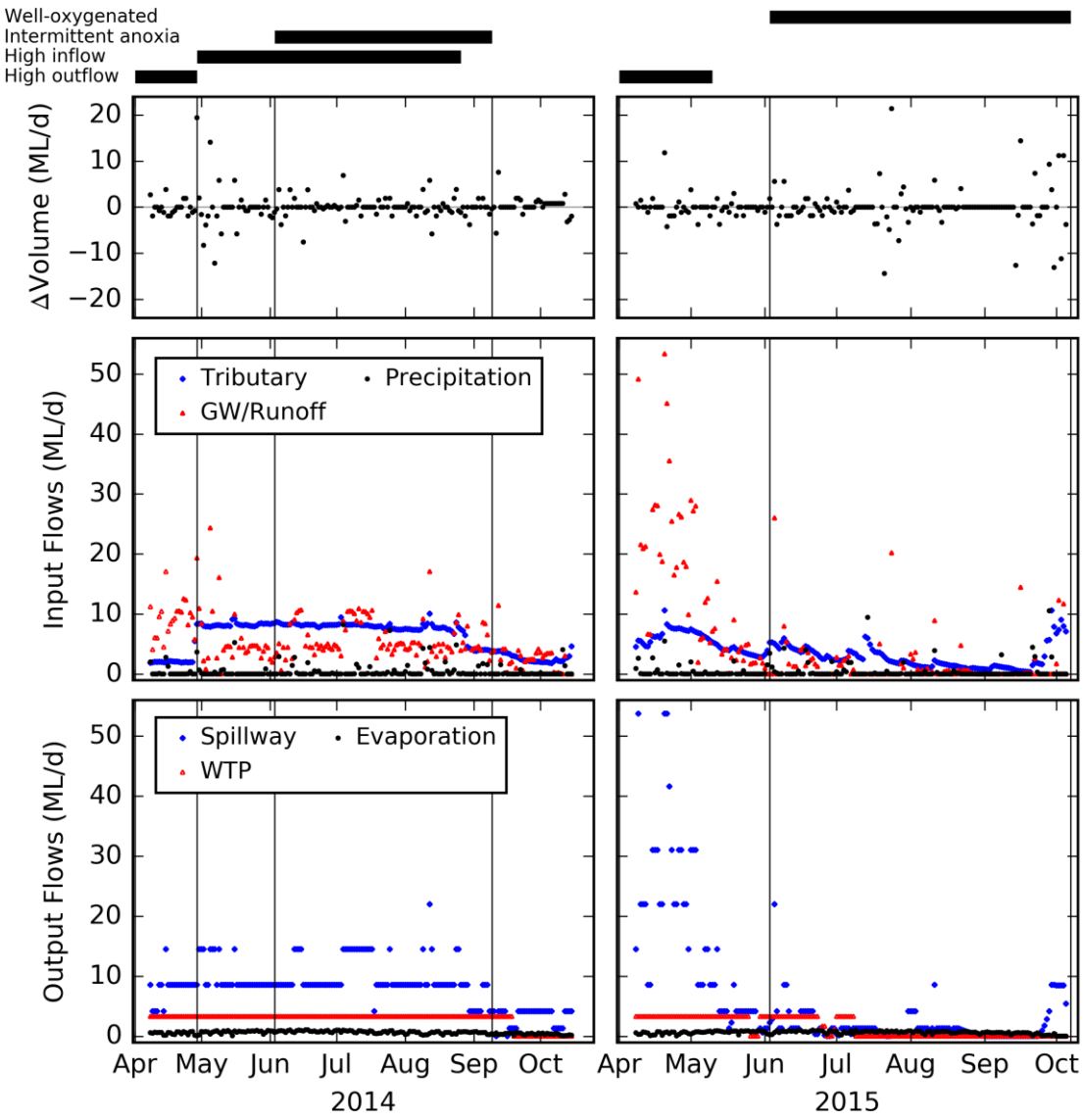

Figure 4.3. Daily change in reservoir volume (top); surface water inflow, groundwater/runoff discharge, and precipitation entering FCR (middle); and spillway discharge, water treatment withdrawals, and direct evaporation, from FCR (bottom) in 2014 (left) and 2015 (right). Vertical lines in the plot area indicate the beginning and end of the hydrologic and redox manipulations. The black bars at the top of the figure indicate the periods of high outflow, of high outflow discharge, high inflow discharge,

intermittent anoxia in the hypolimnion, and well-oxygenated conditions in the hypolimnion.

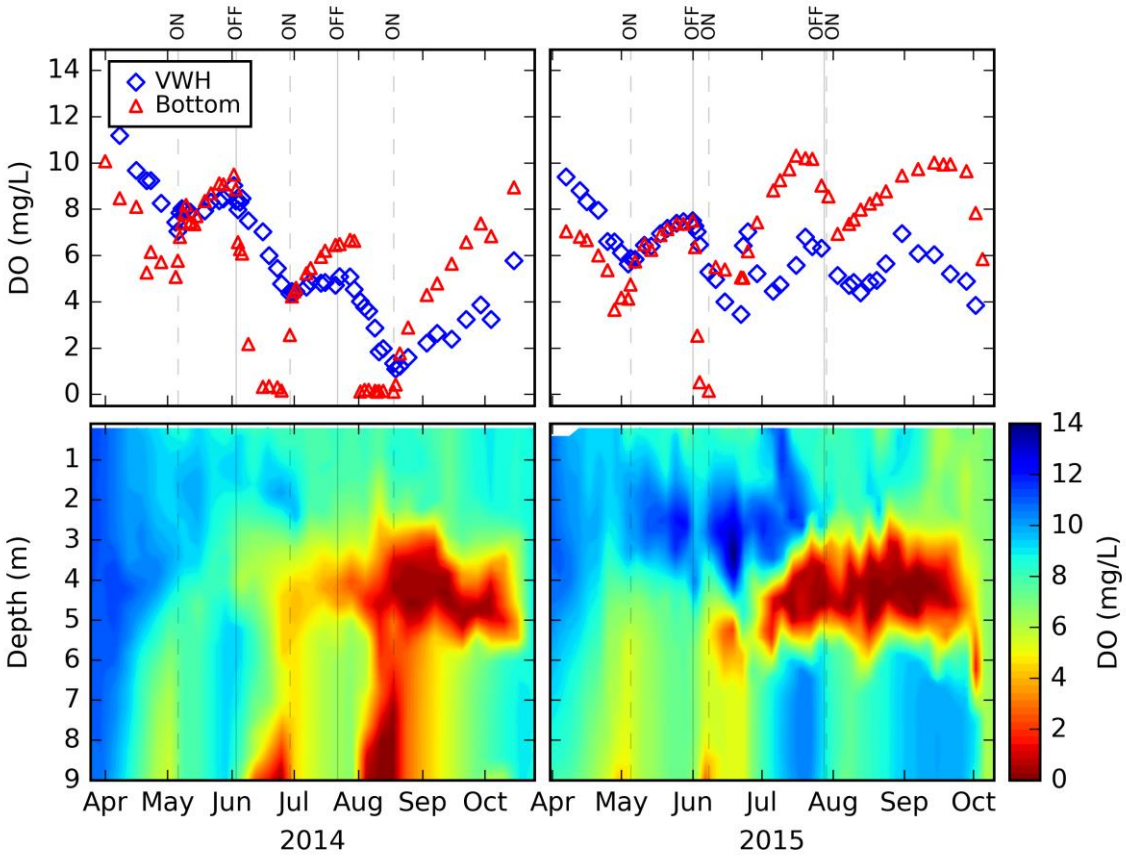

Figure 4.4. The volume-weighted mean hypolimnion DO concentrations and benthic (9-9.3 m depth) DO concentrations (top). Contoured DO concentrations (bottom) at sampling site in FCR during 2014 (left) and 2015 (right). Vertical dashed and solid lines indicate when the HOx system was activated (’ON’) and deactivated (’OFF’), respectively.

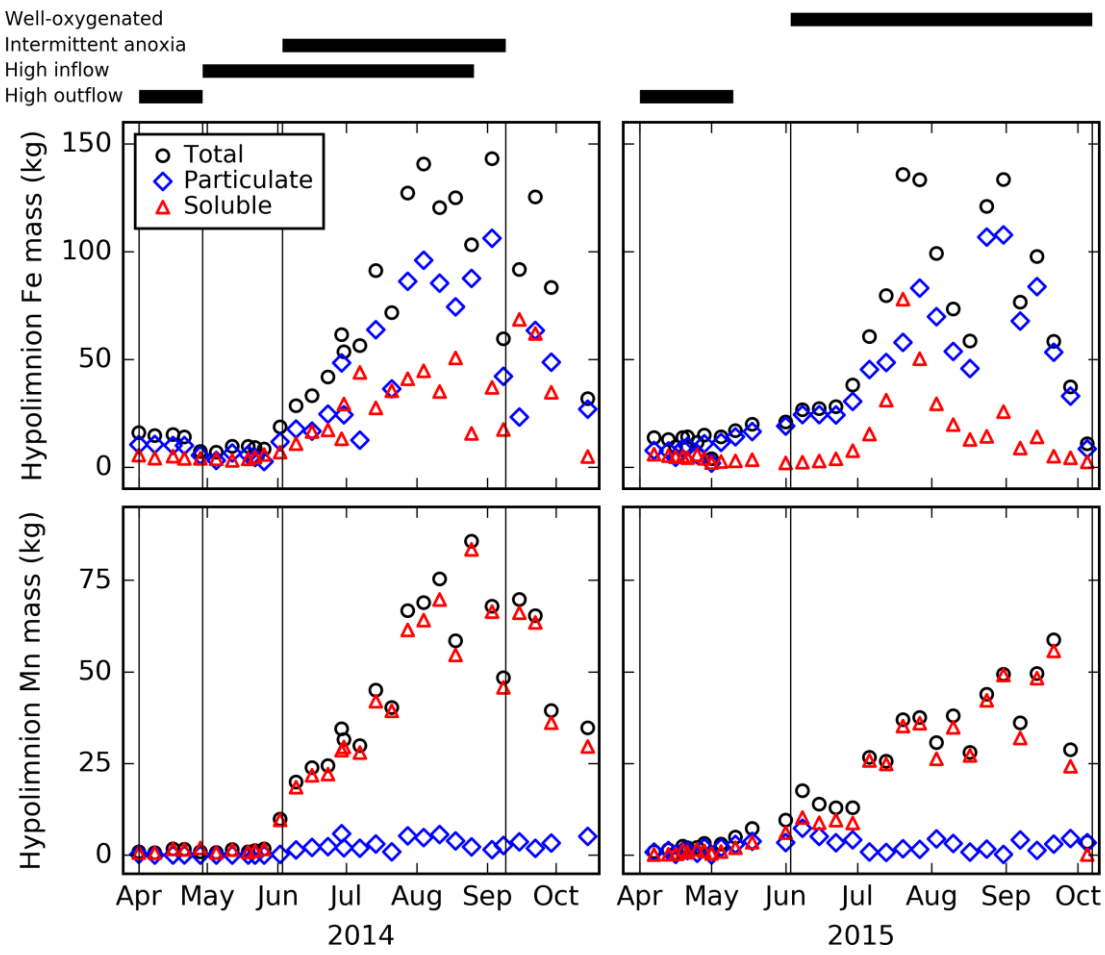

Figure 4.5. The mass of total Fe (top) and Mn (bottom) in the hypolimnion water column in 2014 (left) and 2015 (right). Vertical lines in the plot area indicate the beginning and end of the hydrologic and redox manipulations. The black bars at the top of the figure indicate the periods of high outflow, of high outflow discharge, high inflow discharge, intermittent anoxia in the hypolimnion, and well-oxygenated conditions in the hypolimnion.

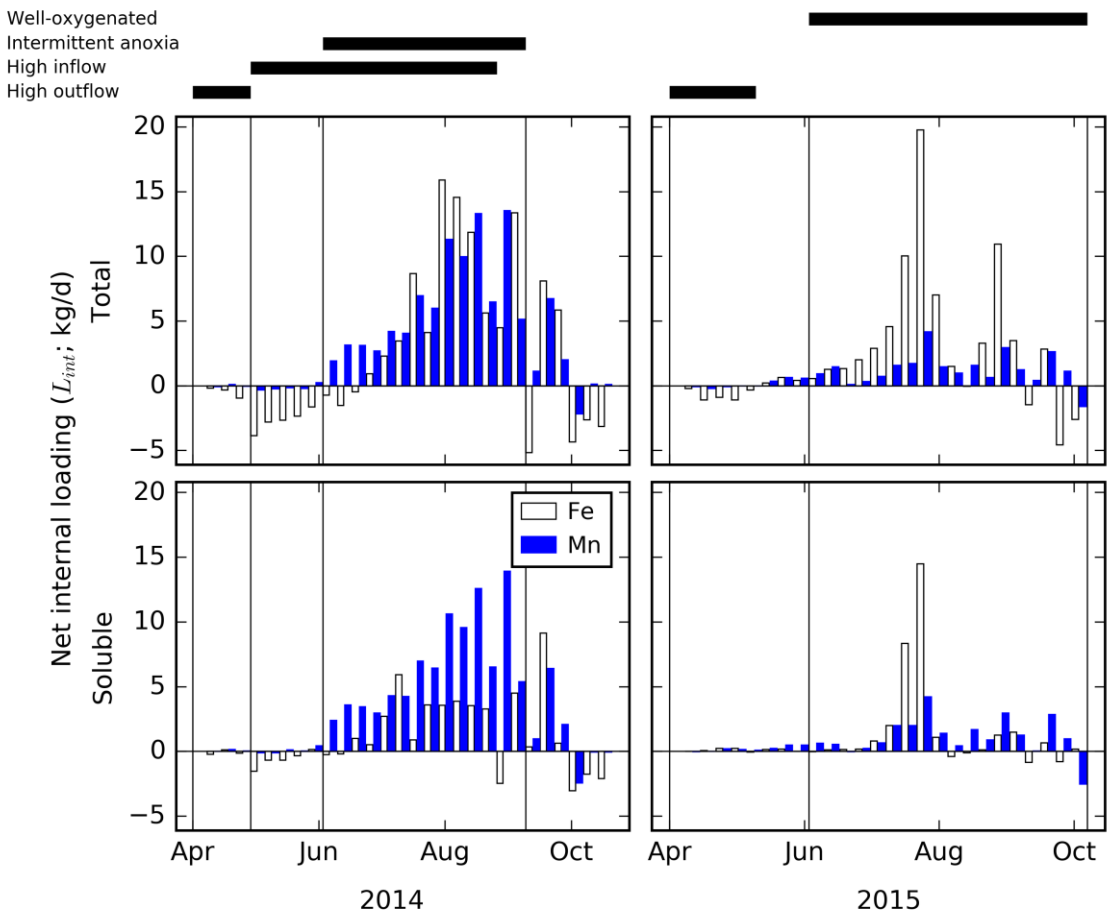

Figure 4.6. Net internal loading (L_{int}) of total (top) and soluble (bottom) Fe and Mn in the hypolimnion of FCR in 2014 (left) and 2015 (right). Positive net internal loading indicates that the release of mass from the sediments to the water column exceeds the return of metals from the water column to the sediments. Vertical lines in the plot area indicate the beginning and end of the hydrologic and redox manipulations. The black bars at the top of the figure indicate the periods of high outflow, of high outflow discharge, high inflow discharge, intermittent anoxia in the hypolimnion, and well-oxygenated conditions in the hypolimnion.

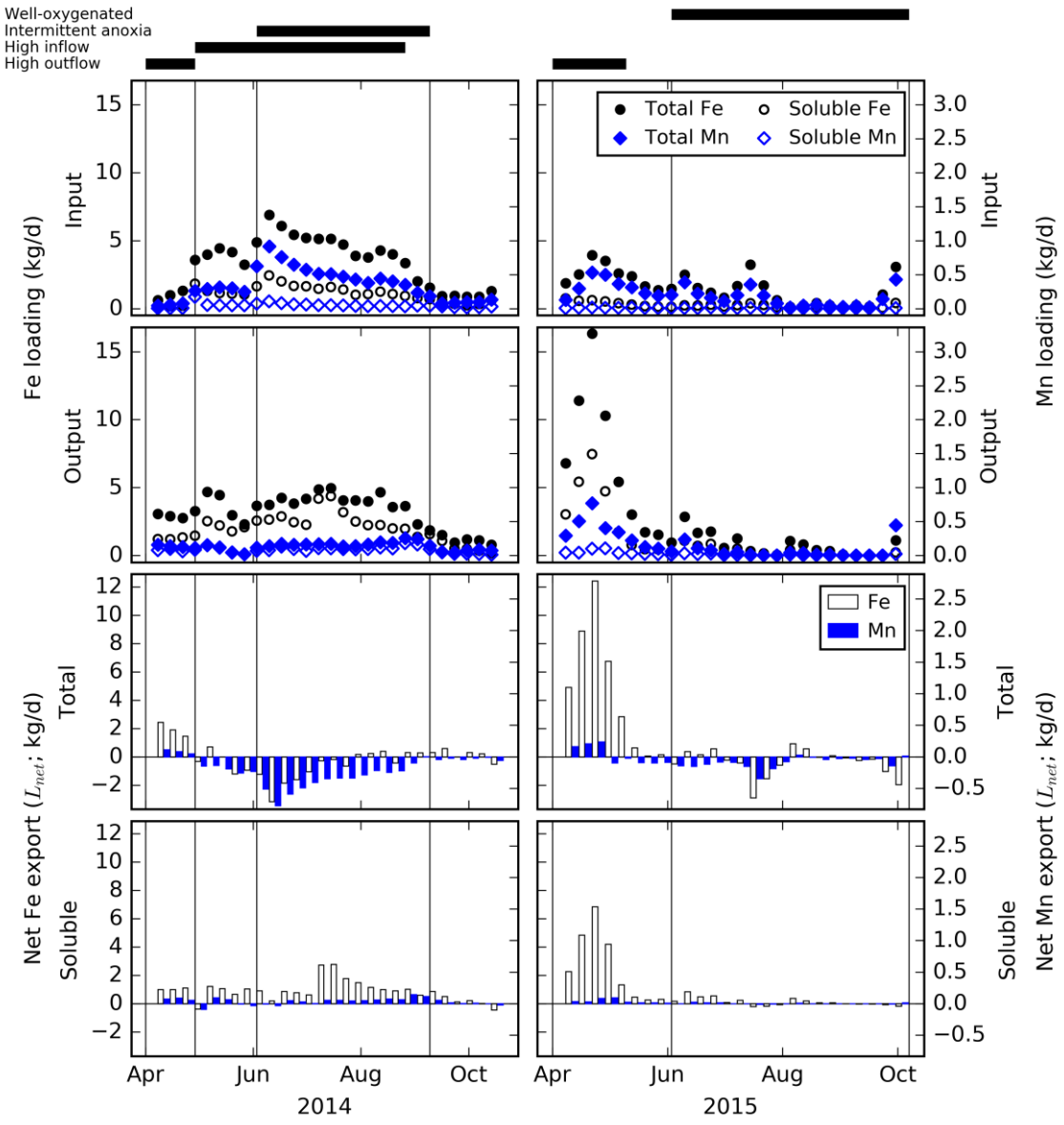

Figure 4.7. Loading of Fe and Mn in the inflows and outflows (top half) and net export of total and soluble Fe and Mn (L_{net}; bottom half) from FCR to the watershed in 2014 (left) and 2015 (right). In all of the panels the right tick marks on the y-axes correspond to the Mn data. Positive L_{net} indicates intervals when the metal loading in the outflows exceeds metal loading in the inflows. Vertical lines in the plot area indicate the beginning and end of the hydrologic and redox manipulations. The black bars at the top of the figure indicate the periods of high outflow, of high outflow discharge, high inflow discharge,

intermittent anoxia in the hypolimnion, and well-oxygenated conditions in the hypolimnion.

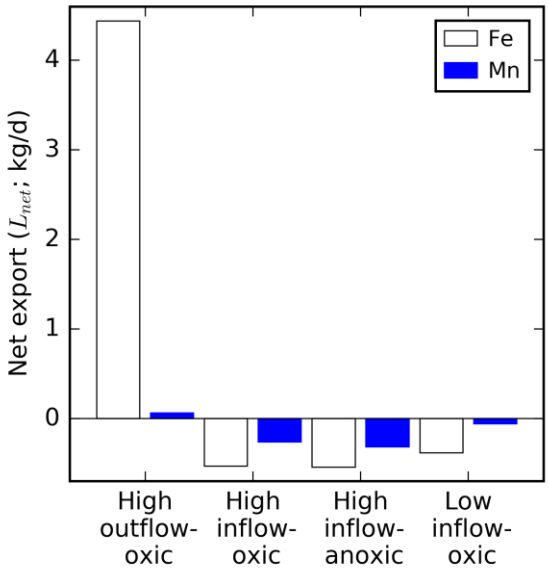

Figure 4.8. Net export of total Fe and Mn (L_{net}) in FCR during high outflow discharge and oxic hypolimnion conditions (1 April through 28 April 2014 and 1 April through 10 May 2015), high inflow discharge and oxic hypolimnion conditions (28 April through 3 June 2014), high inflow discharge and intermittent anoxia in the hypolimnion (3 June through 8 September 2014), and low inflow discharge and well-oxygenated hypolimnion conditions (3 June through 5 October 2015). Positive L_{net} indicates that metal loading in the outflows exceeds metal loading in the inflows.

CHAPTER 5. DISSERTATION SUMMARY AND FUTURE RESEARCH

Controlling Fe and Mn in surface water supplies is a serious challenge for water utilities because of their widespread distribution in watershed sediments and the difficulties in preventing conditions favorable for their ingress to surface waters. Hydrologic factors, such as precipitation and streamflow, are particularly important for the transport of Fe and Mn from the watershed into the water bodies (i.e., rivers, lakes, and reservoirs) that supply the majority of the world's water supply, while biogeochemical factors, such as redox potential, pH, and microbial respiration, control metal speciation and their distribution between insoluble (sediment) and aqueous phases. Both the hydrologic and biogeochemical factors are driven by a combination of climatic, geologic, and biologic processes that occur in all natural systems, which complicates controlling them at the watershed scale. However, accurate characterizations of these factors is essential for informing the management of river, lake, and reservoir water resources.

In Chapter 2, I examined how the sources of Fe and Mn change along a dammed river watershed and the effects of seasonal reservoir conditions on downstream river water quality. Results showed that both the reservoir and tributaries along the watershed were important sources of Fe and Mn to the river, with the relative influence of these sources shifting from reservoir-dominated to tributary-dominated with increased distance from the dam. Furthermore, the magnitude of metal loadings from the reservoir and tributary sources were most strongly influenced by seasonal and hydrologic factors, respectively. These findings demonstrate that, although the sources of Fe and Mn within a watershed may vary both spatially and temporally, systematically characterizing Fe and Mn concentrations with respect to temporospatial watershed characteristics can be

effective for predicting when and where Fe and Mn are likely to be problematic. The relationships between the drivers of reservoir water quality and downgradient river water quality investigated in this study also emphasize the importance of treating water quality management as a holistic endeavor. From the perspective of a drinking water utility responsible for treating river water downgradient from a reservoir, deficiencies in the approach to reservoir water quality management can have a direct economic impact on the water utilities activities, thus studies similar to Chapter 2 are useful not only for informing water quality management practices, but also for informing pollutant discharge regulations.

In Chapter 3, I investigated the effects of hypolimnetic oxygenation on Fe and Mn oxidation and removal in a drinking water reservoir by systematically manipulating hypolimnetic DO concentrations during thermal stratification. Results showed that establishing well-oxygenated conditions increased the oxidation rate of both Fe and Mn. While the enhanced oxidation of soluble Fe was able to successfully prevent it from accumulating in the water column, soluble Mn, and both total Fe and total Mn still accumulated in the hypolimnion while the water column was well-oxygenated. Furthermore, I found that the rate of Mn oxidation was strongly influenced by the activity of metal oxidizing microbes. The findings from this study provide a contrast to several other oxygenated reservoirs where soluble Mn was effectively controlled by increasing DO concentrations, suggesting that although hypolimnetic oxygenation mitigates Fe and Mn problems to a degree, additional characteristics of the reservoir biogeochemistry (e.g., pH, microbial activity, or biochemical oxygen demand) also play an important role in the redox cycles of Fe and Mn.

In Chapter 4, I characterized the effects of internal reservoir conditions and watershed characteristics on the sources and cycles of Fe and Mn in an oxygenated drinking water reservoir. Similar to the findings of Chapter 2, results showed that hydrologic conditions drive the transport of Fe and Mn from the watershed into the reservoir, where the biogeochemical factors in the reservoir strongly influence the accumulation of these metals in the reservoir water column. To quantify the effects of these factors on Fe and Mn cycles, both the discharge in the primary reservoir tributary and DO concentrations in the reservoir hypolimnion were manipulated, as hydrologic and biogeochemical factors have complementary effects on reservoir water quality. Flow conditions in the tributary inflow were a major factor on the import of metals to the reservoir, such that the reservoir tended to behave as a metal sink when the discharge from the tributary inflow into the reservoir was elevated, but behaved as a metal source when discharge in the tributary inflow was low relative to discharge in the reservoir outflows. The tributary flow conditions had a negligible effect on Fe and Mn concentrations in the hypolimnion water column, but played a major role in bringing Fe and Mn into the system that could later be released from the sediments into the water column. Conversely, DO concentrations influenced the release and accumulation of soluble metals in the hypolimnion; when the hypolimnion was well-oxygenated, soluble Fe concentrations were generally low and the rate of Mn oxidation was enhanced. While these internal cycles had a large impact on the exchange of metals between the sediment and water column, they had a relatively minor effect on the source/sink behavior of the reservoir, which was dominated by the hydrologic conditions in the reservoir inflows and outflows.

Despite the advances in our understanding of Fe and Mn cycles resulting from this dissertation, many questions still remain relating to the complexities of Fe and Mn cycles and their implications for water quality. In the context of the dammed river watershed, how might the geomorphology of the watershed, geochemistry of the watershed sediments, or structure of the dam cause the Fe and Mn concentrations in the river to differ from the results in the study presented in Chapter 2? For example, we examined a meandering river that traverses geologic units that have been historically mined for Mn. The dam feeding the river has hourly releases that withdraw water from mid-depths in the water column (below the thermocline during thermal stratification). While the processes driving Fe and Mn entrainment in the watershed and their reductive dissolution in the reservoir are likely to still occur in different environments, their importance may be dramatically different. For example, in a watershed with relatively low concentrations of Fe and Mn in the sediments, even with high erosion and eutrophic conditions, Fe and Mn are unlikely to become problematic. Conversely, some oligotrophic reservoirs may never develop sufficiently reducing conditions to cause the reductive dissolution of Fe and Mn, thus it would not behave as a source of Fe and Mn to the downstream river. Understanding how these vastly different watershed characteristics can influence the distribution of Fe and Mn along a watershed is an important step to improve the application of the findings in Chapter 2 to the systems found globally in different climes.

The internal redox cycles of Fe and Mn also remain difficult to predict from abiotic redox conditions alone. In Chapter 3, I examined the response of Fe and Mn concentrations in the water column of an oxygenated drinking water reservoir. Surprisingly, total Fe and soluble Mn accumulated in the water column even during well-

oxygenated conditions. Numerous studies have examined both the abiotic and biotic oxidation kinetics of Fe and Mn in natural systems, yet these cycles remain poorly understood. In particular, determining where metal-oxidizing microbes exist in the water column and what geochemical variables are optimal for their activities could be essential for elevating the *in situ* management of these metals in drinking water reservoirs. Relating the redox environments in reservoir sediment pore waters, where the bulk of the Fe and Mn reduction occurs, to water column conditions will help to further optimize whole-lake management strategies such as hypolimnetic oxygenation.

REFERENCES

Aguilar, C., Nealson, K.H., 1998. Biogeochemical cycling of manganese in Oneida Lake, New York: whole lake studies of manganese. J. Gt. Lakes Res. 24, 93–104.

American Public Health Association, American Water Works Association, Water Environment Federation, 1998. Standard methods for the examination of water and wastewater, 20th ed. American Public Health Association, Washington, DC.

Amirbahman, A., Pearce, A.R., Bouchard, R.J., Norton, S.A., Kahl, J.S., 2003. Relationship between hypolimnetic phosphorus and iron release from eleven lakes in Maine, USA. Biogeochemistry 65, 369–386.

Anselmetti, F.S., Bühler, R., Finger, D., Girardclos, S., Lancini, A., Rellstab, C., Sturm, M., 2007. Effects of Alpine hydropower dams on particle transport and lacustrine sedimentation. Aquat. Sci. 69, 179–198.

Appelo, C.A.J., Postma, D., 2005. Geochemistry, groundwater and pollution, 2nd ed. CRC press, Boca Raton, Florida.

Ashby, S.L., Myers, J.L., Laney, E., Honnell, D., Owens, C., 1999. The effects of hydropower releases from Lake Texoma on downstream water quality. J. Freshw. Ecol. 14, 103–112.

Balistrieri, L.S., Murray, J.W., Paul, B., 1994. The geochemical cycling of trace elements in a biogenic meromictic lake. Geochim. Cosmochim. Acta 58, 3993–4008.

Baxter, R., 1977. Environmental effects of dams and impoundments. Annu. Rev. Ecol. Syst. 255–283.

Beutel, M.W., Horne, A.J., 1999. A review of the effects of hypolimnetic oxygenation on lake and reservoir water quality. Lake Reserv. Manag. 15, 285–297.

Beutel, M.W., Leonard, T.M., Dent, S.R., Moore, B.C., 2008. Effects of aerobic and anaerobic conditions on P, N, Fe, Mn, and Hg accumulation in waters overlaying profundal sediments of an oligo-mesotrophic lake. Water Res. 42, 1953–1962.

Boogerd, F., De Vrind, J., 1987. Manganese oxidation by Leptothrix discophora. J. Bacteriol. 169, 489–494.

Brown, B.V., Valett, H.M., Schreiber, M.E., 2007. Arsenic transport in groundwater, surface water, and the hyporheic zone of a mine-influenced stream-aquifer system. Water Resour. Res. 43.

Bryant, L.D., Hsu-Kim, H., Gantzer, P.A., Little, J.C., 2011. Solving the problem at the source: controlling Mn release at the sediment-water interface via hypolimnetic oxygenation. Water Res. 45, 6381–6392.

Burdige, D.J., 1993. The biogeochemistry of manganese and iron reduction in marine sediments. Earth-Sci. Rev. 35, 249–284.

Burns, F.L., 1998. Case study: Automatic reservoir aeration to control manganese in raw water Maryborough town water supply Queensland, Australia. Water Sci. Technol. 37, 301–308.

Chapnick, S.D., Moore, W.S., Nealson, K.H., 1982. Microbially mediated manganese oxidation in a freshwater lake1. Limnol. Oceanogr. 27, 1004–1014.

Cook, P.L., Aldridge, K.T., Lamontagne, S., Brookes, J., 2010. Retention of nitrogen, phosphorus and silicon in a large semi-arid riverine lake system. Biogeochemistry 99, 49–63.

Creed, J., Brockhoff, C., Martin, T., 1994. Method 200.8: Determination of trace elements in waters and wastes by inductively-coupled plasma-mass spectrometry, 5th ed. Environmental Monitoring Systems Laboratory, Office of Research and Development, US Environmental Protection Agency, Cincinnati, Ohio.

Csiki, S., Rhoads, B.L., 2010. Hydraulic and geomorphological effects of run-of-river dams. Prog. Phys. Geogr.

Dai, Z., Liu, J.T., 2013. Impacts of large dams on downstream fluvial sedimentation: An example of the Three Gorges Dam (TGD) on the Changjiang (Yangtze River). J. Hydrol. 480, 10–18.

Davis, J.C., Sampson, R.J., 1986. Statistics and data analysis in geology. Wiley New York et al.

Davison, W., 1993. Iron and manganese in lakes. Earth-Sci. Rev. 34, 119–163.

Davison, W., 1981. Supply of iron and manganese to an anoxic lake basin. Nature 290, 241–243.

Davison, W., Woof, C., 1984. A study of the cycling of manganese and other elements in a seasonally anoxic lake, Rostherne Mere, UK. Water Res. 18, 727–734.

Debroux, J.-F., Beutel, M.W., Thompson, C.M., Mulligan, S., 2012. Design and testing of a novel hypolimnetic oxygenation system to improve water quality in Lake Bard, California. Lake Reserv. Manag. 28, 245–254.

Dent, S.R., Beutel, M.W., Gantzer, P., Moore, B.C., 2014. Response of methylmercury, total mercury, iron and manganese to oxygenation of an anoxic hypolimnion in North Twin Lake, Washington. Lake Reserv. Manag. 30, 119–130.

Diem, D., Stumm, W., 1984. Is dissolved Mn 2+ being oxidized by O2 in absence of Mn-bacteria or surface catalysts? Geochim. Cosmochim. Acta 48, 1571–1573.

Dortch, M.S., Hamlin-Tillman, D.E., 1995. Disappearance of reduced manganese in reservoir tailwaters. J. Environ. Eng. 121, 287–297.

Downing, J., Prairie, Y., Cole, J., Duarte, C., Tranvik, L., Striegl, R., McDowell, W., Kortelainen, P., Caraco, N., Melack, J., others, 2006. The global abundance and size distribution of lakes, ponds, and impoundments. Limnol. Oceanogr. 51, 2388–2397.

Dripps, W., Granger, S.R., 2013. The impact of artificially impounded, residential headwater lakes on downstream water temperature. Environ. Earth Sci. 68, 2399–2407.

Edwards, T.K., Glysson, G.D., 1999. Field methods for measurement of fluvial sediment, in: Techniques of Water-Resources Investigations. United States Geological Survey, p. 89.

Espenshade, G.H., 1954. Geology and mineral deposits of the James River-Roanoke River manganese district, Virginia (No. Bulletin 1008). United States Geological Survey.

Fetter, C.W., 2000. Applied hydrogeology. Prentice hall.

Fu, G., Charles, S.P., Chiew, F.H., 2007. A two-parameter climate elasticity of streamflow index to assess climate change effects on annual streamflow. Water Resour. Res. 43.

Gantzer, P.A., Bryant, L.D., Little, J.C., 2009. Controlling soluble iron and manganese in a water-supply reservoir using hypolimnetic oxygenation. Water Res. 43, 1285–1294.

Gerling, A.B., Browne, R.G., Gantzer, P.A., Mobley, M.H., Little, J.C., Carey, C.C., 2014. First report of the successful operation of a side stream supersaturation hypolimnetic oxygenation system in a eutrophic, shallow reservoir. Water Res. 67, 129–143.

Gerling, A.B., Munger, Z.W., Doubek, J.P., Hamre, K.D., Gantzer, P.A., Little, J.C., Carey, C.C., 2016. Whole-catchment manipulations of internal and external loading reveal the sensitivity of a century-old reservoir to hypoxia. Ecosystems 19, 555–571.

Gordon, J.A., 1989. Manganese oxidation related to the releases from reservoirs. J. Am. Water Resour. Assoc. 25, 187–192.

Gordon, J.A., Bonner, W.P., Milligan, J.D., 1984. Iron, manganese, and sulfide transformations downstream from Normandy Dam. Lake Reserv. Manag. 1, 58–62.

Graham, M.C., Gavin, K.G., Farmer, J.G., Kirika, A., Britton, A., 2002. Processes controlling the retention and release of manganese in the organic-rich catchment of Loch Bradan, SW Scotland. Appl. Geochem. 17, 1061–1067.

Hem, J.D., 1981. Rates of manganese oxidation in aqueous systems. Geochim. Cosmochim. Acta 45, 1369–1374.

Hem, J.D., 1972. Chemical factors that influence the availability of iron and manganese in aqueous systems. Geol. Soc. Am. Spec. Pap. 140, 17–24.

Hem, J.D., 1963. Chemical equilibria and rates of manganese oxidation, Water Supply Paper. United States Geological Survey.

Hess, G.W., Kim, B.R., Roberts, P.J.W., 1989. A manganese oxidation model for rivers. J. Am. Water Resour. Assoc. 25, 359–365. doi:10.1111/j.1752-1688.1989.tb03072.x

Hongve, D., 1997. Cycling of iron, manganese, and phosphate in a meromictic lake. Limnol. Oceanogr. 42, 635–647.

Horne, A.J., Goldman, C.R., 1994. Limnology, 2nd ed. McGraw-Hill New York.

Johnson, D., Chiswell, B., O'halloran, K., 1995. Micro-organisms and manganese cycling in a seasonally stratified freshwater dam. Water Res. 29, 2739–2745.

Jones, B.F., Bowser, C.J., 1978. The mineralogy and related chemistry of lake sediments, in: Lakes. Springer, New York, New York, pp. 179–235.

Kawashima, M., Takamatsu, T., Koyama, M., 1988. Mechanisms of precipitation of manganese (II) in Lake Biwa, a fresh water lake. Water Res. 22, 613–618.

Kohl, P.M., Medlar, S.J., 2006. Occurrence of manganese in drinking water and manganese control. American Water Works Association, Denver, Colorado.

Köhler, J., Hilt, S., Adrian, R., Nicklisch, A., Kozerski, H., Walz, N., 2005. Long-term response of a shallow, moderately flushed lake to reduced external phosphorus and nitrogen loading. Freshw. Biol. 50, 1639–1650.

Krenkel, P., 2012. Water quality management, 1st ed. Elsevier.

Ku, H., 1966. Notes on the use of propagation of error formulas. J. Res. Natl. Bur. Stand. 70.

Kurunc, A., Yurekli, K., Okman, C., 2006. Effects of Kilickaya Dam on concentration and load values of water quality constituents in Kelkit Stream in Turkey. J. Hydrol. 317, 17–30.

Lane, S., Flanagan, S., Wilde, F., 2003. Selection of equipment for water sampling (ver. 2.0), in: Techniques of Water-Resources Investigations. United States Geological Survey, p. 101.

Lerman, A., Imboden, D., Gat, J., 1995. Physics and chemistry of lakes, 2nd ed. Springer, New York, New York.

Löfgren, S., Boström, B., 1989. Interstitial water concentrations of phosphorus, iron and manganese in a shallow, eutrophic Swedish lake—implications for phosphorus cycling. Water Res. 23, 1115–1125.

Lovley, D.R., 1987. Organic matter mineralization with the reduction of ferric iron: a review. Geomicrobiol. J. 5, 375–399.

Marsden, M.W., 1989. Lake restoration by reducing external phosphorus loading: the influence of sediment phosphorus release. Freshw. Biol. 21, 139–162.

Menne, M.J., Durre, I., Korzeniewski, B., McNeal, S., Thomas, K., Yin, X., Anthony, S., Ray, R., Vose, R.S., Gleason, B.E., Houston, T.G., 2016. Global Historical Climatology Network - Daily (GHCN-Daily). Version 322 NOAA Natl. Clim. Data Cent. Accessed April 5 2016.

Millero, F.J., Sotolongo, S., Izaguirre, M., 1987. The oxidation kinetics of Fe (II) in seawater. Geochim. Cosmochim. Acta 51, 793–801.

Morgan, J.J., 1967. Chemical equilibria and kinetic properties of manganese in natural waters, in: Principles and Applications of Water Chemistry. Wiley, New York, New York, pp. 561–624.

Nealson, K.H., Saffarini, D., 1994. Iron and manganese in anaerobic respiration: environmental significance, physiology, and regulation. Annu. Rev. Microbiol. 48, 311–343.

Nearing, M., Lane, L., Lopes, V.L., 1994. Modeling soil erosion. Soil Eros. Res. Methods 2, 127–156.

Olivie-Lauquet, G., Gruau, G., Dia, A., Riou, C., Jaffrezic, A., Henin, O., 2001. Release of Trace Elements in Wetlands: Role of Seasonal Variability. Water Res. 35, 943–952. doi:http://dx.doi.org/10.1016/S0043-1354(00)00328-6

Orihel, D.M., Schindler, D.W., Ballard, N.C., Graham, M.D., O'Connell, D.W., Wilson, L.R., Vinebrooke, R.D., 2015. The "nutrient pump:" Iron-poor sediments fuel low nitrogen-to-phosphorus ratios and cyanobacterial blooms in polymictic lakes. Limnol. Oceanogr. 60, 856–871.

Peters, A., Lofts, S., Merrington, G., Brown, B., Stubblefield, W., Harlow, K., 2011. Development of biotic ligand models for chronic manganese toxicity to fish, invertebrates, and algae. Environ. Toxicol. Chem. 30, 2407–2415.

Read, J.S., Hamilton, D.P., Jones, I.D., Muraoka, K., Winslow, L.A., Kroiss, R., Wu, C.H., Gaiser, E., 2011. Derivation of lake mixing and stratification indices from high-resolution lake buoy data. Environ. Model. Softw. 26, 1325–1336.

Richardson, L.L., Aguilar, C., Nealson, K.H., 1988. Manganese oxidation in pH and O2 microenvironments produced by phytoplankton1, 2. Limnol. Oceanogr. 33, 352–363.

Rimstidt, J.D., 2013. Geochemical rate models: an introduction to geochemical kinetics, 1st ed. Cambridge University Press, New York, New York.

Rosenberry, D.O., Winter, T.C., Buso, D.C., Likens, G.E., 2007. Comparison of 15 evaporation methods applied to a small mountain lake in the northeastern USA. J. Hydrol. 340, 149–166.

Rounds, S., Wilde, F.D., 2001. Alkalinity and acid neutralizing capacity, in: National Field Manual. United States Geological Survey, p. 45.

Rozan, T.F., Taillefert, M., Trouwborst, R.E., Glazer, B.T., Ma, S., Herszage, J., Valdes, L.M., Price, K.S., Luther III, G.W., 2002. Iron-sulfur-phosphorus cycling in the sediments of a shallow coastal bay: Implications for sediment nutrient release and benthic macroalgal blooms. Limnol. Oceanogr. 47, 1346–1354.

Sear, D., 1996. Sediment transport processes in pool–riffle sequences. Earth Surf. Process. Landf. 21, 241–262.

Shaked, Y., Erel, Y., Sukenik, A., 2004. The biogeochemical cycle of iron and associated elements in Lake Kinneret 1, 2. Geochim. Cosmochim. Acta 68, 1439–1451.

Singleton, V.L., Little, J.C., 2006. Designing hypolimnetic aeration and oxygenation systems-a review. Environ. Sci. Technol. 40, 7512–7520.

Skalak, K., Pizzuto, J., 2010. The distribution and residence time of suspended sediment stored within the channel margins of a gravel-bed bedrock river. Earth Surf. Process. Landf. 35, 435–446.

Smith, D.B., Cannon, W.F., Woodruff, L.G., Solano, F., Kilburn, J.E., Fey, D.L., 2013. Geochemical and mineralogical data for soils of the conterminous United States. US Geol. Surv. Data Ser. 801, 19.

Smith, R.A., Alexander, R.B., Wolman, M.G., 1987. Water-quality trends in the nation's rivers. Science 235, 1607–1615.

Sommerfeld, E.O., 1999. Iron and manganese removal handbook, 1st ed. American Water Works Association, Denver, Colorado.

Stauffer, R.E., 1986. Cycling of manganese and iron in Lake Mendota, Wisconsin. Environ. Sci. Technol. 20, 449–457.

STORET, 2015. STOrage and RETrieval, The US EPA Water Quality Database. US Environmental Protection Agency.

Stumm, W., Lee, G.F., 1960. The chemistry of aqueous iron. Schweiz. Z. Für Hydrol. 22, 295–319.

Tebo, B.M., Johnson, H.A., McCarthy, J.K., Templeton, A.S., 2005. Geomicrobiology of manganese (II) oxidation. TRENDS Microbiol. 13, 421–428.

Teefy, S., 1996. Tracer studies in water treatment facilities: a protocol and case studies. American Water Works Association.

Tipping, E., Thompson, D., Davison, W., 1984. Oxidation products of Mn (II) in lake waters. Chem. Geol. 44, 359–383.

Turnipseed, D.P., Sauer, V.B., 2010. Discharge measurements at gaging stations, in: Techniques of Water-Resources Investigations. United States Geological Survey, p. 65.

United States Environmental Protection Agency, 2016a. Table of Regulated Drinking Water Contaminants [WWW Document]. URL https://www.epa.gov/ground-water-and-drinking-water/table-regulated-drinking-water-contaminants (accessed 6.6.16).

United States Environmental Protection Agency, 2016b. Secondary Drinking Water Standards: Guidance for Nuisance Chemicals.

United States Environmental Protection Agency, 1995. Method 3051: Microwave assisted acid digestion of sediments, sludges, soils, and oils, in: Test Methods for Evaluating Solid Waste. United States Environmental Protection Agency, Washington, D.C.

Van der Molen, D.T., Boers, P.C., 1994. Influence of internal loading on phosphorus concentration in shallow lakes before and after reduction of the external loading, in: Nutrient Dynamics and Biological Structure in Shallow Freshwater and Brackish Lakes. Springer, pp. 379–389.

Vörösmarty, C.J., Green, P., Salisbury, J., Lammers, R.B., 2000. Global water resources: vulnerability from climate change and population growth. Science 289, 284–288.

Wada, Y., Wisser, D., Bierkens, M., 2014. Global modeling of withdrawal, allocation and consumptive use of surface water and groundwater resources. Earth Syst. Dyn. 5, 15.

Ward, J.V., Stanford, J., 1995. Ecological connectivity in alluvial river ecosystems and its disruption by flow regulation. Regul. Rivers Res. Manag. 11, 105–119.

Wasserman, G.A., Liu, X., Parvez, F., Ahsan, H., Levy, D., Factor-Litvak, P., Kline, J., van Geen, A., Slavkovich, V., Lolacono, N.J., others, 2006. Water manganese exposure and children's intellectual function in Araihazar, Bangladesh. Environ. Health Perspect. 124–129.

Wei, G., Yang, Z., Cui, B., Li, B., Chen, H., Bai, J., Dong, S., 2009. Impact of dam construction on water quality and water self-purification capacity of the Lancang River, China. Water Resour. Manag. 23, 1763–1780.

Whiting, P.J., Matisoff, G., Fornes, W., Soster, F.M., 2005. Suspended sediment sources and transport distances in the Yellowstone River basin. Geol. Soc. Am. Bull. 117, 515–529.

Wielicki, B.A., Barkstrom, B.R., Harrison, E.F., Lee III, R.B., Louis Smith, G., Cooper, J.E., 1996. Clouds and the Earth's Radiant Energy System (CERES): An earth observing system experiment. Bull. Am. Meteorol. Soc. 77, 853–868.

World Commission on Dams, 2000. Dams and Development: A New Framework for Decision-making: the Report of the World Commission on Dams. Earthscan.

World Health Organization, 2004. Guidelines for drinking-water quality: recommendations, 3rd ed. World Health Organization, Geneva, Switzerland.

Zarfl, C., Lumsdon, A.E., Berlekamp, J., Tydecks, L., Tockner, K., 2015. A global boom in hydropower dam construction. Aquat. Sci. 77, 161–170.

Zaw, M., Chiswell, B., 1999. Iron and manganese dynamics in lake water. Water Res. 33, 1900–1910.

Zhang, J., Huang, W., 1993. Dissolved trace metals in the Huanghe: the most turbid large river in the world. Water Res. 27, 1–8.